UNIVERSITAT POLITÈCNICA DE VALÈNCIA

_ TELECOM ESCUELA TÉCNICA VLC SUPERIOR DE UPV INGENIEROS DE TELECOMUNICACIÓN

Experimental Analysis of LoRa LPWAN technology in Smart City and Open Environments

Author: Carlos Adrián Sánchez Mompó

Tutor: Víctor Miguel Sempere Payá

Co-Tutor: Salvador Santoja Climent

Trabajo Fin de Grado presentado en la Escuela Técnica Superior de Ingenieros de Telecomunicación de la Universidad Politécnica de Valencia, para la obtención del Título de Grado en Ingeniería de Tecnologías y Servicios de Telecomunicación

Curso 2017-18

Valencia, agosto de 2018

Agradecimientos

Deseo agradecer el apoyo y colaboración de las personas e instituciones que me han ayudado a llegar hasta aquí.

Al Instituto Tecnológico de Informática (ITI) de la UPV, por la cesión de las instalaciones. Al Servicio de Seguridad de la UPV por facilitar el acceso a los edificios desde los que se han hecho varios de los ensayos. Al profesor Víctor Miguel Sempere, por la dirección del proyecto. A mi cotutor Salvador Santoja, por guiarme durante todo el proceso. A José Vera y Rubén Ponce, por su compromiso y ayuda durante todo el desarrollo del trabajo. A José Ramón Navarro, por las "tutorías" sobre estadística. A Juan Carlos García, por toda la ayuda prestada.

A mis padres, por estar ahí cuando más los necesitaba y por su apoyo incondicional; y en particular, a mi padre, profesor de la Escuela de Caminos de la UPV, por el ánimo y la grandísima ayuda en la revisión formal del trabajo.

Y a todos los profesores, amigos y familiares que, de una manera u otra, me han enseñado, ayudado o acompañado en estos años.

Resumen

La revolución tecnológica de las últimas décadas nos está llevando a un mundo conectado en el que cada vez un mayor número de dispositivos adquiere conexión a Internet. Estos dispositivos son parte del IoT (*Internet of Things*), y suelen presentar fuertes restricciones de coste y duración de batería.

Debido a estas limitaciones, los dispositivos requieren de soluciones de conectividad con una baja complejidad y consumo. Además, para despliegues extensos también es conveniente que estas tecnologías sean de largo alcance para reducir costes de infraestructura. Al tipo de redes que cumplen estas características se las denomina LPWANs (*Low Power Wide Area Networks*).

En este Trabajo Fin de Grado se busca estudiar el desempeño de una de estas tecnologías (LoRa) en diferentes tipos de escenarios abiertos como *Smart City*, *Smart Campus* y Entorno Agrícola. Para ello se procede, en primer lugar, al análisis de las diferentes tecnologías de transmisión disponibles en el mercado que hayan sido diseñadas o adaptadas para su uso en dispositivos IoT.

A continuación, se selecciona la más apropiada para el proyecto (LoRa) y se procede a su análisis en profundidad. Después, se diseñan y realizan diversas pruebas con el objetivo de medir el rendimiento de esta tecnología en términos de capacidad y distancia.

En último lugar, se procede al análisis de los resultados obtenidos en las pruebas y se extraen las conclusiones sobre el comportamiento de LoRa en los diferentes escenarios propuestos. Como resultado del trabajo realizado y de los datos recogidos, se pretende extenderlo mediante una publicación de investigación para posteriormente continuar con la línea de investigación abierta.

Resum

La revolució tecnològica de les últimes dècades ens està portant a un món connectat en el qual cada vegada un major nombre de dispositius adquirix connexió a internet. Estos dispositius són part del IoT (Internet of Things), i solen presentar fortes restriccions de cost i durada de bateria.

A causa d'estes limitacions, els dispositius requerixen de solucions de connectivitat amb una baixa complexitat i consum. A més, per a desplegaments extensos també és convenient que estes tecnologies sigan de llarg abast per a reduir costos d'infraestructura. Al tipus de xarxes que complixen estes característiques se les anomena LPWANs (Low Power Wide Area Networks).

En este Treball Fi de Grau es busca estudiar l'acompliment d'una d'estes tecnologies (LoRa) en diferents tipus d'escenaris oberts com *Smart City, Smart Campus* i Agrícola. Per a això es procedix, en primer lloc, a l'anàlisi de les diferents tecnologies de transmissió disponibles al mercat que hagen segut dissenyades o adaptades per al seu ús en dispositius IoT.

A continuació, se selecciona la més apropiada per al projecte (LoRa) i es procedix al seu anàlisi en profunditat. Després, es dissenyen i realitzen diverses proves amb l'objectiu de mesurar el rendiment d'esta tecnologia en termes de capacitat i distància.

En darrer lloc, es procedix a l'anàlisi dels resultats obtinguts en les proves i s'extrauen les conclusions sobre el comportament de LoRa en els diferents escenaris proposats. Com a resultat del treball realitzat i les dades obtingudes, es pretén estendre-ho mitjançant una publicació d'investigació per posteriorment continuar amb la línia d'investigació oberta.

Abstract

Over the last decades, a technological revolution has led to a connected world where an increasing number of devices requires an Internet connection. These devices are part of the IoT (Internet of Things) and usually present strict cost and energy restrictions.

Due to these limitations, IoT devices require low-complexity, low-power connectivity solutions. In addition, for wide-area implementations, it is also convenient to use long-range technologies to reduce infrastructure costs. This type of network is called LPWANs (Low-Power Wide-Area Networks).

The aim of this project is to study the performance of one of these technologies (LoRa) in scenarios such as Smart City, Smart Campus and Smart Countryside. To achieve this objective, in the first place, an analysis of the State of the Art of the transmission technologies available for the IoT is conducted.

Secondly, the technology that best fits the project (LoRa) is chosen, and a deeper analysis of it is performed. Then, different experiments are designed and conducted to measure the real-world capacity and range of this technology.

In the last place, an analysis of the results obtained in the different experiments is performed, from which the conclusions regarding the performance of LoRa in the proposed scenarios will be extracted. As a result of this work and based on the data collected, it will be extended with a research publication to later continue with the opened research line.

TABLE OF CONTENTS

INDEX OF TABLES

INDEX OF FIGURES

Chapter 1: INTRODUCTION

1.1 THE HISTORY OF NETWORKING

Data communication networks have been around since the beginning of the computing age and, even before, other types of communication networks such as the telegraph existed to share information across distances.

The first data communications between computers were application specific and usually point to point. The creation of ARPANET revolutionised this state of affairs, being a network able to communicate any type of information between machines, with routing and path redundancy capabilities. This was a network designed to enable machines with information interchange capabilities.

The next revolution was the appearance of the World Wide Web, which enabled users to interact directly with other computers or servers connected to the network, obtaining information from them in the form of web pages. Its use was initially limited to universities, but it progressively spread to the general public, becoming more accessible by adapting old communications networks as the POTS (Plain Old Telephone Service) to carry Internet data.

Afterwards, purpose-built infrastructure for Internet access as coaxial and optical fibre networks were deployed to the user's homes.

In 2007, with the appearance of the first iPhone, another revolution had place, the revolution of the Smart Phones. With these electronics devices, users could access all the information in the web from practically anywhere. New wireless communications networks were developed and deployed to provide of high access mobile Internet connectivity to these devices, while web services were adapted for their use and access from portable devices.

As citizens became familiarised with the use of multiple devices (such as computers, Smart Phones, wearables, smart TV's, etc.) to access the information available on the Internet and to interact with it, a need for instant access to all types of information appeared.

Thereafter, the number of connected devices raised almost exponentially as devices ranging from appliances to parking sensors became connected to the Internet, as a response to the users' need to access information from virtually any place.

The cities have begun to undergo a change on how users interact with the city and how the city offers its services to its users. Besides, citizens are beginning to get involved in the decision making that occurs on the different services offered by the city.

To enable an efficient infrastructure of services, the cities need to become smart, leading to the Smart City movement. Nowadays, the cities begin to incorporate sensors to gather all kinds of data from their infrastructures. These range from parking sensors for a better parking space management to environmental and soil moisture sensors for the efficient maintenance of the cities' parks.

1.2 THE INTERNET OF THINGS

The "Internet of Things" or IoT is a naming convention which comprises a group of devices connected to the internet which are usually characterized by their low power-consumption and

their low complexity, such as battery-powered sensors connected to the internet. The market that it represents is in a constant and exponential growth. The increasing number of IoT devices demands an increasing network capacity, which results in the need of new radio technologies and modern network architectures.

Although the name IoT was not used in a publication until the year 2009, when Kevin Ashton used it in an article in the RFID journal [1], it had already been in use in the scientific community for over a decade; in fact, considering its definition, devices which could have been defined under the category of the IoT existed even earlier.

In the present, the number of connected devices is well over the population of the world, with more than 50 billion devices. The smartification of everything leads to the need of communications solutions capable of handling a massive number of devices spread across vast territories.

To provide of connectivity to such a large number of devices, some legacy solutions have already been adapted and implemented, such as large-area deployments of Wi-Fi networks, the use of existing WAN technologies, the deployment of mesh networks as ZigBee, etc.

The problem with classic networking solutions is that to achieve a viable economical design, the networks need to provide the devices with a very low power communications solution, something that most of these networking solutions do not provide. The network should allow the device to enter sleep mode whenever no data needs to be transmitted, therefore avoiding an almost constant connection just for link maintenance purposes (which classic networks usually need). A new category of networks re-emerged in the 2000's to fill this gap: the LPWANs (Low Power Wide Area Networks).

The LPWANs provide of low power network access to wide areas. There are many technologies of this type competing for their market share as they are still in their early stages. Therefore, the scientific community needs to understand the capabilities and boundaries of these new types of networks, as well as analyse how they perform in certain environments and use-cases.

To this purpose, there are multiple studies that simulate the behaviour of some of the existing technologies. However, there are not as many practical studies where a case-scenario or use-case is defined and tested. The lack of practical studies is due to their higher difficulty and the variability observed in their results depending on the specific conditions of the experiment.

Therefore, in this document, an LPWAN technology will be tested with a series of practical experiments to help further advance the knowledge about the behaviour of that technology and possible use-cases. The use-cases chosen (which will be explained in the following sections) range from Smart City to agricultural.

Chapter 2: PROJECT OBJECTIVES AND METHODOLOGY

2.1 OBJECTIVES

The objectives pursued in this project are:

- To Evaluate the capacity of the LoRa protocol when only one channel and one Spreading Factor is used.
- To Evaluate the performance of the LoRa PHY communications layer (when the gateway is installed on the roof of a building) in:
    - A Near Line of Sight environment (nodes are on other roofs of the campus' buildings).
    - A No Line of Sight environment (nodes are in campus at ground level).
    - A mixed Line of Sight agricultural environment (nodes are at ground level outside the campus).
    - A very obstructed Fresnel zone Near Line of Sight environment (nodes are at ground level in port facilities).

In the next section, the methodology used to achieve these objectives during the course of this work will be explained.

2.2 METHODOLOGY

The steps which have been followed to accomplish the objectives of this project are:

- INITIAL RESEARCH
    - To Evaluate the project's viability.
    - To Study the State-of-the-Art of the different LPWAN technologies available in the market.
    - To Choose the PHY interface which suits best the type of experiments that are conducted.
    - To Choose a development platform (both hardware and software) that fits best the experiments that are going to be conducted.
    - To Familiarise with the platform and technologies chosen and to do some preliminary testing in order to dimension the experiments and to know what results to expect.
- DESIGN
    - To Design a MAC layer to support the necessary experiments and tests of the LoRa PHY layer.
    - To Design the underlying control and supervision layer to be used in the experiments.
    - To Design and assemble the necessary hardware for the project.
    - To Design the tests.
- DEVELOPMENT
    - To Program the devices' firmware to include the MAC, control and supervision layers of the tests.
    - To Carry out the Capacity Laboratory Experiment.
    - To Install the gateway in the roof of the building 8E.
    - To Conduct the In-Campus experiments.
    - To Conduct the Out-Campus experiments.

- ANALYSIS
    - To Analyse the results obtained in each one of the experiments.
    - To Analyse the results of all the experiments together and to reason the findings of the project.
    - To Extract the conclusions of the project.
    - To Devise and design future work that could be conducted after this work is finished.

Due to the limitation in the number of pages recommended for this document, only the most relevant steps followed and conclusions drawn are documented.

Chapter 3: LPWAN STATE OF THE ART

3.1 INTRODUCTION

In order to select the communications technology to be used in the experiments, a state-of-the-art analysis is carried out in the next sections. In it, some of the most relevant low-power long-range technologies available on the market are analysed. At the end of this analysis, the technology that best fits the intended application is chosen.

3.2 LORA

LoRa is a radio interface designed to satisfy the increasing demand of low-power high-range radio modulation technologies for IoT LPWANs. It can either be used with the LoRaWAN Wide Area Network MAC layer and network architecture on top, with another MAC layer or alone.

3.2.1 Technical Overview

LoRa [2] is a low-level physical interface (PHY) for very low data-rate, low-power, high-range communications. It achieves these characteristics by using Semtech's implementation of the Chirp Spread Spectrum (CSS) modulation technology which is a modification of a technology used for continuous wave RADAR applications since 1961 [3]. Semtech's achievement has been to compact all the necessary circuitry into a small-factor, low-power inexpensive chip.

The bands of operation in Europe are the 868 MHz, the 433 MHz and the 169 MHz ISM (Industrial, Scientific and Medical) bands. LoRa uses a CSS modulation scheme to overcome interferences from other sources. Because of this choice, in some regions, limitations to the duty cycle may apply. In the EU, the local radio regulations allow for a maximum duty cycle of up to a 10% in some channels and 1% and 0.1% in others [4]. For a bandwidth of 125 kHz, the data rates range from 0.293 kbps to 9.375 kbps, for spreading factors ranging from 12 to 6 respectively.

The total capacity using a single 125 kHz LoRa channel is, as shown in (1), the sum of the bitrates of all the SFs.

$$\begin{aligned} Capacity_{LoRa} &= 1 \times (SF12 + SF11 + SF10 + SF9 + SF8 + SF7 + SF6) \\ &= 1 \times (293 + 537 + 976 + 1{,}757 + 3{,}125 + 5{,}468 + 9{,}375) \\ &= 21{,}531\ b/s \end{aligned} \quad (1)$$

The payload is limited to 255 bytes of content at the physical layer. However, when using high spreading factors which need more air-time per byte, it is not recommended to transmit large packets, as the receptor may de-synchronize or the transmission may get interfered. However, if a large packet needs to be transferred using high SFs, there is an option in the radio that increases the chances of a correct reception called low data rate optimise.

The link Budget of the LoRa radio interface for Europe, achieved using the maximum transmission power (14 dBm), using the maximum permitted ERP (Effective Radiated Power) (14 dBm) and using the strongest radio configuration is of 156 dB.

3.2.2 Use Cases

As LoRa is a low-power, low-capacity and long-range physical interface technology, it is well suited for IoT-driven applications involving medium to long range communications (≈10 km). While it is designed to work with the LoRaWAN protocol and architecture, it can also accommodate other WAN protocols such (as the one designed in future sections) as well as other non-WAN protocols such as ZigBee or DigiMesh. While mesh architectures as DigiMesh can be implemented, it is not recommended (by Semtech), due to the long preambles and variable bit rates of LoRa.

3.2.3 Usage, Availability and Cost

LoRa has already been used in many deployments of the LoRaWAN protocol and network architecture in different countries. LoRaWAN gateways are available in the market with price tags as low as 230€. This is achieved using low cost development components as the Raspberry Pi [5]. Prices are higher for other commercial alternatives which allow for more channels in a single gateway, multiplying the number of devices a single gateway can handle. These options can reach price tags of thousands of euros for ready-to-use models rated for exterior use [6]. Most of the communications ICs for both the gateways and the nodes are usually provided by the Semtech Corporation.

LoRaWAN gateways which allow for low-level firmware access to the radio can also be used for any LoRa-based protocol, given the shared PHY layer.

The typical price of a node ranges from 20-60 euros, depending on the processing power and if other communications solutions or sensors are integrated in the boards.

3.3 LoRaWAN

LoRaWAN is a wide area networking protocol and architecture for long range IoT communications which makes use of the LoRa and FSK radio modulations. Its design makes use of a gateway to end-node communication scheme, similar to the mobile-station to base-station scheme used in GSM. It is not capable of peer to peer (end device to end device or gateway to gateway) communications.

3.3.1 Technical Overview

There are 4 different types of devices recognized in the LoRaWAN [7] [8] architecture:

- The end devices or nodes which usually generate the data. The purpose of the network is to provide communications to these devices. An end node can be a sensor, an actuator or any other type of device that does not need a high-speed connection to the network. The data it produces can consist of temperature readings, status of a process, etc.
- The application servers are the controllers to which the different nodes are linked. These servers receive the information sent by the nodes and can also send configuration parameters to them. Their role is to process the received information and configure the nodes linked to them. They might also convert this information to a human-understandable format and of utility to the end user or for an automated process. These servers are property of the customers.
- The Network Server acts as a concentrator of all the communications that take place in the LoRaWAN network. It communicates with both the application servers and the gateways and is a key component to both deliver the data provided by the nodes such as sensor information to the application servers and the control messages from the

application servers to the end nodes. It could be understood as the router of the LoRaWAN network.

- The Gateway acts as a connector between the end devices and the network server. More than one Gateway can exist in the same LoRaWAN network. There are some rules to deal with this situation:
    - On the one hand, as all the packets received by a Gateway are forwarded to the network server and there can be multiple gateways in the reach of a node, a network server might receive the same packet more than once.
    - On the other hand, when the network server wants to send a packet to an end node, it chooses the gateway with the best connection with the end device to forward it.

In LoRaWAN, different data rates are defined depending on the band of operation and region. These data rates use different SFs and BWs to achieve different bit rates. It also allows for the use of the FSK modulation instead of LoRa to achieve up to 50 kbps. Table 1 contains the data rates for the European EU868 band of operation.

DataRate	Configuration	Indicative Physical bit rate (bit/s)
0	LoRa: SF12 / 125 kHz	250
1	LoRa: SF11 / 125 kHz	440
2	LoRa: SF10 / 125 kHz	980
3	LoRa: SF9 / 125 kHz	1,760
4	LoRa: SF8 / 125 kHz	3,125
5	LoRa: SF7 / 125 kHz	5,470
6	LoRa: SF7 / 250 kHz	11,000
7	FSK: 50 kbps	50,000
8-14	RFU	
15	Defined in LoRaWAN Specification	

Table 1: LoRaWAN DRs for the EU868 band

The application payload for the lowest data rates is limited both by the FCC to a maximum of 11 bytes per packet in the United States of America and by the ETSI to a maximum of 51 bytes per packet in Europe. For the highest transmission rates, the application payload can reach up to 222 bytes.

There are several transmission powers defined in the standard. The transmission power is ERP dependant and therefore adjusted accordingly to comply with the established maximum ERP. For the European band EU868, the transmission powers available and the corresponding value of the TXPower parameter are defined in Table 2.

TXPower	Transmission Power (ERP)
0	Max ERP
1	Max ERP – 2 dB
2	Max ERP – 4 dB
3	Max ERP – 6 dB
4	Max ERP – 8 dB

TXPower	Transmission Power (ERP)
5	Max ERP – 10 dB
6	Max ERP – 12 dB
7	Max ERP – 14 dB
8-14	RFU
15	Defined in LoRaWAN Specification

Table 2: LoRaWAN TXPowers for the EU868 band

3.3.2 Use Cases

LoRaWAN is a protocol and architecture which was designed for its use with the LoRa PHY Layer in IoT wide-area low-power wireless network communications. Some examples of possible implementations are process monitoring in industrial and construction environments, temporal deployment of sensors, smart cities, agricultural automation, etc.

3.3.3 Usage, Availability and Cost

As already stated in the LoRa section, the combination of the LoRa physical layer and LoRaWAN network architecture and protocol has already been deployed in multiple regions. LoRaWAN gateways are available from hundreds of euros in components using a Raspberry Pi [5] to thousands of euros for ready-to-use multichannel equipment rated for exterior use [6].

3.4 IEEE 802.11AH (WI-FI HALOW)

IEEE 802.11ah is an amendment to the IEEE 802.11 (Wi-Fi) standard. It enables devices with new power-saving and advanced contention avoidance techniques. One of the drawbacks of this standard against others available such as Zigbee is the lack of products in the market, even a year after the official release of the standard.

3.4.1 Technical Overview

The IEEE 802.11ah PHY and MAC layers conform a low power, low data rate communications networking solution designed for the growing need of M2M (Machine to Machine) and IoT communications [9]. It is one-hop capable and each AP can manage up to 8,191 hierarchically organized devices. It operates in sub-GHz unlicensed bands, such as the 915 MHz and 868 MHz bands. The devices connected to an AP are sorted in groups, therefore supporting a larger number of stations than other IEEE 802.11 networks.

The PHY layer of the IEEE 802.11ah standard is a sub-GHz version of the PHY layer found on the IEEE 802.11ac. The MAC layer incorporates most of the main IEEE 802.11 characteristics, adding extra power management mechanisms [10].

The frequency spreading and division modulation technique used in IEEE 802.11ah is OFDM, as in all the other IEEE 802.11's PHYs. The use of a spread spectrum technology gives the IEEE 802.11ah the possibility to use a 2.8% duty cycle [11] in the aforementioned sub-GHz frequency bands, instead of the 1% duty cycle that would be enforced in some countries with the use of a UNB technology.

The transmission rate can be configured up to 347 Mbps (with four spatial streams), while the maximum packet sizes are 7,991 bytes for a single packet and 65,535 bytes for an aggregated packet.

When compared with LoRa and Sigfox, IEEE 802.11ah outperforms them in terms of data rates and therefore network capacity in exchange of a lower range.

3.4.2 Use Cases

The main application for IEEE 802.11ah is IoT communications in a domestic environment, but it could also be expanded for its use in Smart Cities to handle sensors and devices of all kinds thanks to its medium-high range, capacity of devices and sectorization capabilities. Another possible usage outside of the home IoT is to communicate the non-mission-critical, temporal or static sensors in an industrial environment.

3.4.3 Usage, Availability and Cost

There is a limited diversity of transceivers available in the market by 2017, although there are multiple designs being discussed [12], and the interest shown by the industry in the standard is not very high. Its cost, if mass produced, could fall between the cost of a LoRa/SigFox transceiver and the cost of an IEEE 802.11n transceiver.

3.5 GSM (EC-GSM-IoT)

Extended Coverage GSM (Global System for Mobile communications) for IoT is a wireless communications solution to provide IoT LPWAN communications in countries where LTE is not widely available [13]. The existing communications equipment (cellular towers) can add this functionality with a software update, enabling IoT communications without expensive deployments. The technology is designed so that it can coexist with other 2G, 3G and 4G networks.

3.5.1 Technical Overview

The technical specifications, as per the release 13 of the GSM specifications by the 3GPP standardization group, are as follow:

- This type of network has a star topology, where end nodes (mobile stations) only communicate with their assigned cellular base station (and with others for handover) and the cellular base station only communicates with the end nodes (via radio). The base stations then communicate with the backend of the network, which has servers that orchestrate their behaviour.
- EC-GSM-IoT works in the same frequency bands as other GSM networks, sharing resources with them. The modulation schemes used are either GMSK and 8PSK over either a Time Division or a Frequency Division Multiple Access (TDMA, FDMA).
- The peak data rates achieved with the use of GMSK (Gaussian filtered Minimum-Shift Keying) and 8PSK (Phase-Shift Keying) modulations are of 70 kbps and 240 kbps respectively, when using a 200 kHz bandwidth per channel. The latency varies from 700 ms to 2 s.
- The power classes available are both the 33 dBm (2 W) power class and the 23 dBm (200 mW) power class.
- For the 33 dBm power class, the link budget available, as described per the 3GPP association, is of 164 dB, and for the 23 dBm power class it is of 154 dB. There is a 10 dB difference between the link budgets due to a 10 dB difference in the transmission power.
- New extended times for the DRx (Discontinued Reception) have been added, the new options are called eDRx (extended idle-mode Discontinuous Reception). The new eDRx

allows the devices to sleep longer times (so that energy can be saved) by avoiding unnecessary transmissions.

Due to the high-power consumption needed in EC-GSM-IoT to achieve link budgets similar to those of LoRa and Sigfox, the technology could have a higher impact in battery life depending on the implementation.

3.5.2 Use Cases

The technology is still in its development and beta deployments stage. Due to this, there are not any real-world applications yet. However, according to the 3GPP [14], the main sectors where this technology would prove useful are:

- Industrial: processes and safety monitoring, machinery control, vending machines alarm and age verification.
- Smart City: monitoring of parking spaces to report availability of spaces, monitoring of waste containers to optimise waste collection and management of traffic lights.
- Agriculture: stock tracking (animals, chemical products, etc.) as well as soil and weather monitoring of the fields.
- Consumer: the technology proposed in this section can also be used in consumer equipment as wearables, smart appliances, smart bicycles (for location services), etc.

3.5.3 Usage, Availability and Cost

EC-GSM-IoT has been developed with one feature in mind, and that is economic viability in developing countries. Therefore, the technology can run in already deployed GSM (2G) infrastructure. To allow for its implementation, manufacturers must issue a software update to their equipment which telecom providers have to apply to their deployed equipment to enable the feature. All of this should result in affordable IoT communications.

3.6 LTE CAT M1 & NB1

LTE Cat M1 and LTE Cat NB1, part of the LTE (Long Term Evolution) Standard [15], are designed with IoT devices in mind. LTE Cat M1 is designed to use the already available infrastructure and bands (as EC-GSM-IoT), while LTE Cat NB1 needs additional infrastructure and bands. LTE Cat NB1 (previously known as NB-IoT) is already available in some parts of Spain, as part of Vodafone Group's telecommunications network.

3.6.1 Technical Overview

LTE networks present a star topology where end nodes (mobile stations) only communicate with cellular base stations and cellular base stations only communicate (via radio) with end nodes. Base stations also communicate with the backend of the network, which has servers that orchestrate their behaviour. This architecture presents similarities to that of EC-GSM-IoT.

When compared with LTE Cat 1 (one of the first LTE categories, designed for high speed communications), LTE Cat M1 provides a 15 dB increase in the link budget, moving from 140.7 dB to 155.7 dB, while maintaining the power consumption of LTE Cat 1. A further increase in link budget is seen in LTE Cat NB1, reaching a class-leading 164 dB link budget, like the GSM-based solution EC-GSM-IoT, but with a power consumption reduced by 10 dB.

LTE Cat M1's upload and download data rates peak in 1 Mbps, while Cat NB1 achieves speeds of up to 50 kbps for both upload and download transmissions according to 3GPP's NB-IoT standard.

Transmission power for both LTE Cat M1 and LTE Cat NB1 peaks at a maximum of 23 dBm. This maximum transmission power is the same as that of LTE Cat 1.

3.6.2 Use Cases

LTE Cat M1 and Cat NB1 allow for similar uses as EC-GSM-IoT, but with the inclusion of some other use cases where a lower power consumption or a higher data rate, with the same range of operation, are needed.

One usage for LTE Cat NB1 is sensors which run on batteries, as parking sensors, pollution sensors, wind sensors, etc. These sensors can be found in Smart Cities.

Another usage for LTE Cat M1 is connecting wearables with voice call capabilities. This is enabled by LTE Cat M1, as it offers native support for VoIP. It also offers higher data transfer speeds than Cat NB1, which is beneficial when downloading data containing images, as notifications or navigation data.

3.6.3 Usage, Availability and Cost

LTE's IoT categories have been designed to compete with technologies like RPMA, Sigfox or LoRa in developed countries. Its implementation cost is higher than that of 2G solutions as EC-GSM-IoT, but they benefit from relying on newer technologies as LTE, that will not be deprecated as soon as 2G technologies, which will be soon replaced by 5G. Another key benefit is the higher link budget per power ratio, which enables longer range with less power. These technologies are already being deployed in some European countries as Spain.

3.7 SIGFOX

The SigFox network provides IoT devices with a low-power low-speed data connection in selected countries around the world. It is a private-initiative paid public-access network. Apart from its own deployments, SigFox licenses other companies (operators) to provide coverage in countries that they do not reach with their own.

The SigFox network protocol and architecture presents some similarities with LoRaWAN. However, contrary to LoRaWAN, it is a proprietary public access network that cannot be used for private LAN networks.

The SigFox network uses ISM bands to communicate, employing the 868 MHz band in Europe and the 902 MHz band in the US.

3.7.1 Technical Overview

Sigfox uses D-BPSK (Differential Binary Phase-Shift Keying) UNB (Ultra Narrow Band) modulation in both uplink and downlink transmissions. The bitrate of its transmission can be either of 100 bps or 600 bps, depending on the region of operation. Accordingly, the bandwidths with a 1 Hz per bit spectrum utilization are 100 Hz and 600 Hz respectively.

As Sigfox uses an UNB radio technology, it is very resistant to in-band interferences generated by other transmissions. This is due to the concentration of all the TX power in a very small bandwidth. In ideal conditions, the maximum sensitivities (BS) are -142 dBm for 100 bps and -134 dBm for 600 bps. This results in a maximum link budget of -163.3 dB when transmitting at a rate of 100 bps with an EIRP (Effective Isotropic Radiated Power) of 16.15 dBm, antenna gains of 2.15 dBi and 5.15 dBi in the device and base station respectively, a receiver sensitivity of -142 dBm and a transmission power of 14 dBm. The calculation of the link budget is given in the equation (2).

$$Link\ Budget = P_{Tx} + G_{TX} + G_{RX} - S_{RX} \quad (2)$$

$$LB = 14\ dBm + 2.15\ dBi + 5.15\ dBi - (-142\ dBm) = 163.3\ dB$$

On the one hand, uplink (MS to BS) messages are of a maximum length of 26 bytes, conformed by a 14 bytes protocol header and a 0, 4, 8 or 12 bytes user data payload. A payload of 0 bytes is used as a heartbeat. The current Sigfox regulation limits the amount of uplink packets to a maximum of 140 messages per day. These messages are usually sensor information.

On the other hand, downlink (BS to MS) messages can handle up to 8 bytes of user data. The current Sigfox regulation limits the amount of downlink packets to a maximum of 4 messages per day. These are usually control messages issued by the owner or operator of the devices.

The architecture is composed by 4 types of devices:

- The Objects, which are the sensors or devices that communicate messages through the network, like the end nodes in the LoRaWAN architecture.
- The Sigfox stations, which are the gateways that connect the objects to the Sigfox cloud through an IP network (the Internet).
- The Sigfox cloud servers, which act as the routers of the network, redirecting all the traffic sent by the objects and received by the gateways to the Customer's IT servers. The same happens for the packets sent by the Customer's IT servers, which are redirected to the corresponding Object through a Sigfox station. The cloud servers are also responsible for the coordination of the network.
- The Customer IT servers, which are the application servers that collect and process the data sent by the objects. They are also in charge of controlling the objects associated to them. These servers are property of the customers.

3.7.2 Use Cases

Since its creation, Sigfox has been a reference in IoT WAN communications and has been deployed (at least partially) in many developed countries (especially European countries). The applications range from smart irrigation in the agricultural sector to predictive maintenance in the industrial sector. There are also solutions for smart cities as traffic lights management and many others.

3.7.3 Usage, Availability and Cost

Prices for communication hubs (end nodes/objects) compatible with Sigfox are as low as 20$ and provide full access to the communication capacities of the network [16].

3.8 RPMA

RPMA (Random Phase Multiple Access) is a communications solution (PHY, protocol and architecture) provided by Ingenu, Inc which claims to provide a much better coverage and several times the capacity that other LPWAN technologies being sold, as LoRa or SigFox offer. The company also states that *RPMA "is far more efficient than cellular technologies and, therefore, a better return on investment is expected".*

3.8.1 Technical Overview

The RPMA network, as many other networks discussed in this document, presents a star topology [17], where end nodes only communicate with the base station and the base station only communicates (via radio) with the end nodes. The base stations or gateways then communicate with the backend of the network, which has servers that orchestrate their behaviour.

The spreading technique used by RPMA is DSSS (Direct-Sequence Spread Spectrum), which allows it to use up to a 100% duty cycle in the 2.4 GHz band of operation, leaving as the only band restriction the EIRP, dependent on the region of operation. Another advantage of using the 2.4 GHz ISM band is that it can be used worldwide, as opposite to other sub-GHz bands, whose allocation is region and country dependant. However, this comes at the cost of higher losses with the distance and lower obstacles penetration.

The main advantage of the RPMA technology is its capacity. The total PHY throughput of an RPMA tower (base station) is shown in Table 3.

Region	Uplink (MSs to BS)	Downlink (BS to MSs)
America, Australia	445,217 bps	122,880 bps
EMEA	222,609 bps	61,440 bps

Table 3: PHY Uplink and Downlink capacity of a single RPMA tower

After the MAC layer overhead is applied, RPMA's throughput values are reduced to the values given in Table 4.

Region	Uplink (MSs to BS)	Downlink (BS to MSs)
America, Australia	38,053 bps	20,480 bps
EMEA	19,026 bps	10,240 bps

Table 4: MAC Uplink and Downlink capacity of a single RPMA tower

The network capacity, in its equivalent 32 bytes packets per hour rate that can be received and sent is shown in Table 5. These numbers are much higher than those achieved with the use of other LPWAN technologies, such as LoRa or Sigfox (for single channel implementations).

Region	Uplink (MSs to BS)	Downlink (BS to MSs)
America, Australia	535,117 pph	288,000 pph
EMEA	267,559 pph	144,000 pph

Table 5: 32-byte packets per hour of a single RPMA tower

RPMA's link-budget with optimal conditions, maximum transmit power and highest gain antennas is of 168 dB in the EMEA and of up to 177 dB in America. This link budget is higher than those of the cellular technologies, LoRa and Sigfox, but at the expense of a higher transmission

power (20 dBm) than LoRa and Sigfox and higher computational cost, due to RPMA's phase calculations.

Packet sizes range from 6 bits to 10 kbits, thanks to Ingenu's RPMA flexible packet size.

3.8.2 Use Cases

RPMA is clearly intended for LPWAN operator use. Its high device count capabilities and its relatively high data rates are a must for an operator-class deployment, where millions of devices will connect to the network in a constrained space (of the size of a city). This renders it a candidate for its use in future Smart Cities and IoT networks deployment.

3.8.3 Usage, Availability and Cost

Some RPMA networks have been deployed (mostly in America), but its high scale world-wide deployment is still pending, and it is not sure that there will be any, because RPMA has not taken over its competitors in its 10 years in the market (by 2018).

Development kits are available from Ingenu, Inc. The cost of the development kits is not specified in their webpage [18].

3.9 TECHNOLOGY SELECTION

From all the technologies revised, there are only a few options that offer the possibility of a custom implementation. Also, only a few of the technologies allow for long range communications.

3.9.1 Comparison of Technologies

In Table 6 is shown a comparison between the technologies revised comparing them by range, type of network and customization options.

Technology	Range	Type of Network	Customization Options
LoRa (PHY Layer)	High	WAN or LAN	Open to Customization
LoRaWAN (MAC Layer)	High (as LoRa)	WAN	Open to some Customization
Wi-Fi HaLow	Medium	LAN	Hardware Unavailable
EC-GSM-IoT	Very High	WAN	Not Open to Customization
LTE Cat M1 & NB1	Very High	WAN	Not Open to Customization
Sigfox	High	WAN	Not Open to Customization
RPMA	High	WAN or LAN	Not Open to Customization

Table 6: Technologies Range, Network Type and Customization Options

In Table 7, there is a comparison between the different technologies reviewed in this section. It shows the differences in frequencies of operation, modulation techniques, transmission speeds, transmission powers and link budgets in their most optimal configuration. All the values provided are for the European region (for other regions, some values may change).

Technology	Band of Operation (Europe) (MHz)	Modulation Technique	Bandwidth
LoRa	169|433|868	CSS	Up to 500 kHz
LoRaWAN	868	CSS/FSK	Up to 250 kHz
Wi-Fi HaLow	868	BPSK/QPSK/16-256 QAM	Up to 16 MHz
EC-GSM-IoT	GSM freq.	GMSK/ 8PSK	200 kHz
LTE Cat M1	LTE Bands	QPSK/16-QAM	1.08 MHz
LTE Cat NB1	LTE Bands + Guard Band	BPSK(UL)/ QPSK [19]	180 kHz
Sigfox	868	D-BPSK	Up to 600 Hz
RPMA	2,400	RPMA	1 MHz

Table 7: Radio Characteristics of Evaluated Technologies

Technology	Transmission Power	Transmission Speed (per Device/Node)	Link Budget
LoRa	Up to 14 dBm	Up to 22 kbps	Up to 156 dB
LoRaWAN	Up to 14 dBm	11 kbps (LoRa) 50 kbps (FSK)	Up to 156 dB
Wi-Fi HaLow	Up to 14 dBm	Up to 347 Mbps (with 4 Spatial Streams)	Config. Dependant
EC-GSM-IoT	Up to 33 dBm	70 kbps (GMSK) 240 kbps (8PSK)	Up to 164 dB
LTE Cat M1	Up to 23 dBm	1 Mbps	Up to 155.7 dB
LTE Cat NB1	Up to 23 dBm	50 kbps	Up to 164 dB
Sigfox	Up to 14 dBm	Up to 600 bps	Up to 163.3 dB
RPMA	Up to 20 dBm	Not Specified	Up to 168 dB

Table 7 (Continuation): Radio Characteristics of Evaluated Technologies

3.9.2 Conclusion

According to the previous analysis, the only technology reviewed that is both long-range and open to customization is LoRa. Therefore, the technology chosen for the different RF studies to be conducted in this project is LoRa's CSS PHY layer.

The reason for using LoRa PHY layer instead of LoRaWAN is due to the lack of benefits of implementing the LoRaWAN MAC layer, which does not add any benefit when testing the PHY layer for its range and capacity and would only add control messages and delays that would render the experimental data less reliable.

A better solution for the experiments conducted and explained in the following chapters of this work is to implement a purpose-built MAC layer and protocol which provides of perfect control over all the radio and architecture parameters. This also makes the data valid not only for LoRaWAN implementations, but also for custom implementations such as IPv6 over LoRa and others.

However, for real-world implementations, LoRaWAN is the popular choice for all WAN telecommunications operators which decide to implement a LoRa-based public access network.

The results obtained when testing LoRa with the custom protocol, MAC and link layer designed in this document on top of it are therefore both valid for LoRaWAN implementations and for any other LoRa-based system.

Chapter 4: LoRa PHY Layer

4.1 Introduction

In this chapter, an introduction and description of the CSS modulation and its implementation on LoRa is described. The options found in LoRa's PHY and their effects in the performance of the radio interface will also be discussed.

4.2 LoRa

LoRa is the name of a CSS radio interface for IoT designed and developed by Semtech. It is based on a RADAR (RAdio Detection And Ranging) technology originally developed for military purposes (frequency modulated continuous wave RADAR), which has been adapted by Semtech to be used in Low Power Wide Area Networks (LPWAN). These networks are well-suited for their use with IoT devices given their low power requirements, long reach and low data rates.

4.2.1 CSS

The Chirp Spread Spectrum modulation consists of a carrier wave which moves in frequency (like a frequency modulated carrier would do), but instead of carrying an analogic signal, it moves up and down in frequency to generate what are called up-CHIRPs and down-CHIRPs. These CHIRPs (Compressed High Intensity Radar Pulses) are used to transmit information over the channel. The chirps' duration varies depending on the spreading factor in use.

4.2.2 Options

In the following subsections, the different configurations of the LoRa radio will be described and their effect in the performance of the transmissions in terms of range and speed will be defined.

4.2.2.1 Spreading Factor

The implementation of CSS by Semtech uses the aforementioned CHIRPs to send data over the air. The air-time of the chirps depends on the spreading factor in use. The spreading factors are represented by a number ranging from 6 to 12 (availability for LoRaWAN is country-dependant) which relates to the duration of the chirps in an exponential way. The rate at which the symbols (CHIRPs) are produced is shown in equation (3), where SR (Symbol Rate) is the rate at which symbols are sent, BW is the bandwidth selected for the system and SF is the spreading factor of choice.

$$SR = BW/(2^{SF}) \tag{3}$$

The higher the SF, the more reliable the transmission will be (more resistant to noise), and the lower the SF is, the higher the data rates achieved.

4.2.2.2 Bandwidth

The bandwidth of LoRa transmissions can be set to many values, being the most common ones: 125 kHz, 250 kHz and 500 kHz. The bandwidth can also be set to lower values as 62.5 kHz, 20.8 kHz and 10.4 kHz, but their use is not recommended due to the tight tolerances needed for their proper function. This can be solved by using a precision frequency reference for bandwidth values below 62.5 kHz.

If LoRaWAN is used, the availability of each bandwidth will depend on the spreading factor selected and the region of operation. The bandwidth defines the width of the frequency channel where the chirps are generated.

The higher the bandwidth, the higher the data rates. The lower the bandwidth, the higher the range.

4.2.2.3 Bands of Operation

The LoRa radio has two main bands of operation: the 900 MHz band for the US and the 868 MHz band for the EU. In this document, given the location of the experiments (in Spain, Europe), the working band will be the 868 MHz ISM band. There are also other bands available in European space as shown in Figure 1, as the 433 MHz and 169 MHz frequency bands.

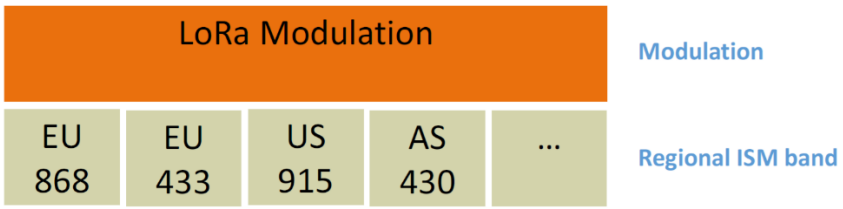

Figure 1: Lora Bands by Regions

In Table 8, the channels available for use in the 868 MHz ISM band are shown. In all but the last two channels, the separation between the centre frequencies of adjacent channels is of 30 kHz.

Channel Number	Centre Frequency
CH_10_868	865.20 MHz
CH_11_868	865.50 MHz
CH_12_868	865.80 MHz
CH_13_868	866.10 MHz
CH_14_868	866.40 MHz
CH_15_868	866.70 MHz
CH_16_868	867 MHz
CH_17_868	868 MHz

Table 8: LoRa Channels available in the EU868 band

4.2.2.4 Duty Cycle

The EU 868 MHz ISM band limits the air-time of devices using certain radio modulation technologies to guarantee the usability of the frequency spectrum, as excessive usage of some frequency bands by some devices may render these bands almost unusable for other devices, as collisions would occur too often.

Each sub-band in the 868 MHz band has its own duty cycle and ERP limitations [20], and, as seen in Table 9, they range from 0.1% to 10% of air-time, depending on the frequency of operation (and therefore, channel). This means that the channel can be occupied 0.1% to 10% of the time, depending on the frequency sub-band.

Lower Frequency	Higher Frequency	Duty Cycle	Maximum ERP
865.0 MHz	868.0 MHz	1%	25 mW – 14 dBm
868.0 MHz	868.6 MHz	1%	25 mW – 14 dBm
868.7 MHz	869.2 MHz	0.1%	25 mW – 14 dBm
869.3 MHz	869.4 MHz	-	10 mW – 10 dBm
869.4 MHz	869.65 MHz	10%	500 mW – 27 dBm
869.7 MHz	870.0 MHz	1%	25 mW – 14 dBm

Table 9: Duty Cycle and ERP for the EU868 sub-bands

The duty cycle represents the percentage of the time that a device can be transmitting in a given sub-band in the period of an hour. In the experiments conducted, conformance with this regulation is not mandatory, speeding up the tests hundreds of times.

The duty cycle only applies if the medium access algorithm used does not comply with the LBT (Listen Before Transmitting) and AFA (Adaptive Frequency Agility) rules.

The duty cycle has no effect in both the data rate nor the range of the LoRa radio. However, the duty cycle limits the length of the transmissions and the air-time.

4.2.2.5 Tx Power

In the EU, the maximum transmission power for a given device on a given frequency band and sub-band is either defined by the ERP or the EIRP. The EIRP accounts for the maximum power density emitted by the device (antenna) in the direction of its strongest beam. It represents the power needed to radiate the same amount of energy in that same direction by an isotropic antenna. Therefore, a device with an omnidirectional antenna can set its transmission power to a higher setting than another device with a directional antenna. The ERP is identical but considering as a reference a half-wave dipole antenna instead of a theoretical isotropic one.

For LoRa's CSS modulation, EU regulation specifies a maximum ERP of 14 dBm. It also specifies a maximum transmitted power of 14 dBm. Is because of this that the most common antenna configuration (and the one used in this project) is an omnidirectional half-wave dipole antenna. With this configuration, 14 dBm of transmission power can be used in the 868.0 MHz band which is the one used in the experiments.

The higher the Tx Power, the higher the link budget and, therefore, the higher the range.

4.2.2.6 Polarization Inversion

There is a mechanism built into LoRa's radio to avoid end nodes receiving other end nodes' transmissions and to avoid gateways listening to other gateways' transmissions. It can be activated in the radio via an option called polarization inversion. This feature reverses the polarization of the CHIRPs so that the messages sent by a given device will not be detected by those devices which do not share the same polarization inversion settings.

This solution is usually implemented (as in LoRaWAN) by activating the polarization inversion either on the upload or on the download as shown in Table 10, so that when a device transmits a packet, the devices with the same configuration (from the same group) can neither receive nor detect that packet.

Device	Upload (transmission)	Download (reception)
Node	Normal Polarization	Inverted Polarization
Gateway	Inverted Polarization	Normal Polarization

Table 10: Polarization Inversion in LoRaWAN

The polarization inversion has no effect in both the data rate nor range of the LoRa radio.

4.2.2.7 PHDR

The physical layer header contains information about: the length of the physical layer payload, the presence of a 6-bit CRC for the payload and the coding rate in use on the rest of the packet. This header may or may not be transmitted depending on the mode of operation of the radio. There are two operational modes available: explicit mode and implicit mode.

In explicit mode, the PHDR is transmitted and, therefore, the receiver of the message does not need to know the length of the payload, its coding rate and the existence of a PHY payload CRC beforehand.

In implicit mode, the PHDR is not transmitted and, therefore, the receiver must know the coding rate, the length of the packet and the existence of a PHY payload CRC beforehand for the correct reception and decoding of the packet.

4.2.2.8 Preamble

The purpose of the preamble is to detect a transmission and synchronise the receptor to the transmitter. In LoRa, the preamble's length can be set through a radio option to values ranging from a length of 0 (+4.25) symbols to 65535 (+4.25) symbols. There are 4.25 symbols whose transmission is mandatory and are omitted in the number giver to the radio. This mandatory part is composed by 2 up-chirps followed of 2 down-chirps and finalizes with ¼ of an up-chirp.

A longer preamble can increase the detection rate of a packet for long distances.

4.2.2.9 Coding Rate

Apart from the spreading factor, transmit power, and bandwidth, LoRa has yet another mechanism to cover long distances. The Coding Rate or CR defines the proportion of the data stream that is formed by useful data and the proportion that is redundant. The redundant bits are used for Forward Error Correction with the use of FEC codes.

The data/total bit proportions available with the LoRa radio are: 4/5, 4/6, 4/7 and 4/8. The lower the proportion, the higher the redundancy, and, therefore, the probability to achieve a successful transmission.

The Coding Rate improves the reception rate for long distances, fixing errors in the message. The lower the data to bits relation, the higher the corruptions that can be corrected in the packet. However, the Coding Rate also lowers the data rate. The higher the redundancy of the FEC code used, the lower the data rate of original message data.

4.2.2.10 CRC

The use of a payload CRC (Cyclic Redundancy Code) of 16 bits (CRC16) is optional. If operating in implicit mode, this setting must be the same and known beforehand in both the receiver and transmitter in order to decode the message correctly. If the operation mode is set to explicit

and, therefore, the package header is sent, there is no need to signal the receiver (locally) whether the packet being received has a CRC or not beforehand.

The CRC does not directly vary the range of LoRa. However, it allows to detect corrupt packets which become more common with the distance.

The CRC does not directly vary the data rate at which the data is sent. However, it adds an overhead to the packet, slowing down the rate at which the packets can be sent.

4.2.3 PHY Packet

The physical layer (PHY) packet is formed by a Preamble, a header (PHDR), a CRC for the header (PHDR_CRC) and a PHY Payload (PHYPayload) with its CRC (PHYPayload_CRC). The only two mandatory fields are the Preamble and the PHYPayload.

Figure 2 shows the arrangement of the different elements in a LoRa packet, as seen in the physical layer, as well as the coding rate and SF used for each section. In the diagram, Header represents the PHDR, CRC represents the PHDR_CRC, Payload represents the PHYPayload and Payload CRC represents the PHYPayload_CRC.

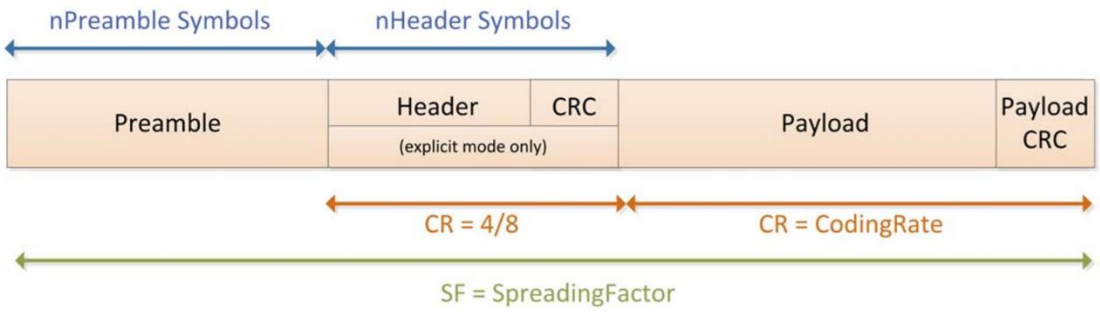

Figure 2: PHY Packet Structure

The preamble, with a length of nPreamble symbols, is not encoded with any coding rate, because it is not composed of bytes but symbols. The entire packet, including packet header and preamble is sent using the same Spreading Factor, as shown in Figure 2.

The nHeader represents the number of symbols that the combination of the Header (PHDR) and CRC (PHDR_CRC) represent.

4.2.3.1 Preamble

The preamble is a mandatory field used for both detection and synchronization with the transmitter. The configurable length of this field of the physical layer ranges from 0 + 4.25 symbols to a length of 65535 + 4.25 symbols.

4.2.3.2 PHDR

The PHY header is optional and will only be sent in the explicit mode of operation, as mentioned before. The length of the header is fixed to 20 bits (counting the extra bits of the coding rate; without the coding rate the length would be of 10 bits). The coding rate used for this field's transmission is always the most reliable setting (4/8) to ensure a correct reception.

4.2.3.3 PHDR_CRC

To ensure the integrity of the header, a CRC of 6 bits (PHDR_CRC) is added following the PHDR. This CRC is not transmitted in Implicit mode, where the PHDR is eliminated.

4.2.3.4 PHYPayload

The PHYPayload could be defined as the data being carried by the physical layer (our application data per se). This is the data that can be modified by the device controlling the transmitter's radio and is also the data that will be forwarded to the device controlling the receptor's.

The length of the PHYPayload can take values ranging from 1 to 255 bytes. Depending on the spreading factor in use, its length should be limited to low values to ensure a correct reception. The LoRaWAN alliance has made a recommendation regarding its length for its use with LoRaWAN's protocol stack.

4.2.3.5 CRC

The last part of the physical packet is the payload CRC (PHYPayload_CRC). This is a 16 bits CRC made from the data sent in the PHYPayload field. Its inclusion is optional, but it is recommended in order to help detect whether a transmission has suffered any corruption.

Chapter 5: RELATED WORK

5.1 PREVIOUS RESEARCH

The research in the field of the LPWANs and IoT is mainly advancing in the direction of Smart Cities, where studies as the research work found in [21] try to evaluate the performance of a LoRa network in a Smart City scenario, achieving a 95% PoS (Probability of Success) in the transmissions. This work was conducted in a simulated environment (with the network simulator ns-3).

In other papers, instead of simulating the results that an implementation would present, a real environment is considered, as in [22], where a pilot implementation of a LoRa Smart City sensor network is designed and deployed in the Italian city of Bologna. Different sensors, measuring parameters such as CO2 and temperature were deployed. The results obtained with this scenario are then introduced in a simulator to guess the performance and coverage that such a network would present if expanded to a whole city.

Research on channel models for Smart Cities with empirical measurements (instead of simulations) has been conducted in paper [23], where the performance of LoRa in both the 868 MHz and 433 MHz European bands is analysed and measured, achieving communications with distances of up to 5.8 km in a Smart City scenario in the area of Dortmund, Germany. However, this study could benefit from more samples in different scenarios that better represent not only the core of a Smart City but its surroundings. This is one of the issues referred to at the end of this section.

In relation with the uses of the LoRa technology, paper [24] studies the possible uses of the LoRa communications technology in a Smart City scenario. The application proposed is to provide remote sampling of electricity metering measurements via a LoRa network for smart meters such as those already installed in Spain and many other countries.

To enable deployments that allow connecting thousands of devices with a single network, as the ones found in a Smart City scenario, the devices need a robust networking layer that allows routing a high number of devices and that offers a great compatibility with other Internet-based devices and services.

To deal with these scenarios, paper [25] tries using IPv6 over LoRa. In it, a basic IPv6 communications scheme over LoRa is successfully implemented with the use of Contiki OS. This system is also later implemented in Zolertia's Re-mote devices.

Referring to the use of IPv6 over LoRa, another research [26] focuses on the use of IPv6 over LoRa for IoV (Internet of Vehicles). In this case, the researchers use datagram compression schemes to fit IPv6 packets in a LoRa transmission. They also implement the system in an experimental (non-simulated) test-bench obtaining great results.

Other studies centre their work on the deployment and implementation of LPWAN technologies. For instance, in [27], the subject of the paper is the use of cable-less deployments to reduce installation costs. This goal is achieved with the use of renewable energy (photovoltaic) and a wireless backhaul to support the gateway's connection to the Internet. The paper is mainly focused in the cost-saving optimization of the system.

Reference [28] also focuses in the wireless (cable-less) LoRa deployment, by using a wireless backhaul for the LoRa network using a GPRS data connection. The devices in this paper are also self-powered, being therefore, a cable-less deployment.

About the adoption of LoRa in smart campus and smart city scenarios, in [29] researchers present a LoRaWAN demonstrator at the Scientific Campus of the University of Lille. The In-Campus tests carried out show the capability of LoRaWAN to provide a good coverage of the campus in both indoors and outdoors environments. However, this study lacks the investigation of both the packet success rate and capacity of the system. It also lacks the study of the performance of the network in open environments which may be found in a Smart City. These are some of the issues to be covered with the tests carried out in this work, as explained at the end of this section.

Most of the papers available talk about the performance of the LoRa network based on the performance shown in a simulation. In this work, the performance of LoRa in different scenarios which can be found in a Smart City and its surroundings will be measured with empirical experiments, to measure real-world performance.

The work will also centre in improving the weaknesses found in the measurements and technique used in related research works, as the ones described in this chapter.

5.2 CONCLUSION

Based on all the papers reviewed –which show how the experimental studies are usually conducted–, as well as the topics of these studies, two categories of tests which have been found relevant to the current research have been defined:

- The first category consists of an analysis of the capacity of a LoRa channel with an experimental base. This would show the total capacity of a channel considering all the effects that both the hardware and environment have in the transmissions.
- The second category includes a series of tests that measure the effects of the distance and therefore path loss in multiple scenarios, which cover Smart City scenario (measured in a Campus) and Open Environments which are measured in an agricultural environment.

Chapter 6: DEVICES SELECTION

6.1 MARKET ANALYSIS

With the radio interface already chosen, the next step was to select the devices to use in the experiments. These devices must have the capabilities necessary to carry out the intended tests and, at the same time, should be reasonably priced.

The devices must have at least a LoRa PHY radio interface built-in and a secondary interface (either included or available) through which an out-of-band management connection can be established. The devices included in the comparison are shown in Table 11.

Product	Underlying Platform	Programming Language	Unitary Price (by 11/06/2018)
LoRa shield for Arduino (Dragino or Adafruit)	Arduino	Arduino Language (C++ based)	17.02€ + Arduino + Wi-Fi
Microchip's LoRa Evaluation Kit	None	All (Windows)	426.44€
Libelium-Multitech-Loriot Development Kit	Libelium	All (Linux)	5,500.00€
Pycom's FiPy	None	µPython	54€+Board

Table 11: Devices Comparison by Price, Programming Language and Unitary Price

The first option to evaluate is the LoRa shield for Arduino, which needs both an Arduino to be controlled and an additional Wi-Fi shield which would provide the out-of-band management channel. The total price for this combination would be of 50€.

The second option is the LoRa evaluation kit from Microchip. This kit has a cost of 426.44€ for a gateway and 3 motes (devices). The capabilities of the gateway included are not those of a multiband gateway that would be used in an operator-class deployment, but it would still be a good start for an IoT project.

The third option is the Libelium-Multitech-Loriot kit. This development kit is based on Linux, which leaves to the user the task of choosing the programming language. It has great capabilities and would be a good choice if it weren't for its price of 5,500.00€ for 3 devices which is too expensive to be justified by its expansion capabilities.

The last device in the comparison is Pycom's FiPy. This device is based on the MicroPython programming language and has many built-in connectivity options, such as LoRa, SigFox, Bluetooth, Wi-Fi and 4G. As it is reasonably priced and integrates all the connectivity needed in a tiny package, this device is the one chosen for the realization of the experiments in this work.

6.2 DEVICES CHOSEN

After the market research and posterior product analysis, Pycom's FiPy along with Pycom's Pysense and Pytrack expansion boards remained as the products chosen. An antenna from the

same manufacturer (Pycom) was also bought for every device, as onboard 800 MHz antenna for LoRa is not included.

6.2.1 Pycom FiPy

As previously stated, after searching the market for development kits and devices to test LoRa's capabilities, Pycom's FiPy resulted the device chosen. Five units of this model were bought: one to be used as a gateway and four to be used as end nodes.

Pycom's FiPy has five communication modules built-in, and, as shown in Table 12, some of them are equipped with on-board ceramic antennas and others with external antenna options.

Technology	Antenna	Characteristics
Wi-Fi	Internal or External	Up to 1 km.
Bluetooth	Internal or External	Only Bluetooth Low Energy (BLE) implemented. Bluetooth Classic to be implemented in the future.
LoRa	External	LoRaWAN and RAW LoRa compatible
SigFox	External	Full Compatibility
LTE	External	Cat M1 and NB1 compatible (only NB1 currently implemented)

Table 12: Communication Modules of Pycom's FiPy

The programming language for the FiPy is MicroPython, a minimalistic implementation of Python, with some embedded systems' functionality implemented through the "*machine*" class.

These devices need an expansion board to provide both power and a programming interface. The expansion board may also provide some enhanced features, such as but not limited to GPS, microSD card slot and sensors.

6.2.2 Pycom Pysense and Pytrack

To provide power and some extra functionalities to the Pycom FiPy devices, there is a range of boards available. The ones chosen for their interest are the Pysense and the Pytrack.

The features of the Pysense expansion board, as shown in Table 13 are: providing power management capabilities with micro USB and battery options as well as a serial connection to an external programmer through the USB port (usually a computer); it also provides some sensors and a micro SD slot to store information in and read from it.

Features
USB Serial interface
Battery Charger
Micro SD card reader
Dual Light Sensor
3 axis Accelerometer
Humidity Sensor
Barometric Pressure Sensor
Temperature Sensor

Table 13: Features Available in Pysense Board

The features of the Pytrack, as shown in Table 14, are very similar to those of the Pysense, lacking a few sensors while gaining a GPS module (Queltec).

Features
USB Serial interface
Battery Charger
Micro SD card reader
3 axis Accelerometer
GPS module (GNSS + Glonass)

Table 14: Features Available in Pytrack Board

6.2.3 Antenna

The antenna selected for the application is a half-wave dipole (2.15 dBi), which provides omnidirectional coverage in the horizontal plane (when oriented vertically). The frequencies suitable for reception with this antenna are both the EU 868 MHz and the US 915 MHz bands. Both the gateway and nodes will implement this antenna during the realization of the experiments.

This antenna was chosen following the recommendation of the manufacturer, which sells this antenna to accompany their devices. The need for an omnidirectional radiation pattern comes from the need of a homogeneous coverage of the horizontal plane.

Chapter 7: MAC AND LINK LAYER DESIGN

7.1 INTRODUCTION

Once the physical interface was chosen (LoRa), a MAC and link layer (OSI Layer 2 - Data link layer) needed to be designed. The options were either to use the LoRaWAN architecture and MAC or to create a new one from scratch. As the control over the packets sent had to be very precise and the packets had to be as small as possible for some of the planned tests, the best option was to design a custom MAC layer/transport protocol.

7.2 FIRST STEPS

The first steps involved in the design of a MAC and link layer are to define the needs of the design in terms of capacity, QoS, acknowledge, optional fields, etc. The constrains of the PHY layer also need to be considered, as the maximum packet size or the duty cycles of the band.

7.3 REQUIREMENTS

After designing the experiments, the requirements for the MAC and link layer are based on the needs of the tests. The requirements for the MAC and link layer are:

- A device identifier to know which device sends the packet in the laboratory capacity experiment.
- A transmission timestamp for all the packets.
- A first transmission timestamp for confirmed packets.
- A sequence number to confirm packets and to keep track of the packet number for statistical and QA (Quality Assurance) purposes.
- A payload to adjust the air-time of the transmission to the desired.
- A code to identify packets which are sent by our devices.
- A code to identify which kind of packet is sent.

7.4 RESTRICTIONS

Having chosen the LoRa PHY radio interface, the restrictions are set by that choice. The main constrain is the maximum packet length that the radio can handle. As the PHY Payload length is represented by a byte, the maximum length of this payload is 255 bytes. The PHY Payload cannot be empty (size 0). With these restrictions, a base is set for the design. The maximum length of the MAC payload will be set accordingly in every packet type to comply with the radio restrictions.

7.5 STRUCTURE

The packet will include a series of fields based on both the requirements and restrictions defined. Other fields will be added as well to obtain a functional MAC and link layer. In the next subsections, the structure, divided by PHY and MAC layers, is represented.

7.5.1 PHY

The physical layer is defined by the LoRa specification and it presents the structure shown in Table 15. As explained in the LoRa section of this document, the Preamble is used to detect a

packet and to synchronize the receptor, the PHDR contains information about the length and coding rate and the CRC serves to check for corruption in the data.

Preamble	PHDR	PHDR_CRC	PHYPayload	CRC
-	-	-	1-255 Bytes	2 Bytes

Table 15: PHY Structure of a LoRa Packet.

7.5.2 MAC and Link Layer (PHYPayload)

The MAC and link layer is designed to provide all the requirements and to fit all the restrictions. It can be divided in two parts: the mandatory part, which all the packets with this MAC layer must have, and the optional fields, which only the packets that need them will include them.

The fields conforming the mandatory MAC Header (MAC_HDR), as can be seen in Table 16**,** are the following:

- Version_Code: A byte containing the version of the LoRa Custom MAC.
- Device_ID: A byte containing an ID unique in the network.
- MType: A byte with a code corresponding to the type of message.
- Payload_Length: A byte with the length of the Payload (0-238/243).
- Seq_Number: A short integer with a counter that increments for every packet sent by a given device.
- Tx_Timestamp: An integer with a timestamp (ms precision, cycles every 24h).

Version_Code	Device_ID	MType	Payload_Length	Seq_Number	Tx_Timestamp
1 Byte	1 Byte	1 Byte	1 Byte	Short 2 Bytes	Integer 4 Bytes

Table 16: Structure of the MAC_HDR of a LoRa Custom MAC Packet.

The fields conforming the optional MAC fields (MAC_OF), as can be seen in Table 17**,** are the following:

- Tx_Try_Number: The retry number of the transmission (for a confirmed message).
- FTx_Timestamp: The Tx_Timestamp of the first time the packet was sent (for a confirmed message).

Tx_Try_Number	FTx_Timestamp
1 Byte	Integer 4 Bytes

Table 17: Structure of the MAC_OF of a LoRa Custom MAC Packet.

7.6 PACKET TYPES

In this revision of the protocol there are 3 packet types which are assigned to a message type code. The table containing all the values that the MType field can have and their respective meaning is given in Table 18.

MType	Description
0-99	Reserved
100	ACK
101	Unconfirmed Message
102	Confirmed Message
103-255	Reserved for Future Use

Table 18: Message Types (MType) values with their Description.

In the following subsections, the unconfirmed message, confirmed message and acknowledge message types will be described, with their structure and size of the fields.

7.6.1 Unconfirmed Message (PHYPayload)

The Unconfirmed Message packet type is composed by the mandatory part of the MAC header (MAC_HDR) and the Payload, which is the data that is sent in the packet. The structure can be found in Table 19.

MAC_HDR	Payload
10 Bytes	0-243 Bytes

Table 19: Structure of an Unconfirmed Message.

The Unconfirmed Message is sent from a Node to a Gateway and does not receive an acknowledge of its correct reception.

7.6.2 Confirmed Message (PHYPayload)

The Confirmed Message packet type is composed by the mandatory part of the MAC header (MAC_HDR), the optional MAC fields (MAC_OF) and the Payload, which is the data that is sent in the packet. The structure can be found in Table 20.

MAC_HDR	MAC_OF	Payload
10 Bytes	5 Bytes	0-238 Bytes

Table 20: Structure of a Confirmed Message.

The Confirmed Message is sent from a Node to a Gateway and the gateway responds with an acknowledge of its correct reception.

This type of packet was used at the first stages of this work but was not used during the experiments. However, it is included because it might be used for experiments in future work.

7.6.3 ACK (PHYPayload)

The ACK (acknowledge) packet type is only comprised of the mandatory part of the MAC header (MAC_HDR). The structure can be found in Table 21 above.

MAC_HDR
10 Bytes

Table 21: Structure of an ACK.

It is the packet sent from a Gateway to a Node to acknowledge the correct reception of a Confirmed Message. The sequence number of the packet to which it refers is the one found in the Seq_Number field of the MAC mandatory part (MAC_HDR).

This type of packet was used at the first stages of this work but was not used during the experiments. However, it is included because it might be used for experiments in future work.

Chapter 8: PROGRAM DESIGN

8.1 INTRODUCTION

As previously stated, the development boards used are Pycom's FiPy five-network IoT development platform. The programming language used in the boards is a custom implementation of Python called MicroPython, which has a much smaller memory footprint than the original Python stack.

To configure and communicate with the radios on the devices, control libraries were provided by Pycom and embedded in the device's firmware. These libraries are supported by Semtech's low-level stack. The device's firmware of both the FiPy and the expansion boards has been periodically updated during the realization of this project, as new features were implemented by the manufacturer.

8.2 REQUIREMENTS

As the experiments required a custom MAC, protocol, testing and supervision environment, a program had to be developed specifically for the realization of these experiments.

The program had to implement the following main features:

- Access to the LoRa Radio
- An implementation of the LoRa Custom MAC and link layer
- Wi-Fi connectivity management
- NTP Time Synchronization
- MQTT Messaging Client
- NVRAM Access (R/W)
- microSD Logging
- LED Control

Apart from all the features stated, the program also had to implement several functions which would control the operative of the devices when the different experiments were running, that would allow access to the device via a control interface (MQTT) and that would log the results of the different tests to the microSD card.

8.3 PRELIMINARY DESIGN

The preliminary design of the controller program was created with the aim of testing the devices and their radios to better understand their capabilities. A first version of the control logic for the tests and an alpha version of the MAC and link layer (which did not include all the fields previously explained in the MAC and link layer design chapter) was also included in this first design.

During the development of this first program, new capabilities were added. At first, the program had only the capability to send and receive simply-formatted messages. The radio settings were hardcoded. Later, a logger was implemented to save experimental data to a microSD.

At the last steps, Wi-Fi connection was added, which led to the use of an MQTT server for logging and devices control. It also enabled the devices to synchronize their time with an NTP server to allow for precise timing in the tests.

The need for a clean and optimized code and a new MAC and link layer with many more fields to allow for further data harvesting made clear that a second program needed to be built from scratch, redesigning it for the final needs.

8.4 FINAL DESIGN

During the second design stage, the program layout was completely redefined. This second design was empowered by the knowledge gained in the first design about both MicroPython and Pycom's FiPy capabilities and limitations.

The program was divided in two parts: a main program orchestrating the execution and several custom-coded libraries to control all the components of the development board. This gives the possibility of quick changes to the behaviour of the board by simple changes in the orchestrator. A scheme of the structure can be found in Table 22.

ORCHESTRATOR
CUSTOM LIBRARIES
EXTERNAL LIBRARIES
FIRMWARE
PHY

Table 22: Second Design's Structure.

The Orchestrator only produces calls to the custom libraries and to some basic firmware utilities. The custom libraries make calls to both the external libraries and to the firmware's functions. The external libraries produce calls to the firmware and to other external libraries. The PHY layer is only controlled by the firmware. A more thorough scheme of the structure can be found in Table 23.

ORCHESTRATOR (main.py and boot.py)				
lora_util.py	general_util.py	GPS_Library.py	LED_Library.py	global_var.py
L76GNSS.py	mqtt.py	pycoproc.py	pytrack.py	
FIRMWARE (MicroPython by Pycom)				
PHY (FiPy + Pytrack/Pysense)				

Table 23: Second Design's Libraries.

The Orchestrator is the highest logical level part of the program. It contains calls to functions which carry-out high-level tasks. An example could be calling a function to recover LoRa radio config parameters from NVRAM, another to initialize the radio with these parameters and a last one sending a confirmed packet and waiting for an acknowledge.

Chapter 9: LABORATORY CAPACITY EXPERIMENT

9.1 TESTS DESIGN

The aim of this test is to find and stress the boundaries of the LoRa radio by using the Custom LoRa MAC protocol described earlier in this document. The objective is to obtain a statistic sample big enough to represent the capacity of each SF with a given number of nodes transmitting at a given rate packets of a given payload size. This will be expressed with an equation which is intended to model the results obtained with the practical tests and therefore, in a real environment, where the only factors which should have a notable impact on the results are the interferences caused between the nodes. These results are evaluated considering the PoS (Probability of Success). The losses due to signal degradation or multipath fading are not considered in this test.

9.1.1 Methodology

In this test, five devices are used: one configured as a Gateway and four as End Nodes. The packets originate from the End Nodes and are received by the gateway. The number of end nodes participating in each test varies from 1 to 4. The SF configured in the device's radios varies from 7 to 12.

The payload transported by the MAC layer is designed in each test so that the total payload sent by the PHY layer fits best to obtain equidistant values of PHY payload, ranging from 1 to 255 bytes. This is necessary to obtain a good statistical sample.

The time during which a node can transmit a message is called Slot Time. The theorical (and practical) time that takes the node to send the packet is called Guard Time. The time of propagation is excluded from the calculations given the short distance between the nodes.

The slot time or inter-packet time on which the packet rate depends, varies between batches to emulate network congestion. The time between the start of the slot and the moment when the packet is sent is randomly chosen between the specified parameters to allow for random collisions as in a real radio environment.

9.1.2 Proposed Tests

The tests are designed in a manner that obtains a good representation of the statistical distribution. To accomplish the requirements without generating a test set that would require months of testing to be completed, an equidistant choice of the values of the variables is adopted as one of the best solutions available. The choice of this variables has been done adhering to the following specifications:

- The number of nodes which participate in each test ranges from 1 to 4, in increments of 1. This value does not affect the duration of the tests or the payload carried in the packages. All combinations of nodes go through the same tests.
- The Spreading Factor ranges from 7 to 12 in increments of 1. For SF greater than 10, the low data rate optimizer bit is enabled, so this is considered for the timing values.
- The values for the payload carried by the PHY layer are chosen so that 5 equidistant values are used, ranging from 51 to 255 bytes. The mathematical operations to produce the values can be found in (4) and the values in Table 24, where Pay_{max} is the maximum PHY payload, Pay_{Part} is a fifth of Pay_{max} and Pay_x are the values for the PHY Payload, where X ranges from 1 to 5 in increments of 1. Also, MAC_{Size} is the size in bytes of the

Custom MAC header and MAC_{Pay_x} is the size of the MAC Payload in bytes. The value 0 for the payload is not used due to the restrictions of the PHY layer.

$$MAC_{Pay_x} = Pay_x - MAC_{Size}$$
$$Pay_x = round(Pay_{Part} * X) \quad (4)$$
$$Pay_{Part} = \frac{Pay_{max}}{5}$$

The values of the MAC Payload (MAC_{Pay_x}) are then selected to comply with the PHY payload chosen (Pay_x).

Value of X	PHY Payload (bytes)	MAC Payload (bytes)
1	51	41
2	102	92
3	153	143
4	204	194
5	255	245

Table 24: Values of PHY and MAC Payloads for the Different Values of X

- The values for the Guard Time are calculated from the PHY payload, Spreading Factor and message length in use following the equation (5), where Payload is the size of the PHY payload in bytes, DE is the low data rate optimize status (0 for SF{7-10}, 1 for SF{11-12}), BW is the bandwidth of the channel (125kHz), SF is the Spreading Factor and n_{Pre} is the number of symbols configured for the preamble via the radio registers (6 symbols).

  In (5), some of the values are fixed by the firmware implementation of the radio library (Pycom's implementation of Semtech's LoRa library). The value IH (Implicit Header) is set to 0 if the PHY Header is used, which in Pycom's firmware is always used. The CRC (Cyclic Redundancy Code) is set to 1 if the PHYPayload_CRC is enabled, which in Pycom's firmware is permanently in use.

$$n_{Pay} = 8 + \max\left(ceil\left(\frac{8 * Payload - 4 * SF + 28 + 16CRC - 20IH}{4 * (SF - 2 * DE)}\right) * 5, 0\right) \quad (5)$$

The Guard Time, represented by $Guard$ in (6), is the time that a device needs to transmit a message with a given length and with a given radio configuration.

$$Guard = t_{Total} = t_{Pre} + t_{Pay}$$
$$t_{Pre} = (n_{Pre} + 4.25) * T_{Sym} \quad (6)$$
$$t_{Pay} = n_{Pay} * T_{Sym}$$
$$T_{Sym} = \frac{1}{R_{Sym}}$$

$$R_{Sym} = \frac{BW}{2^{SF}}$$

- The Slot Time is obtained with an intermediate step where the maximum rate at which packets can be sent is calculated, to be used later in conjunction with the Guard Time to obtain the possible values for the Slot Time.

  The maximum rate at which packets can be sent is the inverse of the Guard Time, given that the Guard Time is the smallest time between transmissions. There is another time between transmissions not considered in these calculations called the processing time, which is necessary for the packets to be processed by the devices before they are sent. This extra time will be addressed at the implementation of the tests in the devices' firmware. The equation (7) shows how the maximum rate is calculated.

$$Rate_{Max} = \frac{1}{G_{Time}} \tag{7}$$

  To choose statistically correct values for the transmission rate, the maximum packet rate $Rate_{Max}$ is divided by 5 and the rates are chosen in increments of that rate, as found in (8), where the value X ranges from 1 to 5 to obtain 5 equidistant values for the rate.

$$Rate_X = Rate_{Max} * (\frac{X}{5}) \tag{8}$$

- The Slot Time is now calculated from the values of the Guard Time and from the different packet rates as shown in (9).

$$Slot_X = \frac{1}{Rate_X} \tag{9}$$

- The last step of the process is to convert the values of the times to millisecond precision, with the appropriate rounding criterium so that, for example, the Slot Time is never shorter than the Guard Time. The process is shown in (10).

$$Guard_{ms} = ceil(Guard * 1000) \tag{10}$$

$$Slot_{ms} = ceil(Slot * 1000)$$

9.1.3 Transmission Times

To guarantee that the transmission times are set correctly, as the manufacturer does not provide reliable information about the matter, the time that a device needs to send a specific packet is

tested and is then compared to the theorical time that it should take (as calculated in the tests planning section) with the assumed configuration.

9.1.3.1 Methodology

The first step was to calculate the transmission times of the packets. The formulas used were the same as in the previous section. These calculations were made considering the parameters in Table 25.

Variable	Value
SF	7-12
BW	125 kHz
PHY Header	Yes (Always)
CRC	Yes (Always)
Preamble	6 (+ 4.25)
DE (Low data rate optimize)	No (Never)
Coding Rate	4/5

Table 25: Preliminary Radio Configurations for the Different Tests

The theorical results for the transmission times were obtained from the equations and the experimental transmission times were obtained through a test program designed to send packets using different configurations and time their transmission time. The results, as shown in Table 26, are different for the theorical calculations with the supposed radio configuration than those of the experimental tests.

SF	Theorical (ms)		Obtained (ms)	
	51 Bytes	255 Bytes	51 Bytes	255 Bytes
7	103	400	103	400
8	185	708	185	708
9	329	1251	329	1251
10	617	2296	617	2296
11	1151	4183	1315	5002
12	2139	7709	2466	9020

Table 26: Theorical and Obtained Transmission Times for the SF and PHY Payload combinations tested

9.1.3.2 Results

When obtaining the theorical transmission times for the “low data rate optimize” parameter enabled, for both SF 11 and 12, all the theorical transmission times match perfectly with the practical ones. Then, the conclusion is that the system is using the initially supposed radio parameters plus the use of the low data rate optimization in the two lowest speed spreading factors: 11 and 12. The new configuration is in Table 27.

Variable	Value
SF	7-12

Variable	Value
BW	125 kHz
PHY Header	Yes (Always)
CRC	Yes (Always)
Preamble	6 (+ 4.25)
DE (Low data rate optimize)	Yes (SF 11 and 12)
Coding Rate	4/5

Table 27:Definitive Radio Configurations for the Different Tests

This configuration will be used for all the calculations related with the experiments and will be the reference when designing all of the experiments found in this document.

9.2 LABORATORY PREPARATION

Once the final design was chosen, as well as implemented in the boards and tested, the next step was to start conducting the laboratory tests. Therefore, the devices were then flashed and positioned in the test area.

The different tests have been classified by the number of nodes and the SF in use, resulting in a series of test batches which can be run in an automated manner. This simplifies the testing stage, keeping operator intervention to a minimum and, therefore, accelerating the process. This also allows for the execution of the programmed tests overnight.

9.2.1 Test Bench

The gateway is 2.75 meters away from the centre of the group of nodes. The nodes are separated by 25 cm between them. The diagram in Figure 3 shows the distribution with the distance between gateway (GW) and nodes.

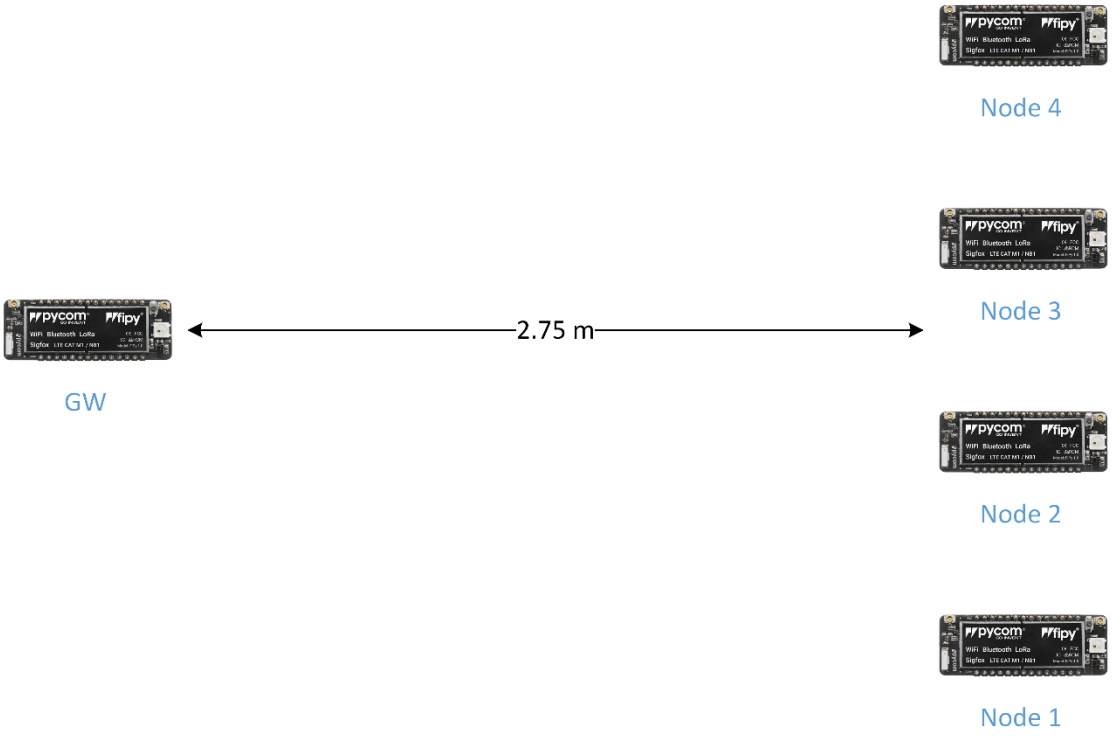

Figure 3: Diagram with the Distance between the Nodes and the Gateway

The elements that participate in the tests are: the FiPy modules with the PySense and PyTrack expansion boards, the 800 MHz half-wave dipoles, a microSD card for the gateway, batteries for power stability when connected to a power supply and the casing for the devices. All the components and their final assembly is shown in Figure 4.

800 MHz Half-Wave Dipole

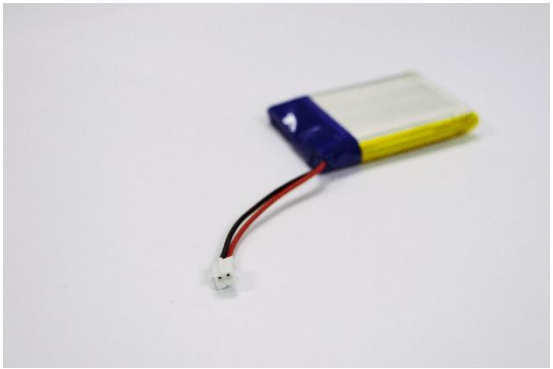

3.7 V - 1400 mAh Battery

2 Gb microSD Card

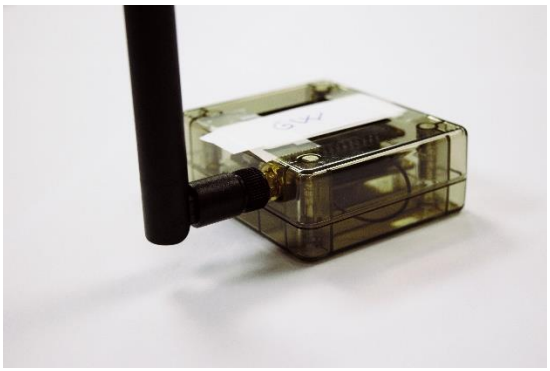

Final Assembly

Figure 4: Components of the Devices and Assembly

9.2.2 Connectivity

The devices are connected to the internet via a tailor-made Wi-Fi network provided by a TP-Link TL-MR3020 router and AP, whose internal logical architecture is shown in Figure 5. This Wi-Fi network is only used by the devices participant in the experiment to avoid incompatibility issues and congestion.

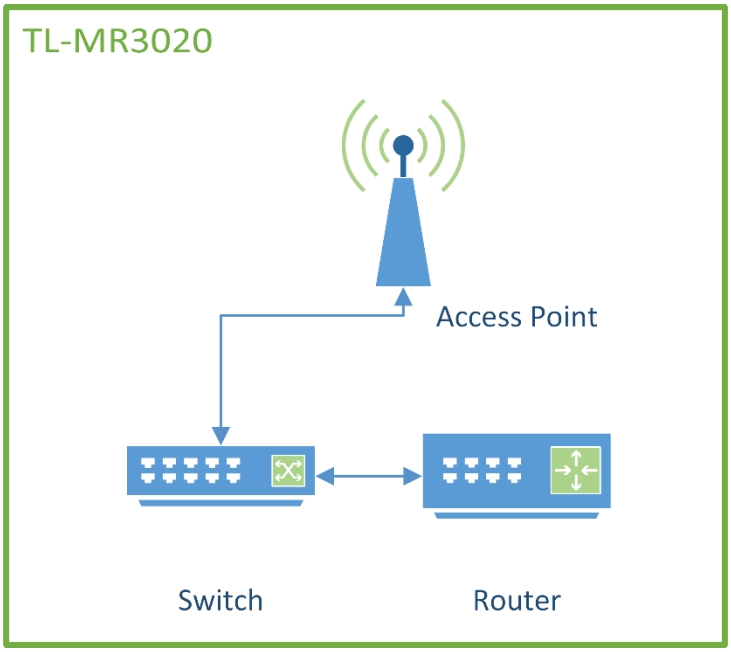

Figure 5: TL-MR3020 Wi-Fi Router Internal Components Diagram

The connection diagram between the devices (nodes and gateway) and the Internet is shown in Figure 6. The connection to the Internet is necessary for both the supervision and control via the MQTT server and the time synchronization between devices (NTP). The TL-MR3020 is connected to the Internet via the UPV wired access network.

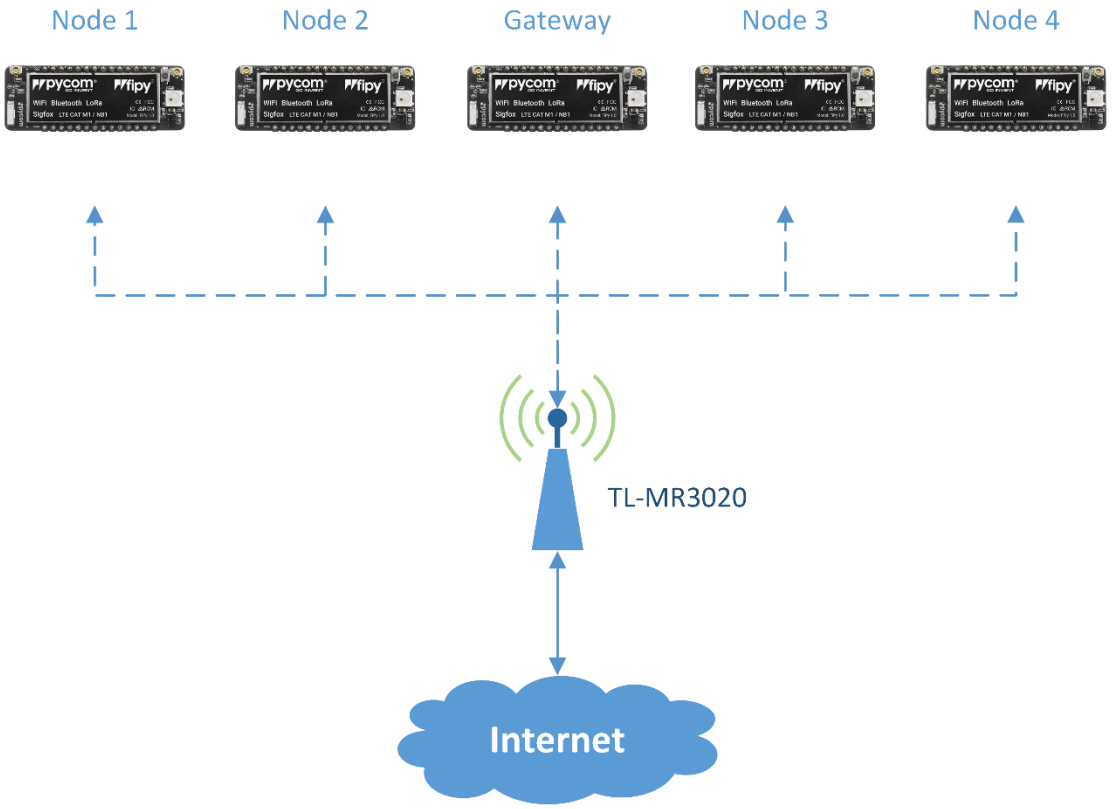

Figure 6: Devices Connection to the Internet

The LoRa connection diagram between the nodes and the gateway, as shown in Figure 7, is a one-way upload communication (nodes to gateway). This is thanks to the off-load of the management to an out-band management interface (the Wi-Fi connection). Depending on the experiment and test, 1 to 4 nodes will participate.

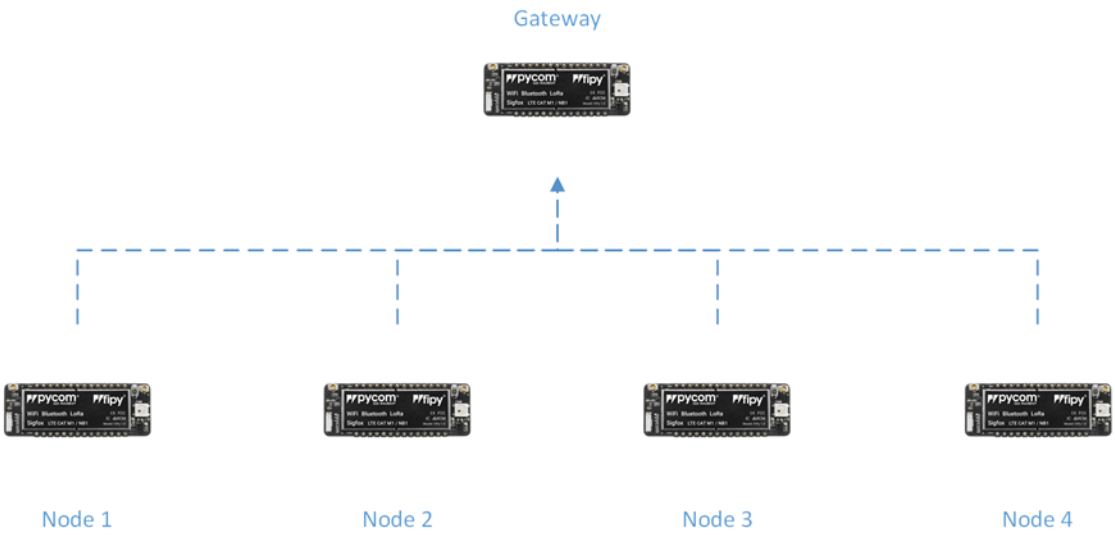

Figure 7: LoRa Connection between Nodes and Gateway

9.2.3 Backend

The backend of the experiments, as shown in Figure 8, is composed of the MQTT Server for the nodes and gateway communications, the supervision station from where the supervisor of the experiment controls and visualizes the activity of the devices and a switch which provides inter-connectivity and access to the Internet.

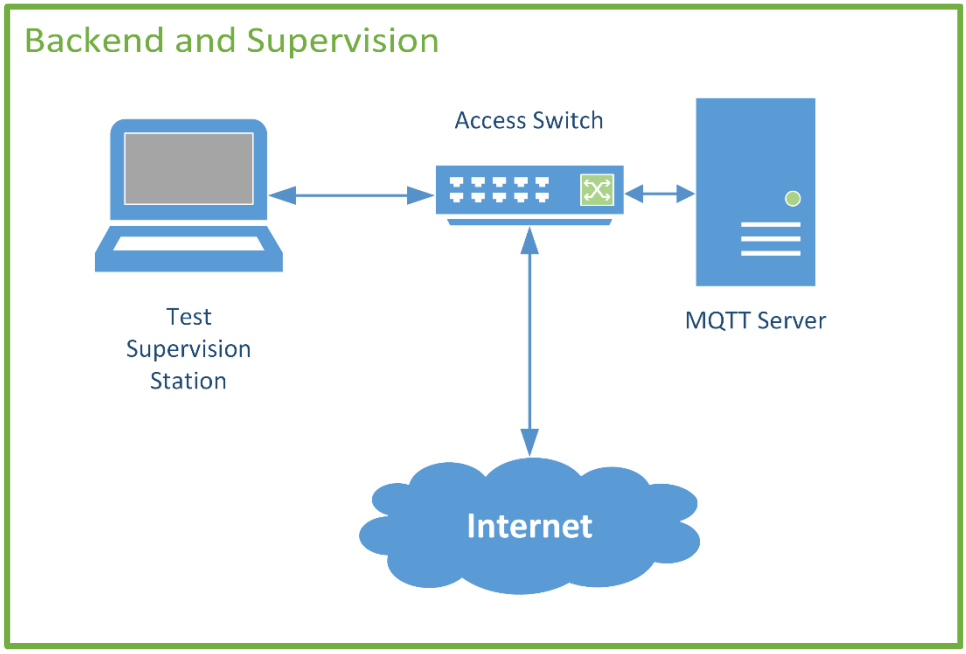

Figure 8: Backend and Supervision Diagram

9.3 Preliminary Tests

Before starting with all the tests of the experiment which will take several days (weeks) to complete, some of the tests are run to check that the results obtained fall within the expected range. In this, a test batch which uses Spreading Factor 7 (the fastest SF) with 3 nodes transmitting is analysed. This test was run several times. The results of the test with Slot Time = Guard Time and PHYPayload = 51 bytes are as follow:

- 85% Received w/o errors
- 10% Received w errors
- 5% Lost

The initially expected result was a 100% of losses, given that all the transmissions would be taking place at the same time. This result totally differs from the result obtained. This led to a review of the program subroutines in the search for bugs in the code. As no error significative to the results obtained was found, other kind of tests were needed to formulate a hypothesis to explain the results.

9.3.1 Oscilloscope Measurements

To determine a relation between the node from which the packets were received and the moment when the packets were sent (represented by the timing of the function calls to the

radio library), an oscilloscope was connected to a pin in 2 nodes and a trigger was introduced in the program in the program in the precise moment of the function calls reviewed.

Once the trigger had been added to the code and the devices were connected to the oscilloscope, the tests started, sending 100 packets using SF7, a PHYPayload of 51 bytes and a Slot Time equal to the Guard Time. The tests were conducted several times, changing the position of the nodes, the orientation of their antennas and the transmission power. While the tests were running, the timing of the triggers was recorded.

After more than 50 tests, a pattern was detected: if the packets of a node were received while another node was also transmitting, when the test is repeated, if the position of the nodes remains the same, the chances of obtaining similar results are very high.

If the dipole antenna of the node of which the packets are being received is turned 90 degrees so that the power received from this node is lower than it would be if oriented correctly, the packets received are not from that node anymore but from the other one transmitting.

In one of the various node distributions that were tested, there were no packets received correctly from any node, which was the initially expected result of the test. However, this result changed when the nodes' position was slightly changed.

The most probable hypothesis that explains the unexpected behaviour of the nodes is that the gateway listens to the medium, synchronizes to the strongest preamble signal and then receives it. This is supported by the fact that LoRa is capable of dealing with very high cochannel interference.

It is also possible that the development boards are making use of Frequency Hopping Spread Spectrum techniques, which would support the previous theory but, as no response from the manufacturer was achieved on this subject, the best that can be done is to explain the behaviour with the information obtained with reverse engineering techniques.

9.4 TESTS REALIZATION

With the final parameters adjusted and corrected, the final tests to obtain all the planned data were run using the test routines developed in the tests planning section. The duration of the tests was of several days, due to the 600 independent tests that were run twice (first run and replica) amounting to a total of 1200 tests.

9.4.1 Test Batches

The 1200 tests that had to be run (including replica), were divided into 8 groups, depending on the number of nodes involved in the test. The summary of the common and varying characteristics of the different tests is shown in Table 28.

Characteristic	Value
Spreading Factor	7-12
Slot Time	0.103-45.097 seconds
Guard Time	0.103-9.02 seconds
Number of Slots	100 slots
Payload	51-255 bytes

Table 28: General Characteristics of the LoRa Capacity Tests.

Parameters such as the Spreading Factor, Slot Time, Guard Time and Payload will be automatically adjusted during the tests. The characteristics of each group can be found in Table 29.

Group Name	Nodes	Run	Tests
1NF	1 Node	First	150
2NF	2 Nodes	First	150
3NF	3 Nodes	First	150
4NF	4 Nodes	First	150
1NR	1 Node	Replica	150
2NR	2 Nodes	Replica	150
3NR	3 Nodes	Replica	150
4NR	4 Nodes	Replica	150
TOTAL	-	-	1200

Table 29: Characteristics of the Different LoRa Capacity Tests.

9.4.2 Methodology

Most of the necessary elements for the tests have been automatized and do not require operator actions. This has been done to keep supervisor intervention and possible error to a minimum.

A series of algorithms to check the correct setup of the devices, as well as their availability and readiness have also been implemented to avoid incorrect experimental data. The system is also capable of self-correcting some of the problems that might appear. If it cannot correct a problem, it will stop the tests until a manual intervention solves the problem.

The devices are all connected to a Wi-Fi network exclusively tailored for the experiment (for compatibility purposes). Through this Wi-Fi connection, several services are provided:

- The devices obtain the current time through the Internet connection provided by the access point, using the Real Time Clock protocol (RTC).
- The devices connect to a local MQTT messaging server which is open to the Internet for external monitoring and future tests.
    - The Gateway uses this messaging service to configure the nodes and pull information from them.
    - All the devices (both gateway and nodes) share their status via information channels to enable any subscribing person to analyse the status of the test and devices.
    - Both the control channels used by the gateway and other extra control channels are available to configure the gateway and nodes; some possible actions are: restarting the device, restarting the automated tests, sending a ping message, configuring a device's radio or even manually defining and starting a custom test.

In order to program the gateway with the tests to be performed, a file containing all the 150 tests of the current batch is stored in an SD card inserted in the gateway. The gateway then

reads the tests from the file and carries them out sequentially. In the event of a power failure, the gateway will recover the last test in progress from NVRAM and will repeat it.

9.4.2.1 Gateway

When performing a test, the basic steps that the gateway goes through are:

- Connecting to the Wi-Fi network.
- Synchronising the local time through NTP.
- Connecting to the MQTT messaging server.
    - Subscribing to the control channels GWControl and Control.
- Reading the tests file from the microSD and choosing the correct test based on the previous test number stored in NVRAM. If all the tests are complete, go to a state of standby waiting for a control message.
- Checking the number of nodes connected and available via the NDControl and GWControl MQTT channels.
    - If the number of nodes available is the same as the number of nodes necessary according to the test under execution, proceed to next step. If not, restart the process.
- Check if the current radio configuration is the one needed for the test.
    - In case the radio configuration needs to be changed or if it is the first test of the file, send a radio configuration command to the nodes through the NDControl channel and configure the onboard radio. Restart to apply the changes.
    - In case the radio configuration does not need to be changed and it is not the first test of the file, continue with the next step.
- Configure the nodes for the current test through the NDConfig MQTT channel. Set the test start timestamp to 10 seconds from the moment of crafting the message.
- Start listening the channel for the duration of the test plus a margin.
    - Store the received unprocessed messages in the RAM memory.
- When the test is finished, stop listening and start processing the LoRa packets stored in the RAM memory.
    - Store the processed packets in a file in the microSD.
- When the processing is finished, store the statistics along with the test characteristics in an information file.
- When everything is finished, restart.

During this process, the Gateway informs of the different events, progress and some results through the GWInfo MQTT channel.

9.4.2.2 Nodes

When performing a test, the basic steps a node goes through are:

- Connecting to the Wi-Fi network.
- Synchronizing the local time through NTP.
- Connecting to the MQTT messaging server.
    - Subscribing to the control channels NDControl and Control.
- Waiting for the gateway to send a radio or test configuration message.
- When a message is received:
    - If the message is a LoRa radio configuration message, apply the configuration changes and restart.
    - If the message is a test configuration message, continue with the next step.

- Configure and prepare the node to start sending messages with the configured parameters at the test start timestamp.
- Disconnect from the MQTT services to avoid execution delays caused by multitasking.
- Send the messages.
- Once the messages have been sent, restart.

During this process, the nodes inform of the events through the NDInfo MQTT channel until the MQTT service is disconnected. The MQTT service is disconnected to achieve a higher precision in the internal timing to send the packet as close as possible to the theorical time.

9.4.3 Beta Tests

So far, the tests design had already been revised, but the stability of the automated testing system still had to undergo a beta run to make sure that the system worked flawlessly and that the logging system recorded every event.

Firstly, the devices were tested in the workbench with a layout different to the final. The devices were programmed with some tests with 1 and 4 devices to check the boundaries (extreme cases) of the system. While the tests where undergoing, the devices were constantly supervised, and extra information was obtained through debug interfaces.

Secondly, the devices were arranged in their final layout while some boundary tests were run. The devices were constantly supervised during this stage and the results were later analysed to make sure that they were correct.

The processes required several iterations to check the effect of the changes to the program.

With the information acquired with these tests, the program was refined. Therefore, the results obtained with these tests were discarded for the final results. The devices were then prepared for the final tests.

9.4.4 Final Tests

The final capacity tests were carried out using the final layout design previously explained in the Laboratory Preparation section. There were 1200 tests to be conducted, which were divided in batches of 150 tests. This division is further explained in the Test Design section.

The tests are divided into 8 batches, as seen in Table 29, where the first digit represents the number of nodes involved and the last character indicates whether it is the first run or the replica of the batch.

The devices which can take part in the tests are shown in Table 30, where the ID of the device represents the last byte of its LoRa radio MAC.

Device Name	Device ID
Gateway	231
Node 1	130
Node 2	180
Node 3	203
Node 4	243

Table 30: Devices and their IDs.

The devices involved in each of the test batches are shown in Table 31. The contents of the "Devices Involved" column contains the IDs of the devices which participate in the test, including the gateway's ID.

Test Name	Devices Involved
1NF	231 & 180
2NF	231 & 180 & 203
3NF	231 & 130 & 180 & 243
4NF	231 & 130 & 180 & 203 & 243
1NR	231 & 180
2NR	231 & 180 & 203
3NR	231 & 180 & 203 & 243
4NR	231 & 130 & 180 & 203 & 243

Table 31: Devices Involved in each of the Capacity Tests.

9.4.5 Anomalous N1 - SF10 Results

After completing the tests, when checking the data obtained, the results showed that the tests with 1 Node using SF10, both in the first run (1NF-SF10) and replica run (1NR-SF10) had anomalous results.

The expected results would be a near-100% success rate. The results obtained with the use of the SF 7, 8, 9, 11 and 12 were as expected, with a success rate greater than 99%, but when transmitting with SF 10 and most evident with PHYPayloads greater than 51 bytes, the success rates fell to a mere 73% average.

A further analysis of the possible underlying causes of this problem is conducted at the results analysis section.

9.5 RESULTS ANALYSIS

9.5.1 Expected Results

The expected results for the Laboratory Capacity Experiment are:

- With one node transmitting, an average PoS (Probability of Success) rate greater than 99.5%.
- With multiple nodes transmitting, the greater the number of nodes while maintaining the other test parameters, the lower the PoS of the transmissions made by those nodes.
- With multiple nodes transmitting, the higher the transmission rate (number of packets per second) —and, therefore, the closer the Slot Time value is to the Guard Time's—, the lower the PoS.

9.5.2 Results

As shown in Figure 9, the results obtained for a Spreading Factor of 7 and a PHY Payload of 51 Bytes show that when only one node is transmitting, the PoS is near the 100% mark for every transmission rate. However, when the number of nodes for a given transmission rate is incremented, the PoS decreases. Also, when for a given number of nodes (different of 1) the transmission rate increases, the PoS decreases.

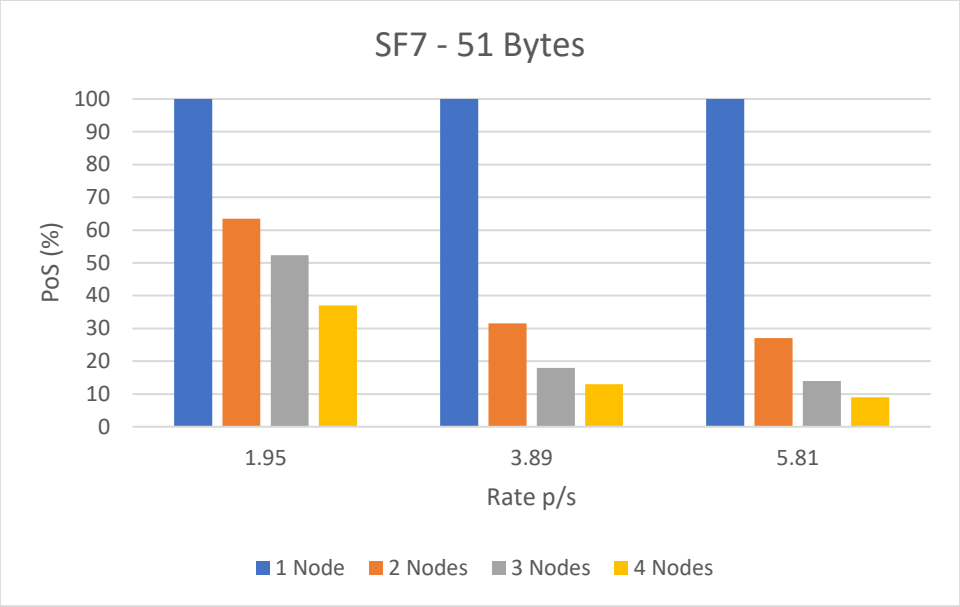

Figure 9: Evolution of the PoS with the Packet Rate for SF 7 and a PHYPayload of 51 bytes

The results shown in Figure 9 are representative of most of the results obtained in the 1200 independent tests realized, but there are some anomalies that appear in a portion of the results that need to be explained.

The results in this section are what seems to be the logical results to obtain from a system of devices transmitting in the same frequency, the same BW and the same SF (their transmissions are not orthogonal).

In the next sections, the anomalous results encountered in the different tests are described and explained. Some extra tests are run to obtain all the necessary data to generate a hypothesis capable of explaining the cause of the anomalies.

9.5.3 Anomalous N1 - SF10 Results

After parsing the results of the 300 tests formed by the tests groups 1NF and 1NR, the expected theorical results would be a success reception rate greater than 99.99% if only considering the effects of power losses and interferences and greater than 99.5% when accounting for all the effects.

These high success rates are expected due to the proximity of nodes and gateway, the fact that only one node is transmitting in this configuration and the transmission power in use (14 dBm). The losses are majorly caused by loss of synchrony between gateway and node and by spike interferences.

While most of the results were near the expected mark, there was an anomaly which appeared in both the first run (1N) and the replica run (1NR), in the SF10 tests. This anomaly caused a severe packet corruption and loss, demonstrated by the 74.0% success rate achieved when the spreading factor 10 was in use in the first run and a 72.1% success rate in the same conditions.

The percentage of packets which were successfully received by the gateway in the replica test can be seen in Figure 10, which shows the PoS for every PHYPayload size tested.

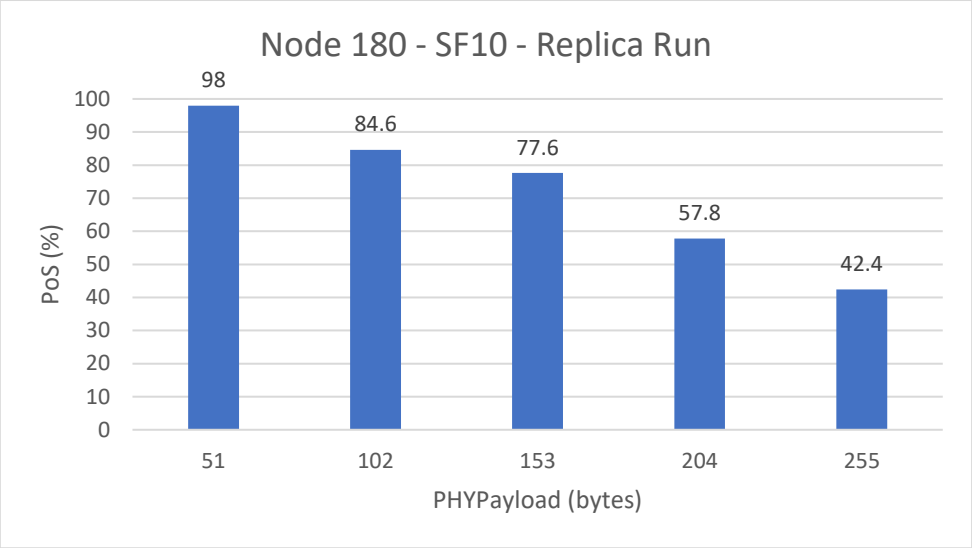

Figure 10: Evolution of the PoS with the PHYPayload for Node 180 using SF 10 in the Replica Run

Other factors which reveal the corruption of the packets and discard the possibility that all the packets not received correctly present a problem with the preamble synchronization, are that most of these packets arrive but have a corruption either in the MAC Header or in the MAC Payload. An average of a 9.12% of the packets sent in the first run and a 10.08% of the packets sent packets in the replica run received by the gateway had corruption in either (or both) of the aforementioned areas.

The percentage of packets which were received with corruption by the gateway in the replica test is shown in Figure 11, which shows the PoC (Probability of Corruption) for every PHYPayload size tested.

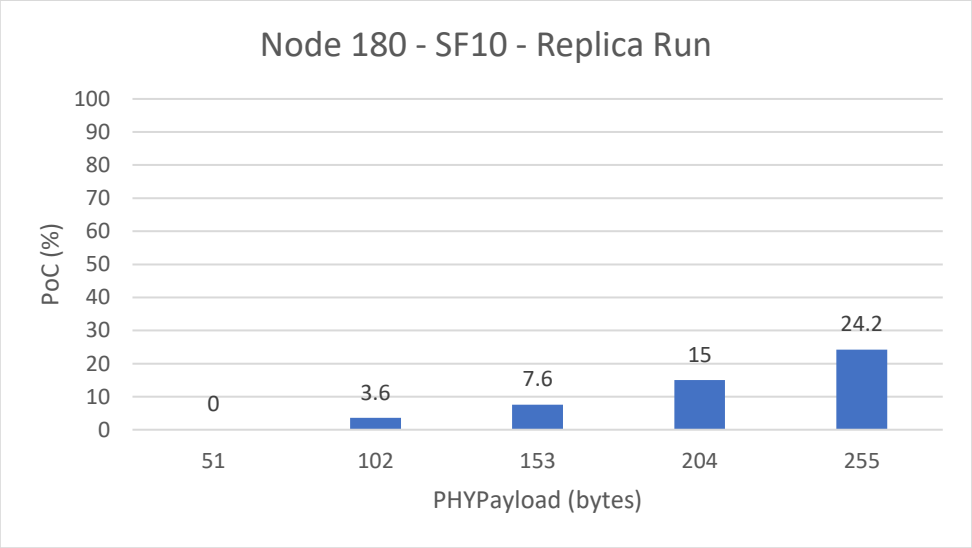

Figure 11: Evolution of the PoC with the PHYPayload for Node 180 using SF 10 in the Replica Run

To further hypothesise about why the node and gateway failed to reliably communicate in the SF10 when the physical payload was greater than 51 bytes, while they functioned perfectly under the other SF configurations, other tests need to be made.

9.5.3.1 Node 180 Re-Run

The 1N – SF10 tests were conducted again with the same node used in the first and replica runs, to determine whether the results were an isolated anomaly or a repeatable event. This node will be called node 180 (last byte of the LoRa MAC).

As shown in Figure 12, the results from the Re-run of the SF10 1N tests with node 180 show that the greater the PHYPayload (and therefore the longer the transmission time), the lower the probability of success.

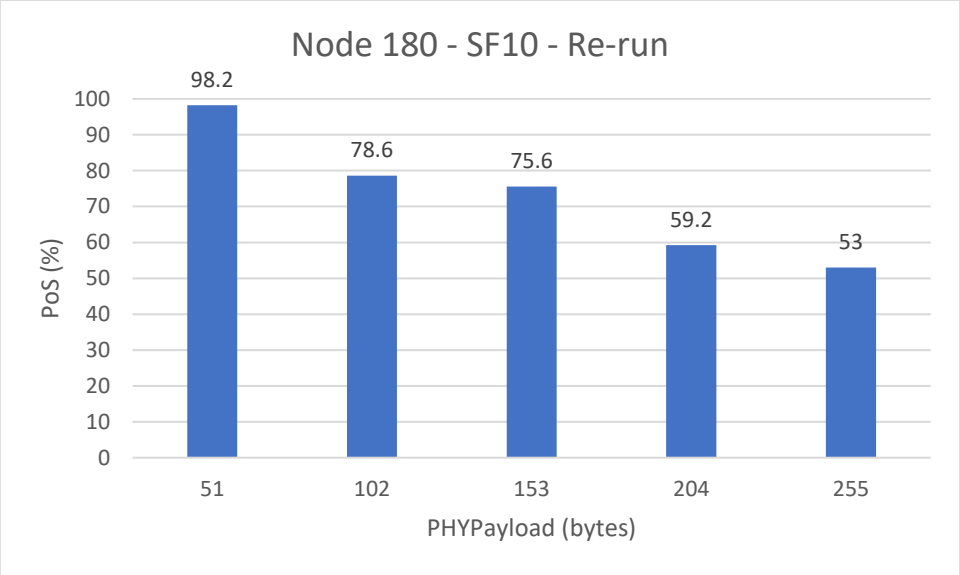

Figure 12: Evolution of the PoS with the PHYPayload for Node 180 using SF 10 in the Re-Run

In Figure 12, the PoS represents the percentage of packages received correctly on average in the 5 tests which use the same PHYPayload length, varying the Slot Time. In Table 32 are defined all the 25 different tests that were run grouped in 5 different groups. All the 25 tests are run by 4 different devices. The variations in the Slot Time should not produce a noticeable effect given that only one node transmits, but it is included due to its inclusion in the previous Capacity Tests (where the anomaly was detected). Each test is comprised of 100 packets and for every SF and PHYPayload configuration a total of 500 packets are sent.

SF	Node	Slot Time (ms)	Guard Time (ms)	MACPayload (bytes)	PHYPayload (bytes)
10	130|180|203|243	617 - 3083	617	41	51
10	130|180|203|243	1027 - 5131	1027	92	102
10	130|180|203|243	1436 - 7179	1436	143	153
10	130|180|203|243	1846 - 9227	1846	194	204

SF	Node	Slot Time (ms)	Guard Time (ms)	MACPayload (bytes)	PHYPayload (bytes)
10	130|180|203|243	2296 - 11480	2296	245	255

Table 32: SF 10 Tests Run grouped by PHYPayload

The results obtained with the node 180 in the Re-run, as represented in Figure 12 were similar to the ones obtained in the original first run shown in Figure 13**.**

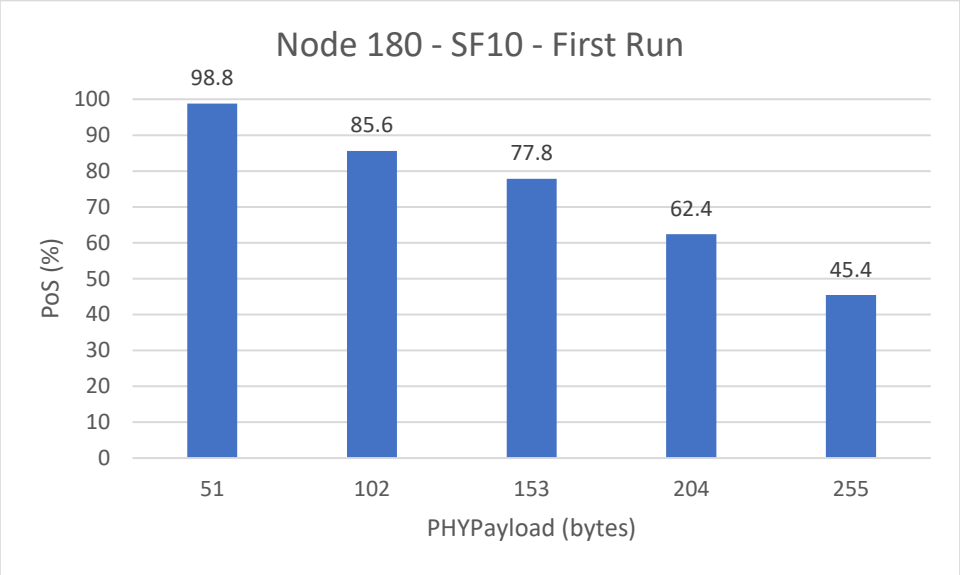

Figure 13: Evolution of the PoS with the PHYPayload for Node 180 using SF 10 in the First Run

- Hypothesis: From this data, could be deduced that the gateway is losing the synchronism with the node 180, given that the longer the transmission time is, the higher the probability of de-synchronization.
- Possible solution to hypothesis: To solve this issue, there is a transmission option called low data rate optimize, which helps solve the issue with long transmission times by making the transmission even longer by adding some elements that help keep the synchronization over such a long period of time (with SF12 up to 45 seconds).

As in Pycom's implementation of Semtech's radio control library low data rate optimization is only applied to SF11 and SF12 disregarding the actual length of the transmission (a transmission using SF11 can be longer than a transmission using SF12 with a lower PHYPayload in SF12 than in SF11), with high Spreading Factors, the probability of losing synchrony is high with big payloads.

9.5.3.2 Node 243

The 1N – SF10 tests were conducted again with a second different node to check whether the error was produced by the gateway or the first node and to obtain more information for further analysis. This node will be called 243 (last byte of the LoRa MAC).

The results obtained with the node 243, as represented in Figure 14 were totally different to those obtained with node 180 and are much closer to what expected, presenting an average PoS (Probability of Success) of 97.92%.

An average 97.92% PoS is less than the average of other spreading factors under the same conditions and with the same PHYPayloads and, therefore, fits the fact that with longer transmission times, losses are greater.

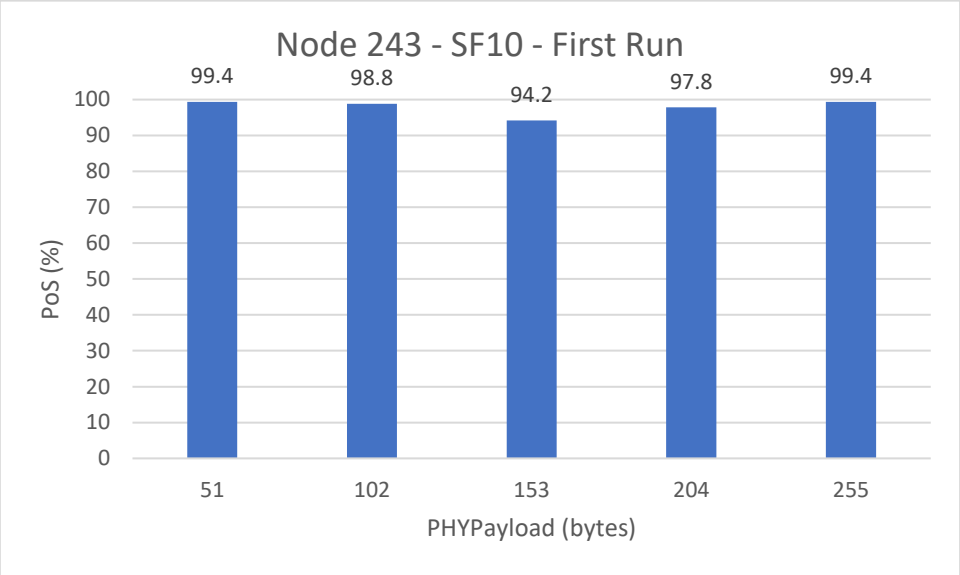

Figure 14: Evolution of the PoS with the PHYPayload for Node 243 using SF 10 in the First Run

As in the first run with node 243 losses for a PHYPayload of 153 bytes are higher than those for 255 bytes, another run of the tests with the same node is conducted to obtain a greater statistical mass.

The results of the second run or replica run with node 243, as shown in Figure 15, are closer to what originally expected, although there is always to expect a statistical deviation given the relatively low size of the sample. The average this time is of a 99.52%, which is still lower to that of lower SFs.

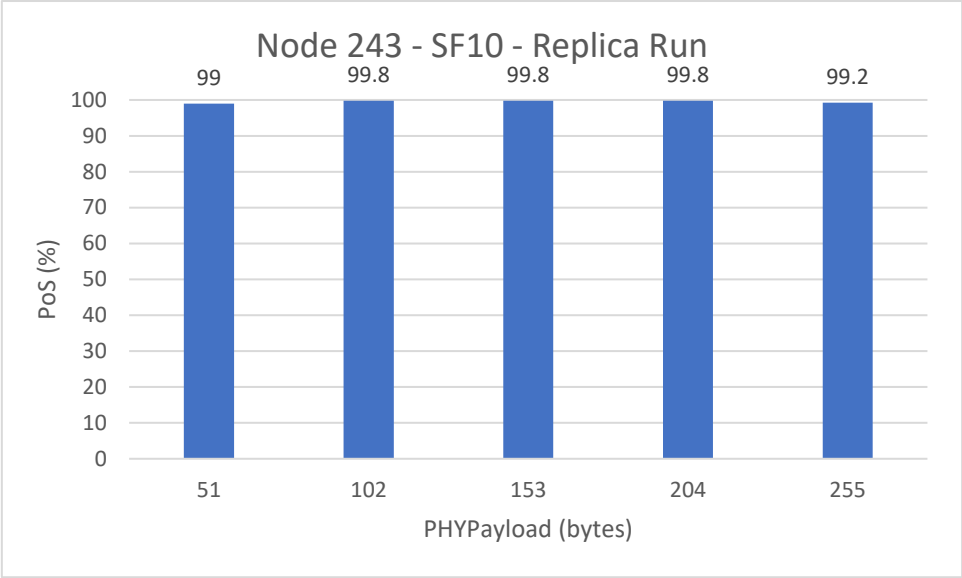

Figure 15: Evolution of the PoS with the PHYPayload for Node 243 using SF 10 in the Replica Run

To check whether any other node shows an anomalous behaviour, the two other nodes will run the 1N SF10 tests as well.

9.5.3.3 Node 203

The node 203, as shown in Figure 16, presents a mostly typical PoS depending on the size of the PHYPayload, with PoS ranging from 98 to 99.5% while showing a tendency to decrease when the PHYPayload is increased. The increase in PoS when PHYPayload is set to 255 bytes is explained by the relatively low size of the statistical sample (500 packets), as with the node 243, which do not guarantee 1 decimal of precision.

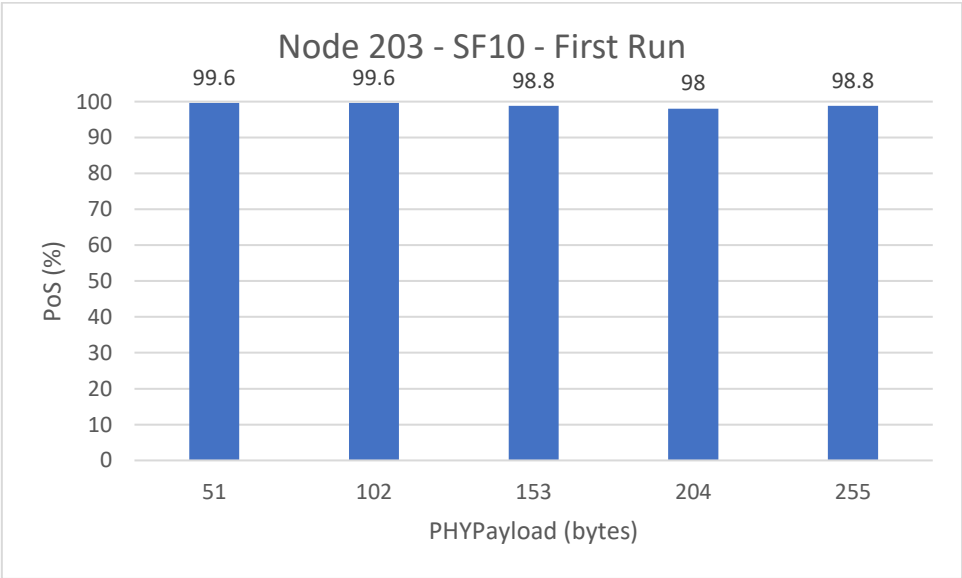

Figure 16: Evolution of the PoS with the PHYPayload for Node 203 using SF 10 in the First Run

The average PoS for the node 203 is of 98.96%, which is well within the expected parameters and consistent with the values obtained for the other nodes.

9.5.3.4 Node 130

The next and last node to check is the node 130. As shown in Figure 17, the results of this node are also within the expected values and show a predictable variance of the PoS in relation with the variation of the PHYPayload.

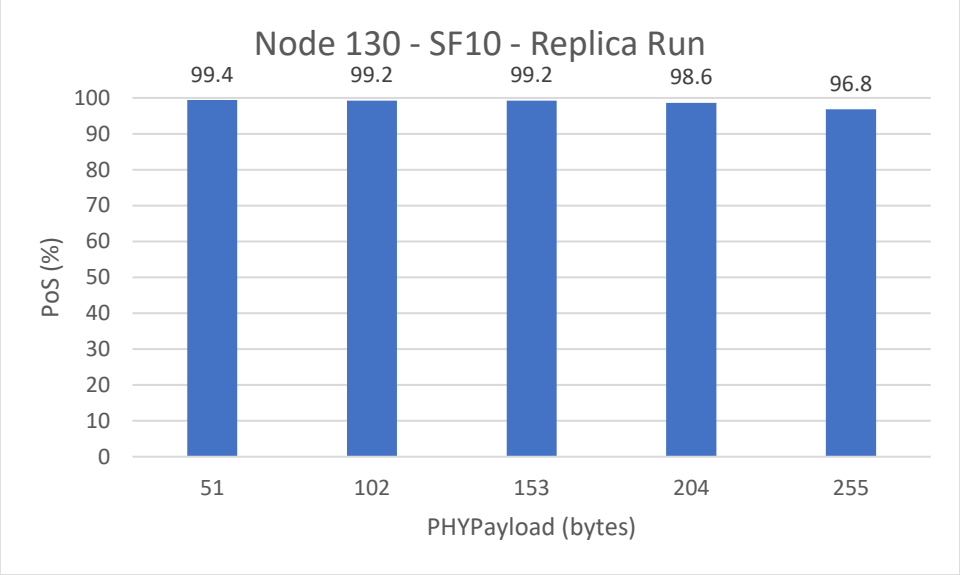

Figure 17: Evolution of the PoS with the PHYPayload for Node 130 using SF 10 in the Replica Run

The average PoS for the node 130 is of 98.64%, which is well within the expected parameters and consistent with the values obtained for the other nodes.

9.5.3.5 Node 180 with 130's antenna

To analyse whether the anomaly has only a dependency on the node or also depends on the antenna in use, another batch of tests was run, but this time with another node's antenna.

The results, as shown in Figure 18, are much more as originally expected than the one's with 180's original antenna in Figure 13.

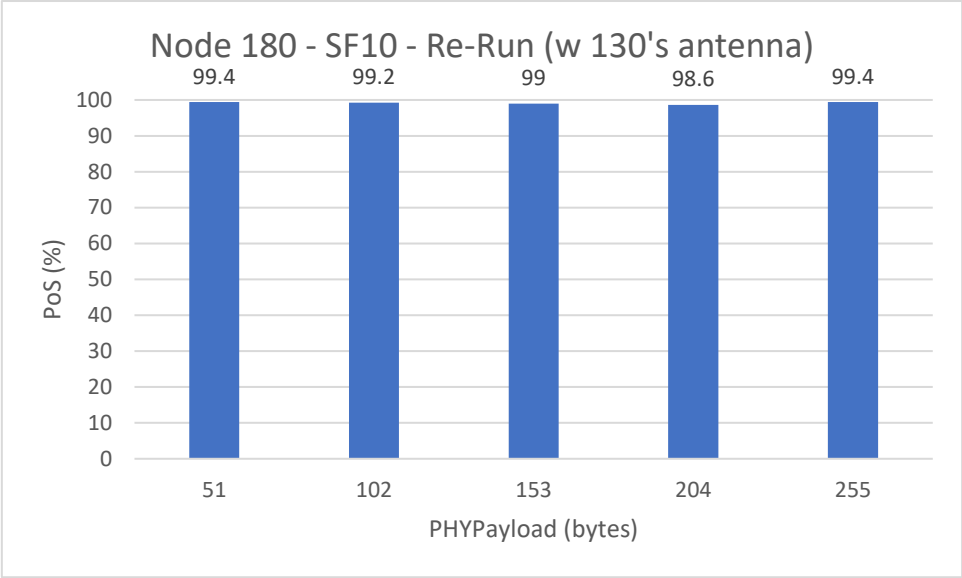

Figure 18: Evolution of the PoS with the PHYPayload for Node 180 with 130's antenna using SF 10 in the Re-Run

The average PoS for node 180 with 130's antenna is of 99.12%, which is well within the expected parameters and consistent with the values obtained for the other nodes.

9.5.3.6 Node 130 with 180's antenna

Another interesting test is using node 180's antenna in another node which has not presented any notable symptoms of anomalies before, as node 130.

The results, as shown in Figure 19, show that the change of antenna has had a considerable effect in the PoS of the node 130.

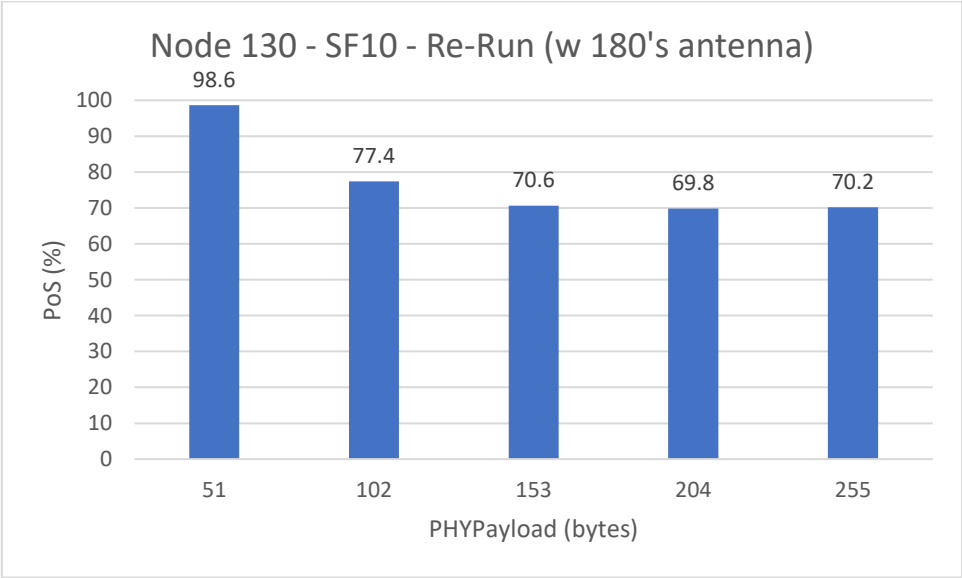

Figure 19: Evolution of the PoS with the PHYPayload for Node 130 with 180's antenna using SF 10 in the Re-Run

The average PoS for the node 130 with 180's antenna is of 77.32%, which is similar to the results obtained with the node 180 with its antenna.

9.5.3.7 Conclusions

After analysing the results and trying to combine node 180 with other antennas, it worked properly, and the results were the expected. Therefore, the antenna used with node 180 might be defective and this defect shows when using the SF10.

The curious thing about these results is that if the problem was of insufficient irradiated power due to a defective antenna, the SF7 would have been affected the most due to its lower sensitivity (because of the faster transmission rate).

A possible explanation for the SF10 with high PHYPayload being affected resides on the fact that, as the SF10 has the longest transmission times without the low data rate optimization activated, its transmissions are the most vulnerable to loss of synchrony between transmitter and receiver.

The anomalies of node 180 might have affected the results of the multi-node tests, such as 2N, 3N and 4N, in which this node was used. But, as this node does not show any other symptoms of being defective, other devices including antennas in similar conditions might have been installed without knowledge of the defects. Therefore, these results are representative of what could be found in a real-world implementation and are therefore included as part of the results.

9.5.4 U-Shaped Results

As previously discussed in the tests realization section, when considering the PoS (Probability of Success or percentage of correctly received packets), there were some tests with anomalous results. These anomalous results appeared in a pseudo-random fashion (which could be modelled with hardware monitoring).

When the anomaly appeared, when the Slot Time was reduced, the number of received packets increased instead of diminishing, which would have been the expected theorical result. This appeared only in tests where multiple nodes were involved, and its hypothetical causes and results will be laid out in this section.

In Figure 20, a result similar to what was originally expected, with the typical deviations expected from the size of the sample chosen is shown. This graph shows that, the greater the rate at which packets are sent with more than one node present, the lower the probability of success (given the greater probability of collision).

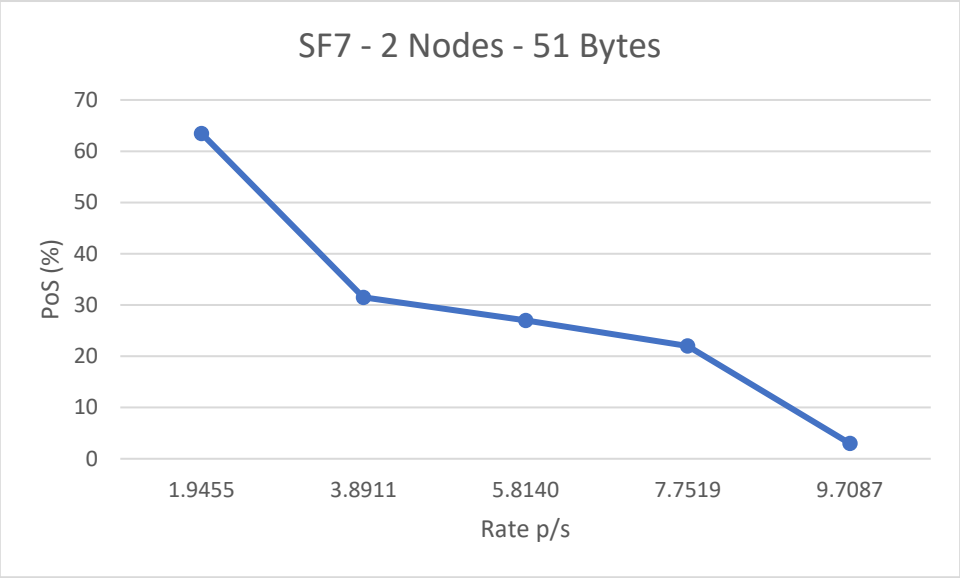

Figure 20: Evolution of the PoS with the Packet Rate for SF 7, 2 Nodes and a PHYPayload of 51 bytes

In contrast with the previous results, in Figure 21, another example is shown where the graph acquires a U-shape.

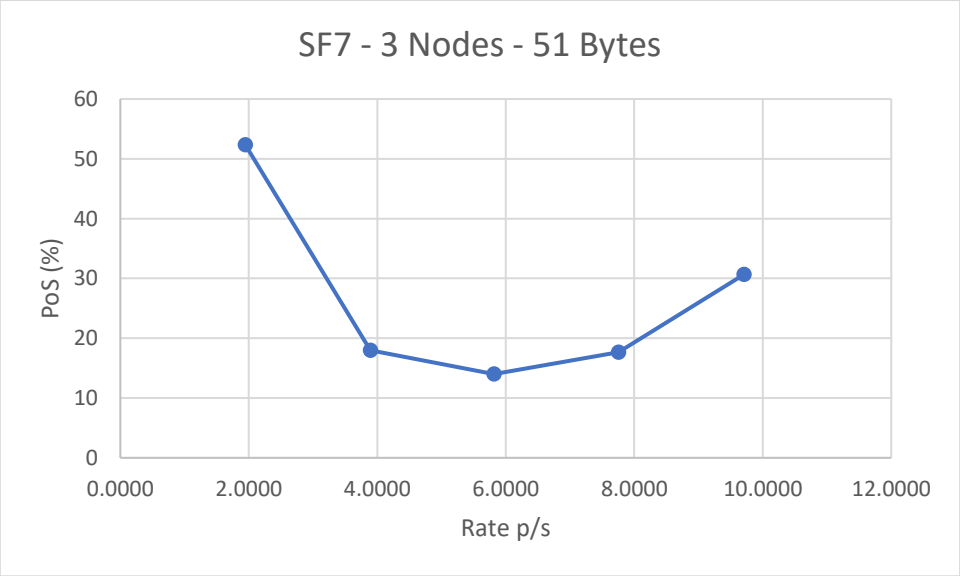

Figure 21: Evolution of the PoS with the Packet Rate for SF 7, 3 Nodes and a PHYPayload of 51 bytes

Another graph with a different scenario using SF 12 instead of SF 7 and 255 bytes of PHYPayload instead of 51 bytes of PHYPayload with 3 nodes obtaining a very similar result is shown in Figure 22. The configuration used produces much longer transmissions, given its lower data rate and bigger payload.

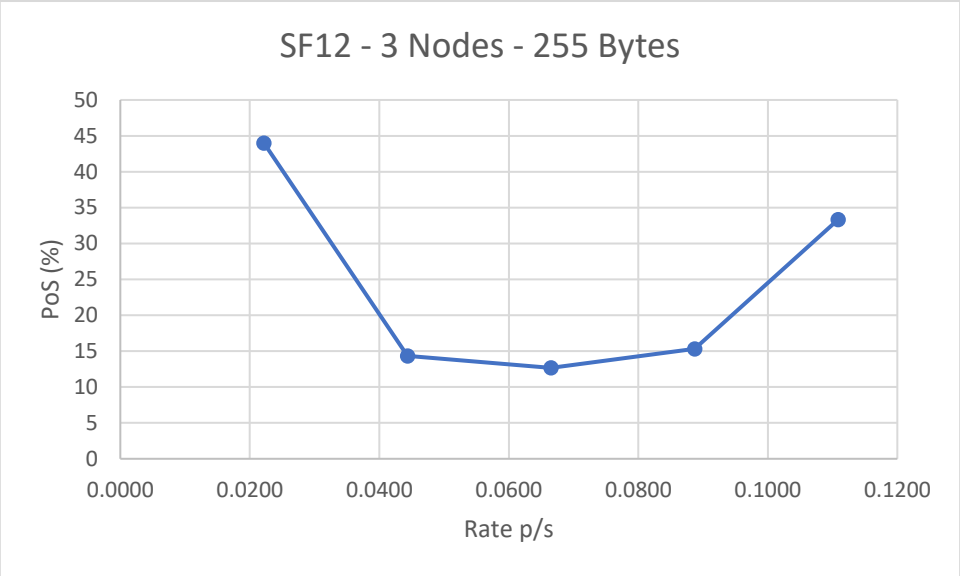

Figure 22: Evolution of the PoS with the Packet Rate for SF 12, 3 Nodes and a PHYPayload of 255 bytes

The explanation for the increase in packet reception when the Slot Time is reduced (and therefore the packet rate is increased) resides in the design of the test and the precision of the devices used.

The phenomenon can be explained by the effect of two characteristics of LoRa:

- The first characteristic would be LoRa's ability to correctly receive a transmission whose signal is endeavouring a co-channel interference from another LoRa transmission of up to -6 dB the strength of the target signal.
- The second characteristic is that, if the devices' timing is slightly off, but enough to allow the reception of the preamble of one of the signals before the others start transmitting and this signal is strong enough, it could be correctly received by the gateway. However, if the first signal is not strong enough, the other LoRa transmissions could interfere the transmission. The time synchro variation is of around ±10 ms, given the lack of a higher time synchronization precision in the implementation of NTP found in MicroPython.

Given that the nodes present some inter-node delay in the experiment's timing, that not all the nodes' signals may have the same path losses and that the power amplifier used by the LoRa IC used does not provide great precision in the power output, the results obtained would be possible. Also, given the volatile nature of the timing precision, the appearance of the U-Shape effect could vary from test to test.

9.5.5 Conclusions

The LoRa communications technology has proven to be very resilient to interference and can withstand noise levels many times higher than the signal level. Is by this reason that if a LoRa receiver starts receiving a LoRa signal and afterwards receives interference (even from other LoRa signals), it will most likely be able to successfully receive the first one.

The so-called U-Shape phenomenon encountered in the results of the experiments seems to be produced from the capability of the LoRa radio to distinguish between two different co-channel

transmissions with only 6 dB of received power differential between them (receiving the most powerful one).

The U-Shape phenomenon also benefits from the characteristic of the LoRa radio, where, when the difference in time between the transmissions of various nodes (produced by the difference in time synchrony) is high enough, the gateway successfully locks to the first node transmission, therefore needing little power difference between the transmissions. This also leads to a more probable correct reception of the first node's transmission (first node transmitting).

Chapter 10: NLoS In-Campus Experiment

10.1 Tests Design and Planning

The objective of this experiment is to assess the robustness of the LoRa radio in a NLoS (Near Line of Sight) environment. The effects that changing some of the radio configurations have on the results are studied as well. The methodology of the test and its characteristics will now be defined.

In this experiment, two devices are used: a gateway and an end node. The experiment takes place at the Polytechnic University of Valencia, were a Smart Campus / Smart City scenario is designed and tested. The devices are at NLoS (Near Line of Sight).

10.1.1 Gateway

The gateway is installed on the roof of the building 8E, access F for the entire duration of the tests. It is placed in an installation pole which has NLoS view to the points where the node will be installed. The gateway is heading towards building 2E/3A *Rectorado*. The exact conditions of the installation are discussed in the realization section of this test.

10.1.2 Node

In this test, the end node is temporarily installed on the roofs of several buildings to measure the effects that variations in the distance in combination with the variation of some radio configurations have in the PoS (Probability of Success). Only one node is used to perform the experiment, which is installed at a given location and uninstalled when the testing in that location has finished. It is then changed to another location where the procedure will repeat. The node is placed on top of a 1.5 meters high tripod in all the locations.

The locations are chosen so that the distance between the gateway and the node is progressively increased. A map with all the locations where the measures are performed is shown in Figure 23.

Figure 23: Buildings where the Node is Placed and their Names

The distance to the gateway is one of the criterium in the selection of the locations and, as shown in Table 33, the distances are distributed in the 100-1100 m range.

Location	Distance to GW
GW	–
8P	97.75 m
7E	390.21 m
7G	540.06 m
4N	825.87 m
2E/3A	1090.00 m

Table 33: Node Locations and their Distance to the Gateway

10.1.3 Radio and Packets Configuration

In this test, both the gateway and the end node vary their SF (Spreading Factor), TX (Transmission) power and CR (Coding Rate) in all the locations where the node is installed. The SF, CR and TX power vary according to the configurations shown in Table 34.

Variable	Value
SF	7-12
BW	125 kHz
PHY Header	Yes (Always)
CRC	Yes (Always)
Preamble	6 (+ 4.25)
DE (Low data rate optimize)	Yes (SF 11 and 12)
Coding Rate	4/5, 4/8
TX Power	8,14 dBm

Table 34: Radio Configurations for the Different Tests

The packet size is fixed to 51 bytes at the PHY layer (PHYPayload). The MAC payload size needed in order to achieve the required PHY payload packet size is of 41 bytes. This is for an unconfirmed packet using the custom LoRa MAC Protocol previously developed and explained in this document.

A modified version of the program used in the Laboratory Capacity Experiment is used in this test. The Slot Time is set to match the Guard Time, given that only one node transmits, and the tests need to be realized as fast as possible. This way more tests can be done and therefore more data for analysis can be obtained.

A total of 24 tests are conducted in each location of the end node. In each of the individual tests, 1500 packets are sent from the node in each location to the gateway, so that the results obtained have the desired precision.

10.2 Preliminary NLoS Tests

After designing the NLoS tests and adapting the program run on the gateway accordingly, the tests could be conducted. The first step was to verify the performance of the devices before starting the final tests.

A special, shorter tests batch was prepared for the occasion with the same configurations of the final tests batch but with only 100 packets per test to save on execution time. The gateway was already installed on its final location during the execution of this test.

10.2.1 Devices Location

The gateway was located on the roof of building 8E access F. The node was located on the 3rd floor terrace of the building 4K. As shown in Figure 24, the distance between the devices is of 713.63m.

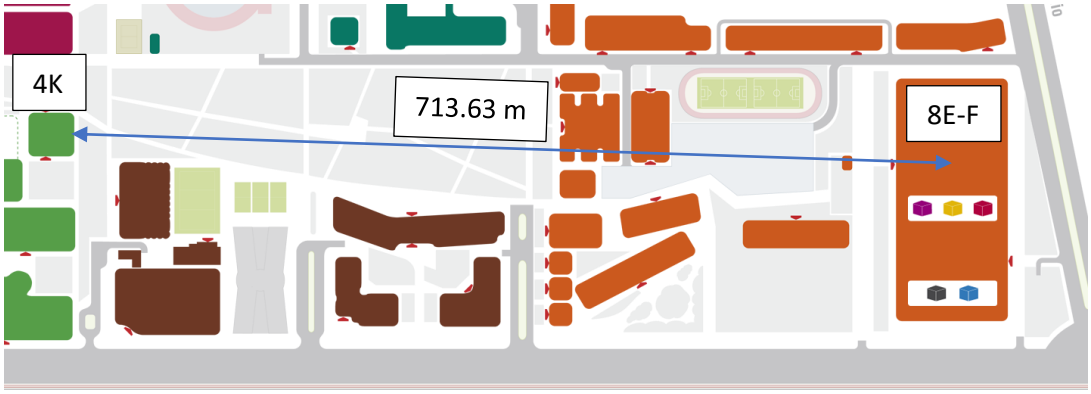

Figure 24: Diagram with Distance between Building 4K and 8E-F

The GPS Coordinates following the WGS84 (World Geodesic System 1984) datum standard are shown in Table 35 for both devices participants in this test.

Device	Location	Latitude (N)	Longitude (E)
Gateway	8E – Access F – Roof	39°28'41.680''	-0°20'02.384''
Node	4K – 3rd floor - Terrace	39°28'50.756''	-0°20'30.162''

Table 35: Devices' Locations and GPS Data for Building 4K

10.2.2 Results

From observations made during the fully-supervised test, excessive delay in some connections of the gateway and some missed MQTT messages were noticed. This lead to discover a problem with the Wi-Fi installed in the roof of the building 8E access F. The problem was solved after several changes and further testing and it resulted in a different placement of the Access Point.

A few extra tweaks to the program were also necessary to adapt to the new test environment. When all the modifications and tests were finished, the system was ready for the final tests.

10.3 Complete NLoS Tests

After the preliminary tests were concluded, the final tests of the experiment started. The first location to test was the nearest building to the gateway and, from there, the testing continued until reaching the farthest building.

10.3.1 Configuration

The gateway was installed in the roof of the building 8E, with access to the internet provided by a Wi-Fi network specifically tailored for this experiment. In Figure 25 is shown the installation of the gateway on the building 8E – access F roof.

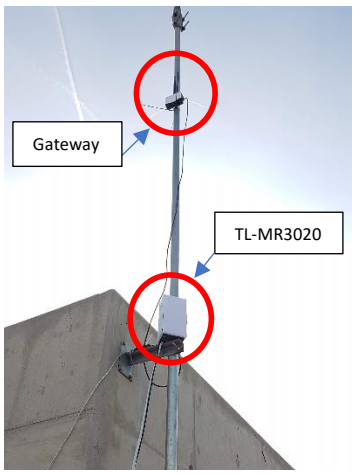

Figure 25: Installation of Gateway and Access Point

The Wi-Fi access point was also installed in the building's roof to provide a reliable connectivity to the gateway. The access point was wired to the network of the UPV via an access switch. As shown in Figure 27, the access point was encapsulated in a box that was then water-proofed (with the use of hot glue and tape) and, as shown in Figure 26, it was also covered by white sheets so that a high percentage of the solar radiation is reflected.

Figure 26: TL-MR3020 Front-Side View

Figure 27: TL-MR3020 Back-Side View

The node was temporarily installed in all the buildings (one by one) where the tests have been conducted. Figure 28 and Figure 29 show the installation of the node in building 8P.

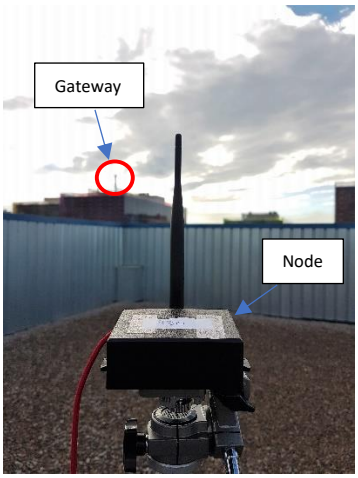

Figure 28: Back view of Node in Building 8P

Figure 29: Lateral view of Node in Building 8P

The node also had access to the internet via another specifically tailored Wi-Fi network provided by a router-AP combo (TL-MR3020) with a Huawei 3G gateway. This device is shown in Figure 30.

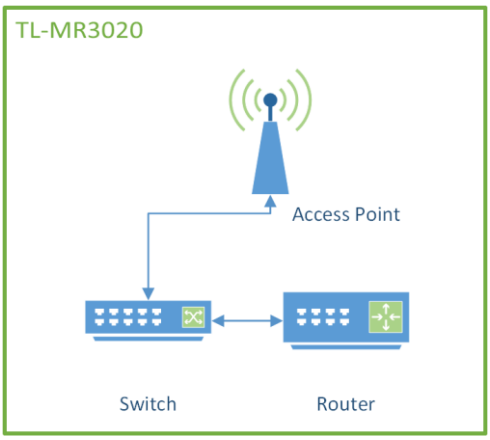

Figure 30: Diagram of TL-MR3020's Components

The LoRa link established between the devices is shown in Figure 31, where the remote building is the building where the node is placed in each of the tests. The LoRa message is sent in an uplink channel (node to gateway).

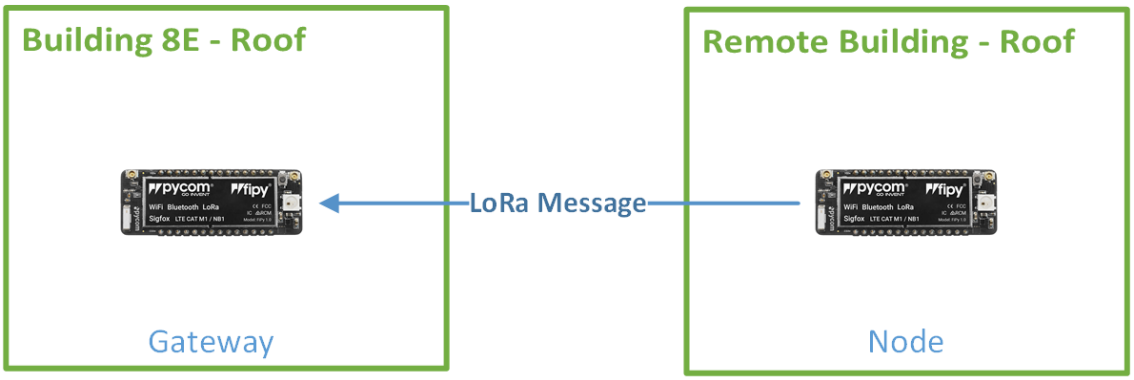

Figure 31: LoRa Link between Node and Gateway

The device utilised to obtain the GPS data has been a Samsung Galaxy S7 (G930F), equipped with a GPS module which in our tests has been capable of obtaining location measurements with an accuracy of up to 2 m by using the following satellite constellations: the American GPS, the Russian GLONASS and the Chinese BeiDou. As by 2018 the BeiDou constellation still does not offer a full global coverage, only a few of its satellites' signals were received in the measuring locations.

10.3.2 Devices Location

The gateway was located on the roof of building 8E access F. The node was installed on the roof of the buildings 8P, 7E, 7G, 4N and 3A. After the measurements in one location were done, the node was then uninstalled from that location and reinstalled in the next one. As previously stated, the order followed in the installations was from the closest to the farthest.

In Figure 23, the different points where the node was installed and the point where the gateway was installed are shown in top of a 2D map of the Polytechnic University of Valencia.

The GPS Coordinates following the WGS84 (World Geodesic System 1984) datum standard are shown in Table 36 for all the locations where the node and gateway were positioned, along with their distance to the gateway.

Name	Location	Latitude (N)	Longitude (E)	Distance to GW
GW	8E – Access F – Roof	39°28'41.680''	-0°20'02.384''	-
8P	8P – Roof (2nd floor)	39°28'41.234''	-0°20'06.606''	97.75 m
7E	7E – Roof	39°28'50.340''	-0°20'14.006''	390.21 m
7G	7G – Roof	39°28'54.623''	-0°20'17.482''	540.06 m
4N	4N – Roof	39°28'49.857''	-0°20'35.445''	825.87 m
3A	3A – Roof	39°28'56.473''	-0°20'44.074''	1090.00 m

Table 36: Devices' Locations and GPS Data for all the buildings

The distances shown in Table 36 are distances in the horizontal plane, due the imprecision of the GPS when measuring height.

10.4 Results Analysis – Effects of the Distance

The effects of the distance on the PoS (Probability of Success) of the packets have not been remarkably notable in this experiment, as the results obtained in the nearest position are very similar to the results obtained in the farthest position. However, there are a few points where the losses in the weakest transmission configurations where notable, located in a middle distance, but with an angle to the gateway and a poorer NLoS. However, while the PoS has not reflected the effect of the distance, the SNR has, and it will be analysed in the RSSI and SNR subsection.

In the first position, as could be expected, the results, as shown in Figure 32, show a near-perfect reception with a PoS greater than 98% sustained over the entire set of radio configurations.

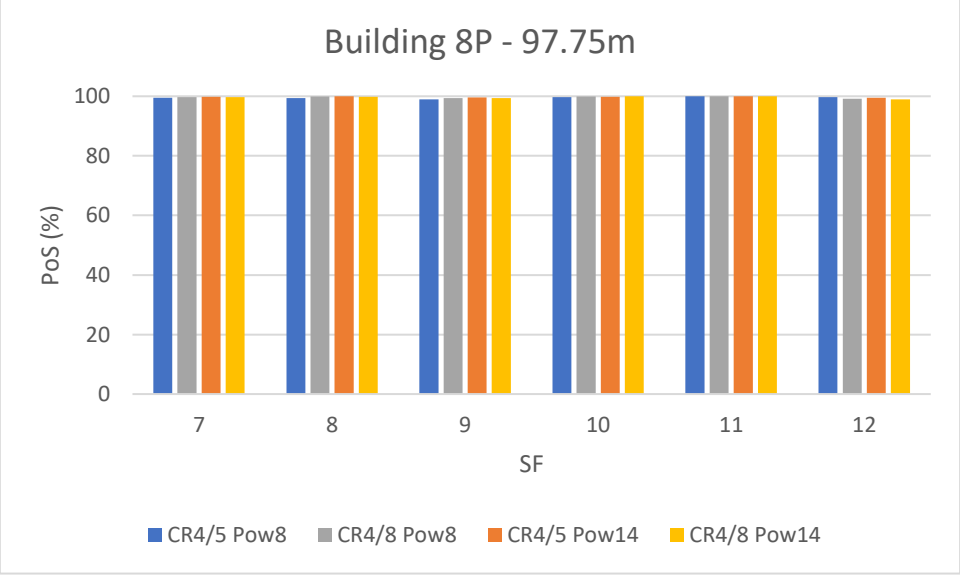

Figure 32: PoS with Transmissions from Building 8P

The results obtained with the node located in the farthest position (building 2E/3A *Rectotado*) are very similar to those found in the nearest position (building 8P). The results obtained in the farthest position are shown in Figure 33, obtaining again a PoS greater than 98%, indicative of a very reliable connection.

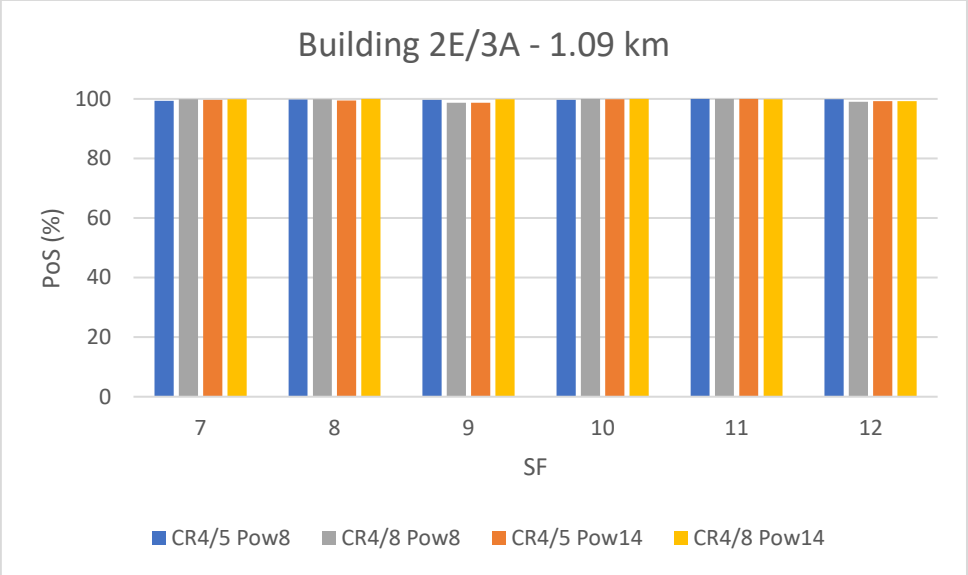

Figure 33: PoS with Transmissions from Building 2E/3A

10.4.1 Losses by Fresnel Zone Obstructions

As discussed earlier, there are two locations where the combined effects of the distance and the obstacles in the 1st Fresnel zone have a notable impact in the weakest transmission configurations.

The first location where this effect is noticeable and the farthest from the gateway of the two is building 7G (Animal Science Department). The results shown in Figure 34 show that the lower SF, lower transmission powers and the less redundant CRs present notable losses.

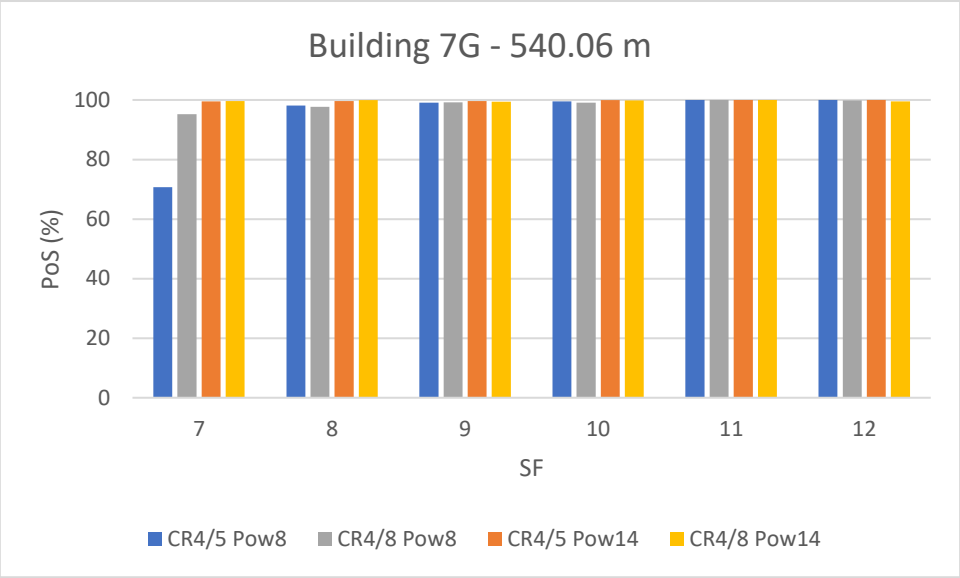

Figure 34: PoS with Transmissions from Building 7G

As expected, the higher the transmission power, the higher the codding rate and the higher the spreading factor, the better the PoS is. This can be clearly observed in Figure 34.

The nearest but also lower in height of the two buildings where the tests present noticeable losses is building 7E (ETSID). As shown in Figure 35, the effects that produce the losses are exacerbated in this location, having a deeper impact in the SF 7 configurations than in the previous building's tests and noticeably affecting the SF 8 and SF 9 configurations.

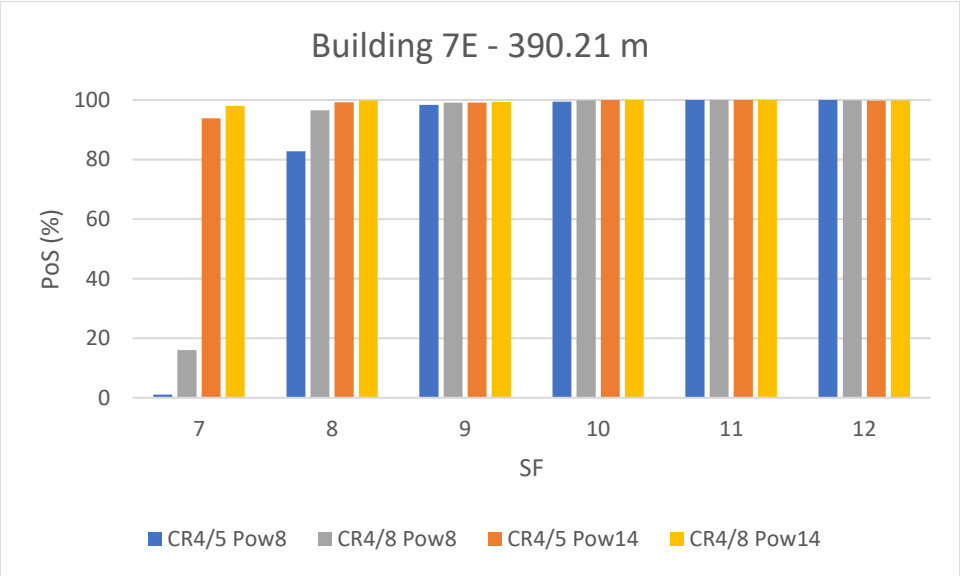

Figure 35: PoS with Transmissions from Building 7E

The cause behind these results (where the distance from the end node and gateway seems to have less weight on the results than other factors) seems to be the poorer visibility in the nearest of the locations with losses when compared to the farthest.

The view of the gateway from the node's point of view when located in building 7E, as shown in Figure 36, shows that the Fresnel zone is partially obstructed by a Vodafone telecommunications tower located in the gateway's building. Both the object and gateway are marked in the image. This image was taken from the node's position with a 50 mm (APS-C) lens and cropped. The real distance between where the picture was taken and the gateway is of 390.21 meters.

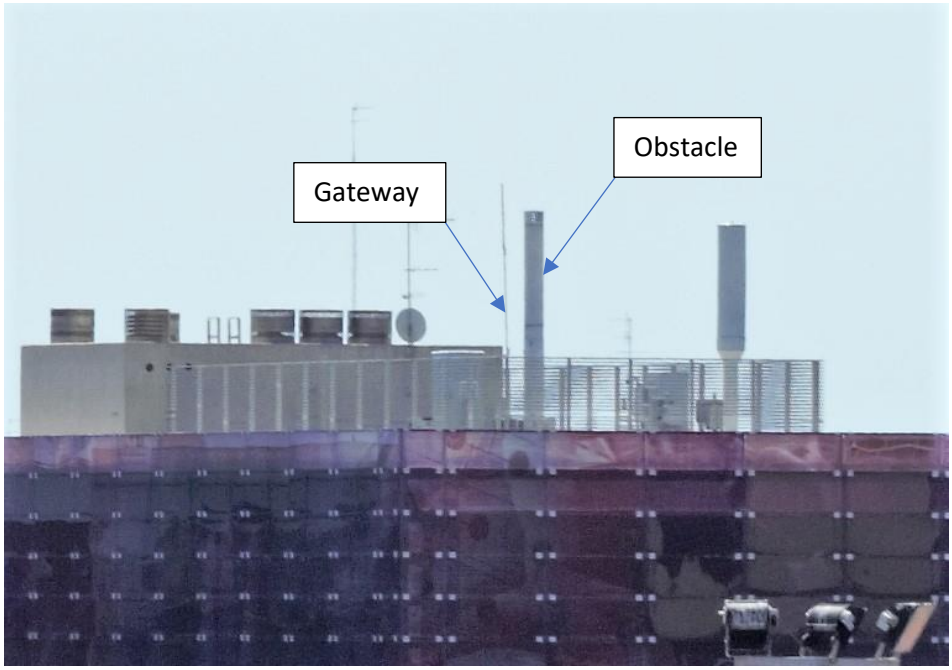

Figure 36: Node's view of the Gateway from Building 7E

The view of the gateway from the node's point of view when located in building 7G, as shown in Figure 37, shows that the Fresnel zone is less obstructed by the Vodafone telecommunications tower located in the gateway's building than the view from the node in building 7E. Both the object and gateway are marked in the image. This image was taken from the node's position with a 50 mm lens and cropped. The real distance between the place where the picture was taken and the gateway is of 540.06 meters. In this case, there are also other obstacles in the transmission path which result in the losses observed.

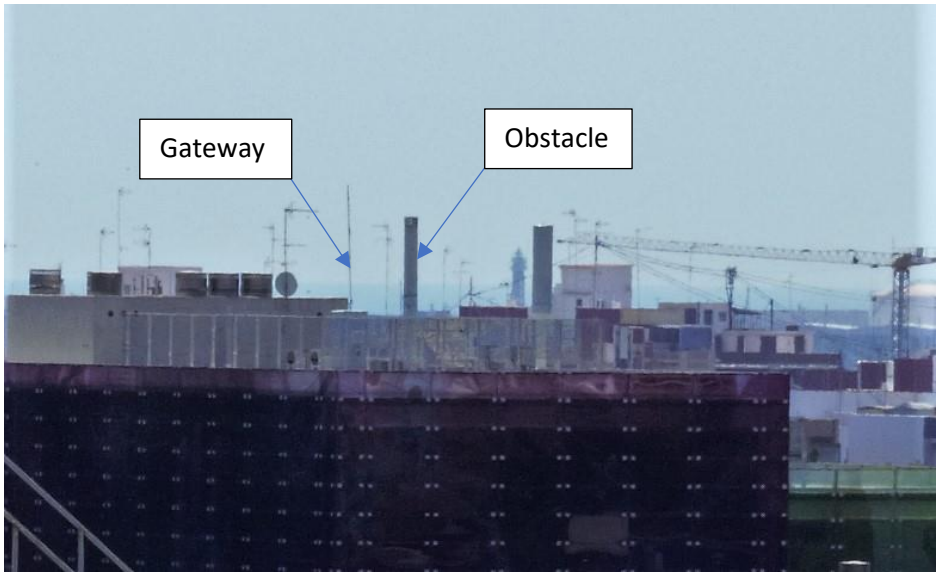

Figure 37: Node's view of the Gateway from Building 7G

10.4.2 RSSI and SNR

After discovering the favourable results obtained presenting very low losses, other tests were conducted to relate the distance to the RSSI (Received Signal Strength Indication) and SNR (Signal-to-Noise Ratio). The locations chosen for this test are the same as the ones of the previous test.

When the distance increases, both the RSSI and SNR decrease. As an example, for the SF 7 CR 4/5, the distance-RSSI and distance-SNR relationships are shown in Figure 38.

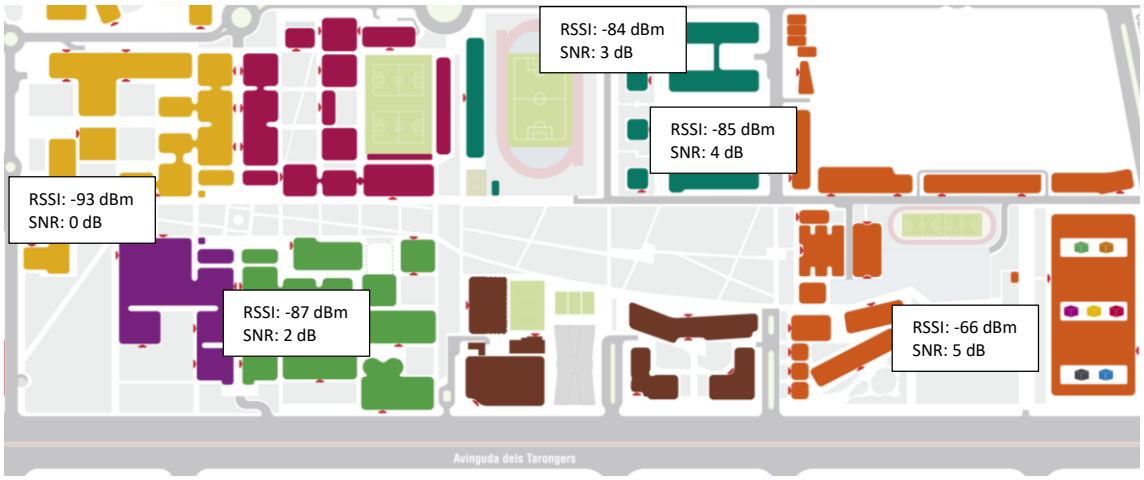

Figure 38: RSSI and SNR with SF 7 and CR 4/5

As shown in Figure 38, the both the Signal-to-Noise Ratio and the RSSI decrement with the distance (in all but buildings 7G and 7E, where the signal from 7E is a bit weaker than the signal from 7G, being 7E nearer to the gateway).

Another interesting example of the results obtained in this experiment is the SF 11 CR 4/8 series of tests. The results of this experiment are shown in Figure 39, including the average results of the RSSI and SNR obtained in each of the locations.

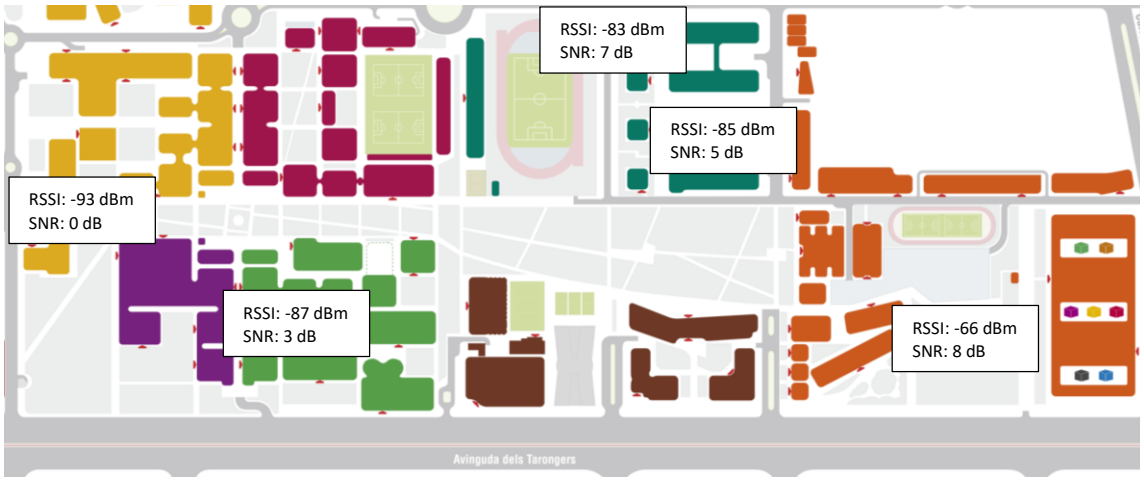

Figure 39: RSSI and SNR with SF 11 and CR 4/8

As shown in Figure 39 and Figure 38, the RSSI stays almost the same when using both the SF 11 and 7. This is due to the transmission power as well as antenna gains and losses staying the same, so that the RSSI stays the same. The SNR varies and that could be caused by the variance of the radio capabilities with different SFs, because of the length of the transmissions or even because of a non-white noise.

In Table 37 are shown the different values that the SNR acquires with the different SF in each location, for a CR of 4/5.

	8P	7E	7G	4N	3A
SF 7	5	4	3	2	0
SF 8	6	5	5	3	0
SF 9	6	4	5	3	-1
SF 10	7	4	5	2	0
SF 11	8	6	7	3	0
SF 12	6	4	5	2	0

Table 37: Values of the SNR with the SF in Different Locations

It may appear from the results shown in Table 37 that the radio has a better SNR when working on the higher spreading factors but the 12, where its SNR returns to lower values. In Figure 40 is shown the evolution of the SNR in the building 8P versus building 7G and building 3A.

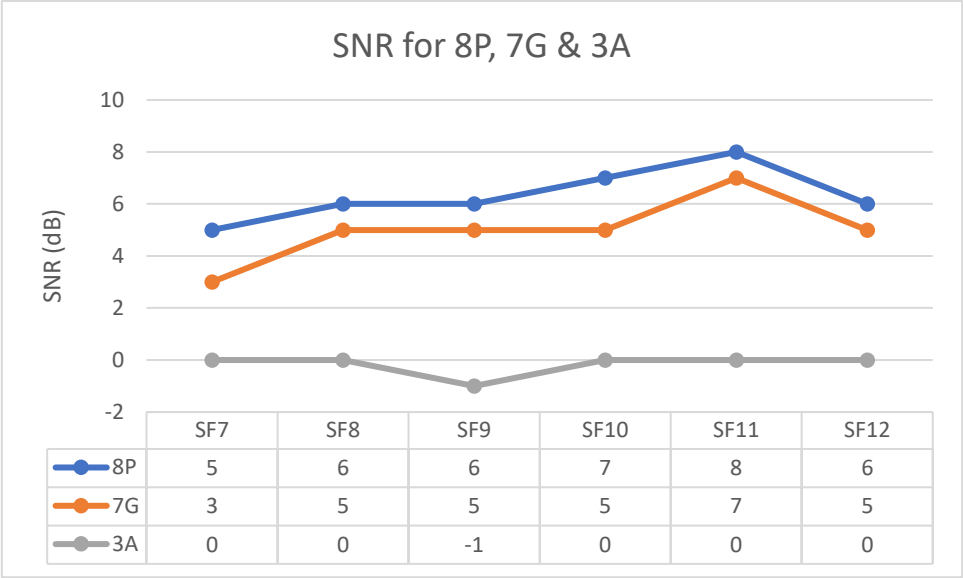

Figure 40: Variation of the SNR with the SF in Buildings 8P, 7G and 3A

As shown in Figure 40, the relation between SF and SNR induces greater variance in the nearest locations as in this case buildings 8P and 7G, but when the distance is greater, where the RSSI and the SNR values are lower, the variance gets reduced.

In the type of environment reviewed, the SNR is a good indicator of whether a packet sent with a given radio configuration will be correctly received and decoded. The higher the SF, the lower the SNR for a correct reception can be. A fitting for the SNR has been conducted in Figure 41.

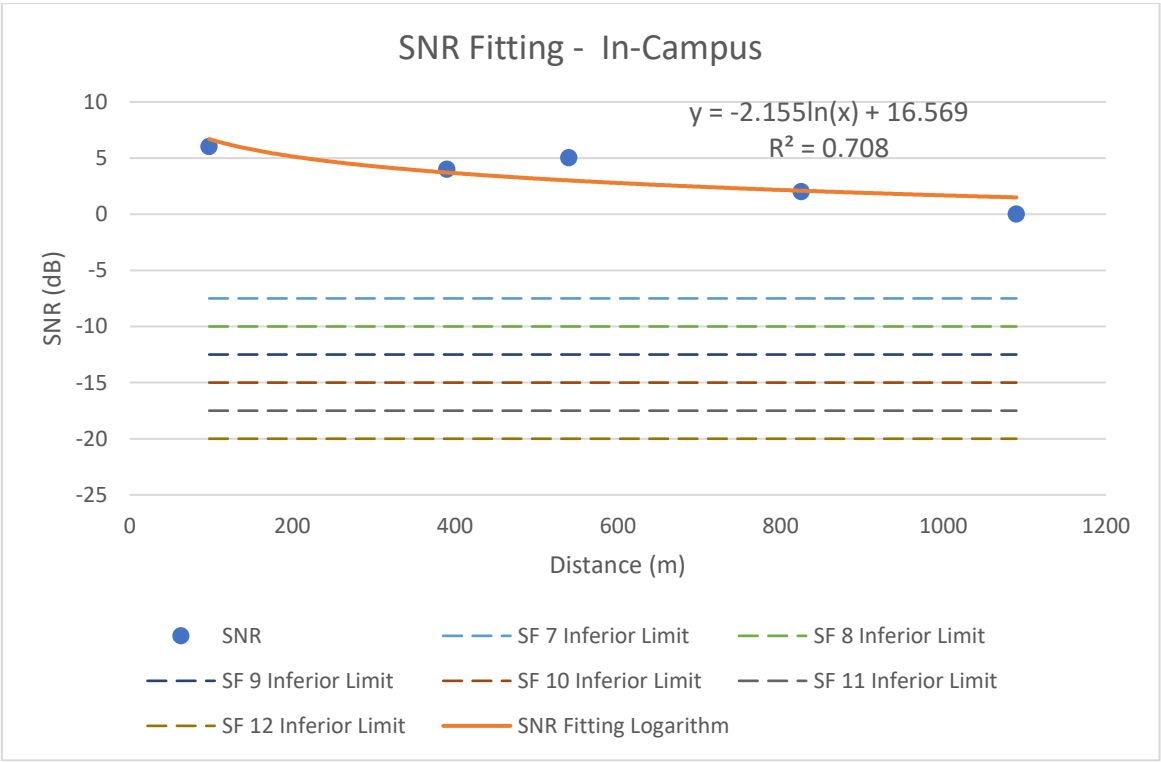

Figure 41: SNR Fitting for In-Campus Experiment

The data for the SNR has been obtained from the packets received with the SF 12 configuration, given that it is the most resilient. The least squares fitting with a logarithmic function obtained for the data of the experiments is not reliable for long-distance predictions because the values of the SNR in short distances are strongly related to the noise introduced in the receiver and not to the “ambient” noise. This is due to how the radio processes the signal and how it obtains the SNR value.

However, when the distances are greater and therefore the RSSI is closer or under the noise floor, the values of the SNR become strongly related with the external noise and RSSI ratio and therefore, they become a good indicator of the distance.

10.4.3 Conclusions

The results analysed show a trend in the SNR evolution with the distance that would lead to a maximum working distance with the most resilient radio configuration of approximately 5 km if the noise and visibility conditions encountered in the experiment were maintained.

The results have also shown that any obstruction in the path of the signal can have a deep effect in the results of a transmission.

Chapter 11: In-Campus No LoS Experiment

11.1 Tests Design and Planning

The No-LoS (No Line of Sight) ground level experiment provides information regarding the use of LoRa in a ground level environment where Line of Sight cannot be easily achieved. It demonstrates how the radio technology handles the extra path losses and lower SNRs (Signal to Noise Ratios).

11.1.1 Gateway

In this test, the gateway remains installed in building 8E, access-F's roof, retaining the same orientation and position on the installation pole as in the NLoS in-campus experiment, with the gateway facing building 2E/3A *Rectorado.*

11.1.2 Node

In this test, the node is temporarily installed in a series of locations where the packet loss, the Signal to Noise Ratio and the Received Signal Strength Indicator are measured while sending a series of packet with different radio configurations in order to assess the effects that different elements in the path of propagation have in the signal, as well as the effects of the distance.

To measure the performance of the LoRa PHY layer, a series of locations with different distances to the gateway and path obstructions were chosen. Some of the locations chosen have buildings between them and the gateway and some only have vegetation.

The number of locations to test was fixed to 9 and the locations were spread over the UPV, choosing those which seemed interesting due to their surroundings and distance to the gateway. The locations are shown in Figure 42.

Figure 42: Locations where the Node is Placed

Given the characteristics of the EU868 band used, the signal is less prone to bouncing and better at breaking through buildings and other obstacles than other higher frequency bands are.

The distance to the gateway is one of the criterium in the selection of the locations and, as shown in Table 38, the distances are mostly distributed in the 700-1400 m range. Less than 700

m produces little losses and 1400 m is the limit of the UPV. Therefore, the density of locations for distances to the gateway lower than 700 meters is reduced, as seen in the table.

Location	Distance to GW
GW	–
1	281.33 m
2	518.97 m
3	706.40 m
4	720.92 m
5	868.57 m
6	1070.76 m
7	1072.59 m
8	1175.61 m
9	1390.02 m

Table 38: Node Locations and their Distance to the Gateway

For some of the distances (700 m and 1070 m), two locations were set: one with only vegetation obstruction and another with buildings obstructing the path. This leads to a better understanding of the effects of the materials and density of the obstructions in the direct (no-bounce) path of propagation.

11.1.3 Radio and Packets Configuration

The program of the gateway and node is the same as in the NLoS experiment's SNR/RSSI measurement. The difference falls both in the locations and in the number of tests per location conducted. As Table 39 shows, the configuration for the radio retains similarities with that of the NLoS tests, but lacks the transmission power variations, staying always in the maximum transmit power setting. This change was to speed up the per-location measurement time and because the Tx power variations showed a very predictable result in the NLoS experiment.

Variable	Value
SF	7-12
BW	125 kHz
PHY Header	Yes (Always)
CRC	Yes (Always)
Preamble	6 (+ 4.25)
DE (Low data rate optimize)	Yes (SF 11 and 12)
Coding Rate	4/5, 4/8
TX Power	14 dBm

Table 39: Radio Configurations for the Different Tests

In this experiment, the tests are composed of 100 packets of 25 bytes, which were found representative of a usual MAC + APP data size for most applications and protocols related to the IoT.

11.2 Experiment Realization

In the next subsections, the installation of the different elements, their locations and their configuration are explained.

11.2.1 Gateway

The Gateway remains installed in the roof of the building 8E, access F. The installation is the same as in the previous experiment (NLoS In-Campus).

11.2.2 Node

The node moves between the positions described in the planning section of this test. In every location the node is placed at ground level + 1.5m by using a tripod to fix its position.

An example of the installation of the node in the locations defined in the planning section is shown in Figure 43, where the node is installed in location 6 near *Rectorado* (as per tests planning section nomenclature), at a distance of 1070.76 meters from the gateway.

Figure 43: Node Installation in Location 6 near Rectorado

The node is connected to the TL-MR3020 router-AP combo which provides of a Wi-Fi connection to the internet. A Huawei 3G internet access point is connected to the router to provide it with a connection to the internet.

A LoRa link is established between the node and the gateway. This LoRa link is shown in Figure 44, where remote location is the location where the node is positioned. The LoRa messages are sent from the node to the gateway.

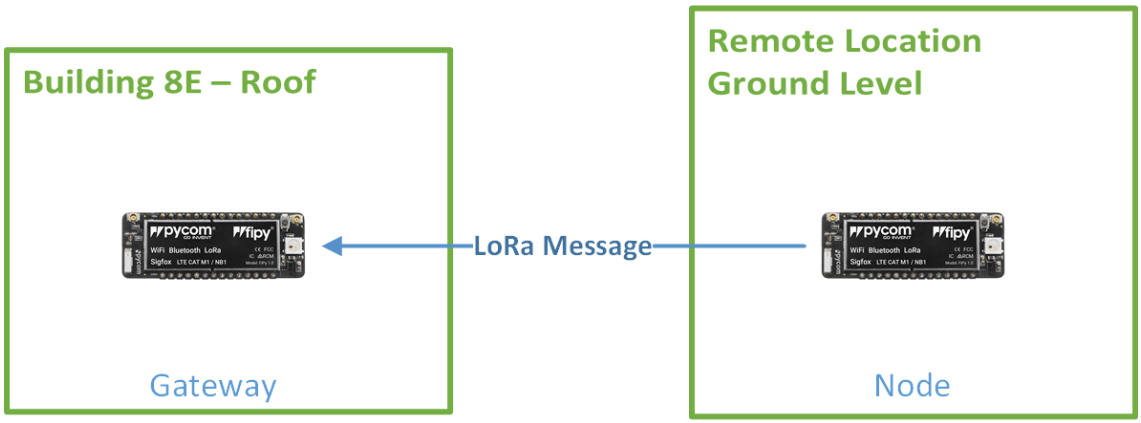

Figure 44: LoRa Link between Node and Gateway

The program run by the node and gateway in this test is the same as the one used in the previous experiment (In-Campus NLoS) when measuring the SNR and RSSI values.

In every one of the locations where the node is placed, the coordinates are recorded to later calculate the distance to the gateway. These coordinates and their respective distances are shown in Table 40.

Location	Latitude (N)	Longitude (E)	Distance to GW
GW	39°28'41.680''	-0°20'02.384''	–
1	39°28'42.788''	-0°20'14.268''	281.33 m
2	39°28'52.368''	-0°20'19.059''	518.97 m
3	39°28'51.300''	-0°20'29.261''	706.40 m
4	39°28'47.219''	-0°20'31.458''	720.92 m
5	39°28'56.789''	-0°20'33.061''	868.57 m
6	39°28'55.848''	-0°20'43.174''	1070.76 m
7	39°28'52.744''	-0°20'45.081''	1072.59 m
8	39°28'58.612''	-0°20'46.486''	1175.61 m
9	39°28'53.765''	-0°20'58.286''	1390.02 m

Table 40: Device's Locations with GPS Coordinates and Distance to GW

The distances shown in Table 40 are distances in the horizontal plane, due the imprecision of the GPS when measuring height.

11.3 Results Analysis

After the NLoS experiment, the No LoS experiment helps achieve a vision of the performance of LoRa in No LoS environments where the gateway and node do not have a direct line of sight, where the Fresnel zone is not respected, and where the nodes are located almost at ground level to simulate a Smart City sensor network environment.

As previously stated in the planning section, the locations have different types of obstacles in their path to the gateway, such as vegetation and buildings. Depending on the distance and the number of obstacles of each type, the SNR and therefore the RSSI will vary from location to

location, and the transmissions will have different PoS for different SF, depending on the SNR requirements of each SF.

11.3.1 Results of Opposite Configurations

The two extremes in the radio configurations tested are SF 7 with a CR 4/5 and SF 12 with a CR 4/8, being the first the configuration that should suffer most from bad SNRs and the later the most resilient. In Figure 45 are shown the results for the RSSI and SNR obtained for the different locations when using the SF 7 CR 4/5 radio configuration.

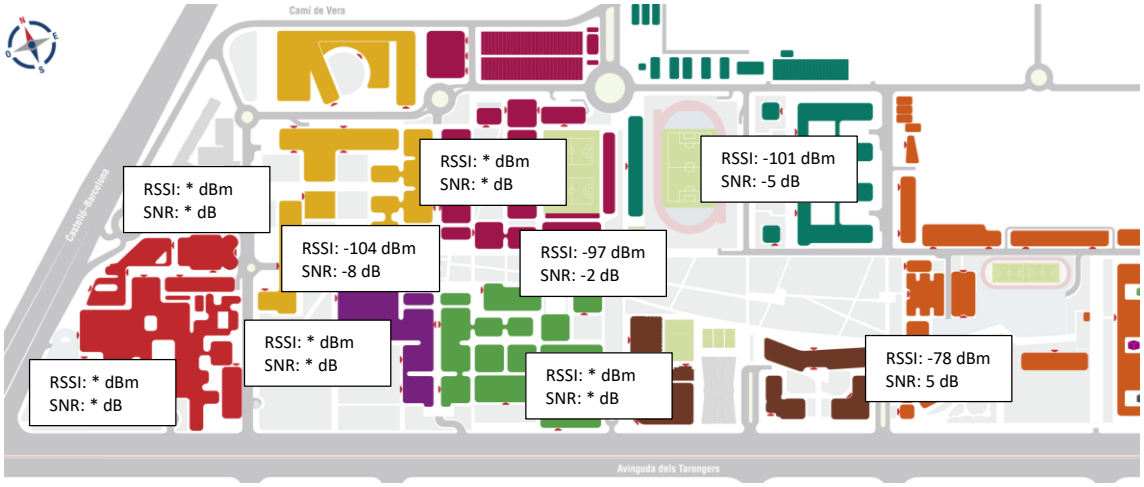

Figure 45: RSSI and SNR Obtained with SF 7 and CR 4/5

The time needed to transmit a 25 bytes packet with the SF 7 CR 4/5 configuration is of 62 ms, and the coverage shown in Figure 45 is for a transmit power of 14 dBm. As shown in Figure 46, the worse the SNR is, the less packets are received (and therefore, the lower the PoS is).

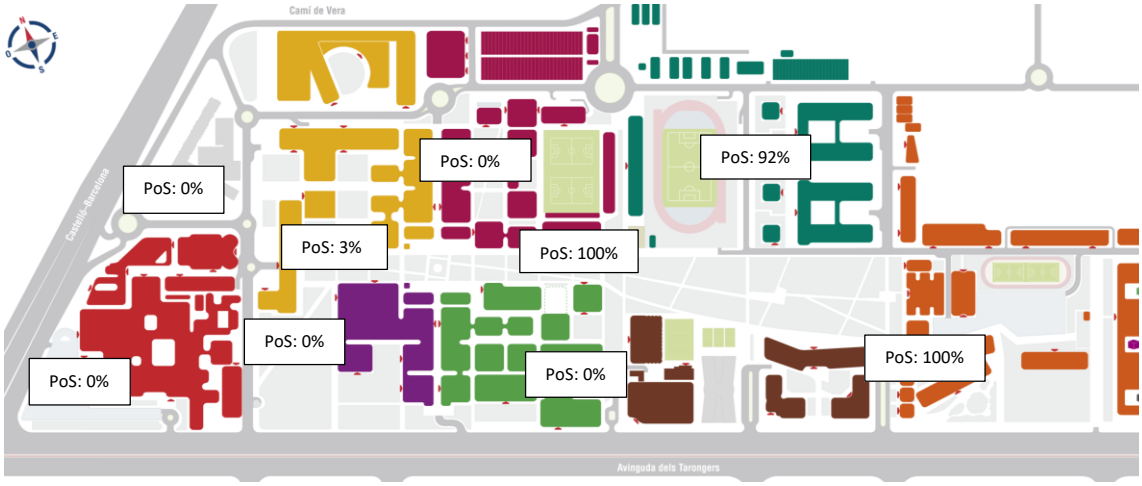

Figure 46: PoS Obtained with SF 7 and CR 4/5

To obtain better results for longer distances and/or paths with more dense obstacles, the solution is to increase the spreading factor and codding rate. The results obtained with the most reliable radio configuration that can be implemented with our current setup are shown in Figure 47, where both the RSSI and SNR obtained for the SF 12 and CR 4/8 radio configuration are shown.

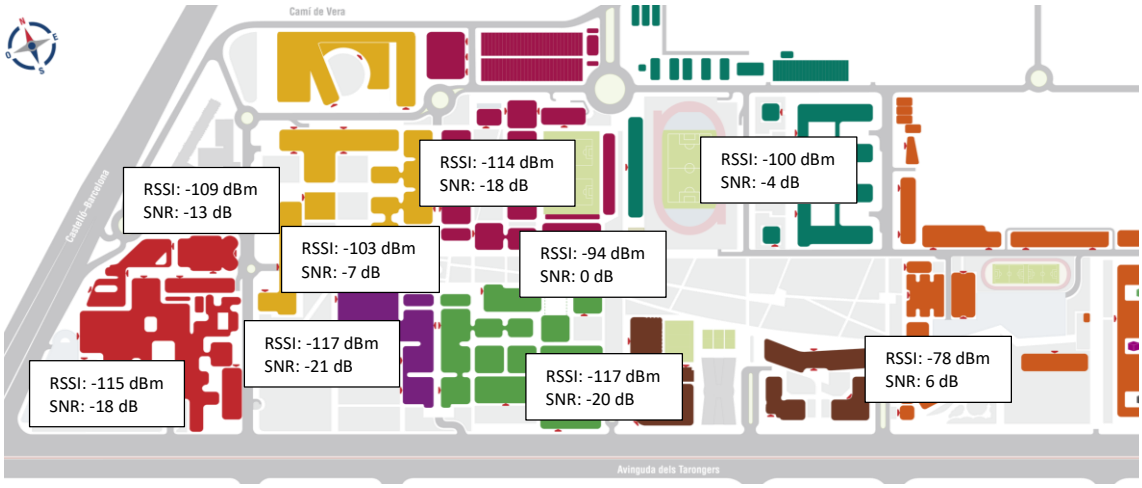

Figure 47: RSSI and SNR Obtained with SF 12 CR 4/8

The time needed to transmit a 25 bytes packet with the SF 12 CR 4/8 configuration is of 1975 ms (which is substantially higher than that of the SF 7 CR 4/5 configuration), and the coverage shown in Figure 47 is for a transmit power of 14 dBm. As shown in Figure 48, the worse the SNR is, the less packets that are received (and therefore, the lower the PoS is).

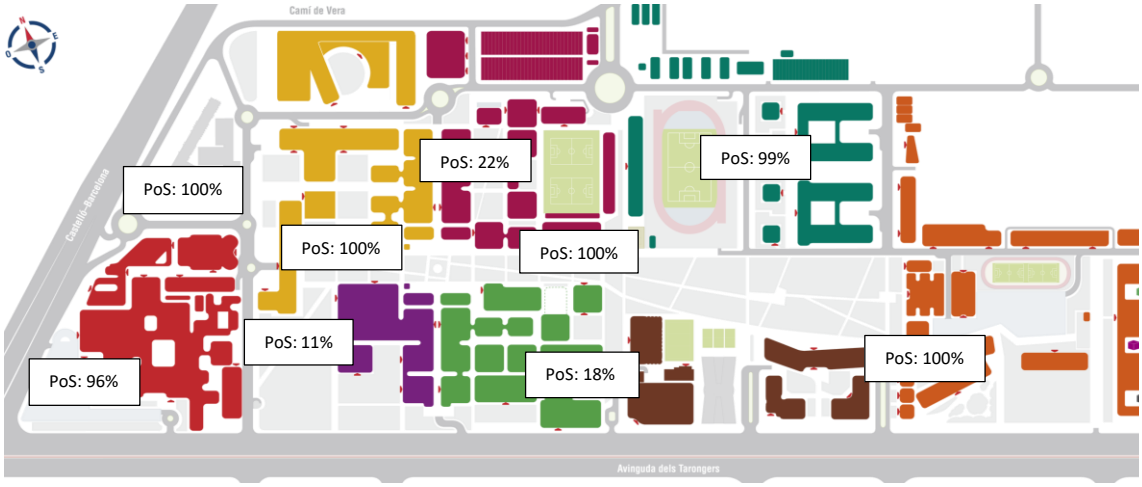

Figure 48: PoS Obtained with SF 12 CR 4/8

11.3.2 Effects of RSSI and SNR in the PoS

According to the manufacturer (Semtech) of the communications solutions implemented in the devices used for the experiment, the radio sensitivity for a 1% PER (Packet Error Rate) (99% PoS equivalent), a CR of 4/6 (a compromise between both codding rates used), a bandwidth of 125 kHz (as the one used), a preamble of 12 symbols (8 optional + 4.5 fixed) and a payload of 64 bytes is as shown in Table 41.

SF	LoRa Sensitivity
7	-123 dBm
8	-126 dBm
9	-129 dBm
10	-132 dBm
11	-133 dBm
12	-136 dBm

Table 41: LoRa Sensitivity by SF According to Semtech

As the data for sensitivity provided by the manufacturer is for an ideal scenario with low noise, the sensitivity values obtained in the experiment are higher than the ones provided by the manufacturer, needing then a higher RSSI to obtain a correct reception of the packet. The preamble configured in the devices used for the experiment is also shorter, leading to a lower probability of packet detection.

The high sensibility is achieved thanks to LoRa's capability to work with negative SNRs (Signal to Noise Ratio). The minimum SNR with which the radio will correctly receive packets is shown in Table 42 for the different SFs.

SF	LoRa Demodulator SNR
7	-7.5 dB
8	-10.0 dB
9	-12.5 dB
10	-15.0 dB
11	-17.5 dB
12	-20.0 dB

Table 42: LoRa SNR by SF According to Semtech

As can be observed from the data provided by Semtech shown in Table 42 about the SNR values for a correct reception, the laboratory values provided are very similar to those obtained in the limits of reception on the No LoS experiment shown in Table 43.

SF	Minimum LoRa Demodulator SNR
7	-8 dB
8	-10 dB

SF	Minimum LoRa Demodulator SNR
9	-14 dB
10	-16 dB
11	-18 dB
12	-21 dB

Table 43: LoRa SNR by SF Obtained in the Experiment

The lower SNR achieved for some of the Spreading Factors is lower (better) than the value provided by the manufacturer of the chip. This is because the codding rate used is 4/8 instead of 4/6 and the values given by the manufacturer are for a 1% PER, while the values obtained in the experiment are for higher PERs.

While the SRN is equal or better than the one offered by Semtech, the minimum RSSI obtained in the experiment for the different SFs is higher than those offered by Semtech shown in Table 41.

11.3.3 Effects of the CR in the PoS

The PoS for each SF in a given location is an indicator of the reliability of the communications. As shown in Figure 49, the PoS in a given location depends on both the SF and the CR in use.

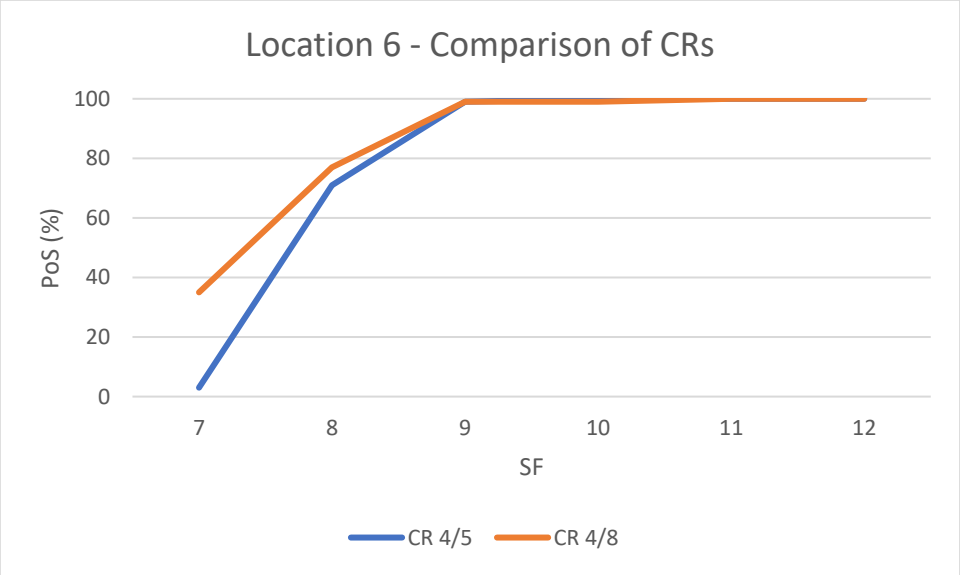

Figure 49: Comparison of CRs in Location 6

The results obtained confirm that the greater the SF and lower CR, the greater the PoS. For example, with SF 7, when the CR is of 4/5 the PoS is of a 3%, while with a CR of 4/8, the PoS elevates to a 35%. This difference between CRs presents greater impact in the PoS with lower SFs than with higher ones in location 6.

Location 8 has its path to the GW more obstructed with buildings than location 6. This extra signal loss causes lower SNR, which, as shown in Figure 50, leads to a total loss of the higher data rate Spreading factors 7 and 8.

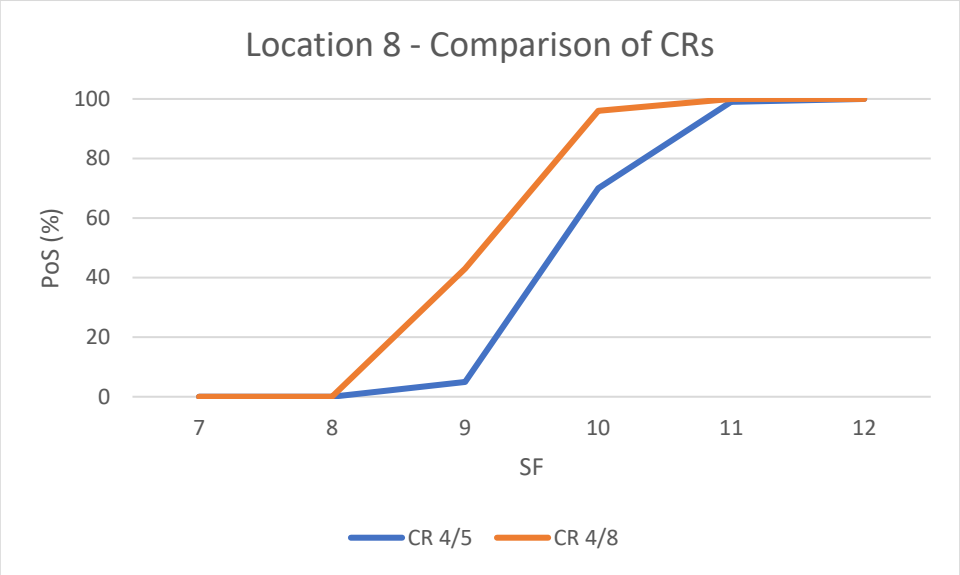

Figure 50: Comparison of CRs in Location 8

The CR also has a great effect in location 8, leading to better PoS when using CR 4/8 than when using CR 4/5. As an example, with SF 10, when the CR is set to 4/5, the PoS is of an unreliable 70%, while when the CR is set to 4/8, the PoS turns to a reliable 96%.

11.3.4 Conclusions

The results obtained in the In-Campus No LoS Experiment show that while the distance is an important factor when considering signal degradation and path loss, two other factors have had a greater impact.

The first factor is the composition, number, volume and position of the obstacles in the path of propagation of the signals, as may be buildings and vegetation.

The second factor to consider are the surroundings of the node's position. Depending on the objects surrounding the node such as buildings, and their position relative to the node, they can have a great inference in the results obtained for both the signal degradation and path loss.

These factors reflect in the SNR and RSSI which finally reflect in the PoS of a given transmission between the two devices (gateway and node).

Chapter 12: OUT-CAMPUS EXPERIMENT

12.1 TESTS DESIGN AND PLANNING

The objective of this test is to assess the robustness and capacity of a LoRa network in a Near Line of Sight environment where the only obstacles in the LoS are vegetation, where there is no intrusion of objects as vegetation and buildings in the direct path between the node and the gateway. The environments reviewed represent an agricultural and port environment.

12.1.1 Gateway

In this test, the gateway remains installed in the same conditions as in the previous experiment (In-Campus No LoS), but with a different orientation, given that the installation pole can become an obstacle for the correct reception when it is on the path between gateway and node, due to the effect it has in the radiation pattern of the dipole.

12.1.2 Node

In this test, the node was temporarily installed in every one of the locations shown in Figure 51 (one by one). It was installed on top of a tripod which is 1.5 meters high. At the end of the tests in each location, the node was then uninstalled from this location and installed in the next one. This procedure was repeated until all the locations were visited.

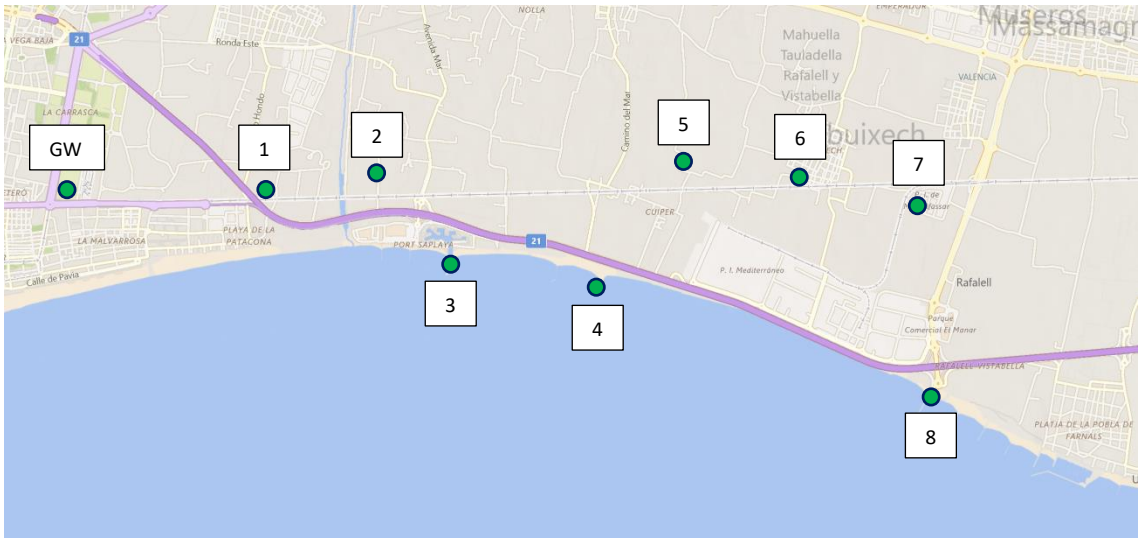

Figure 51: Locations where the Node is Placed

The different locations in the map are at a given distance, which, along with the description of the location are shown in Table 44. The distances are carefully selected to achieve a good representation of the effects of the distance in a long distance NLoS environment, where the only obstructions to the LoS are vegetation (for the agricultural environment). However, for points 3,4 and 8 which represent the port environment, the Fresnel zones are heavily obstructed by a group of buildings located in the signal path.

Location	Description	Distance to GW
GW	Building 8E – Access F – Roof	-
1	“Carrer Camí a la Mar”	2.05 km
2	Unnamed Road near Port Saplaya	3.07 km
3	Port Saplaya – Sea Port’s Breakwater	3.86 km
4	Breakwater near Port Saplaya	5.28 km
5	“Camí de la Mar” near Cuiper	6.06 km
6	Albuixech	7.27 km
7	Industrial Park near Masalfasar	8.38 km
8	Puebla de Farnals	8.71 km

Table 44: Node Locations and their Distance to the Gateway

12.1.3 Radio Configuration

The radio configuration of the node and gateway varies between a given set of parameters. These parameters, as shown in Table 45, are the same as those used in the SNR and RSSI experiment conducted on top of the buildings (NLoS In-Campus Experiment).

Variable	Value
SF	7-12
BW	125 kHz
PHY Header	Yes (Always)
CRC	Yes (Always)
Preamble	6 (+ 4.25)
DE (Low data rate optimize)	Yes (SF 11 and 12)
Coding Rate	4/5, 4/8
TX Power	14 dBm

Table 45: Radio Configurations for the Different Tests

The experiment consists of sending 100 packets with different SF and CR configurations from the node and logging the number of correct and incorrect packets; and logging their SNR and RSSI. The SNR and RSSI are then averaged by radio configuration (for both the correct and incorrect packets separately).

12.2 Experiment Realization

As previously stated in the planning section of this experiment, the gateway remained installed in building 8E, access F’s roof. The heading of the gateway in the installation pole was changed, as shown in Figure 52, to point the path of vision to the locations where the nodes were placed which is shown in Figure 53.

Figure 52: Gateway with new Heading

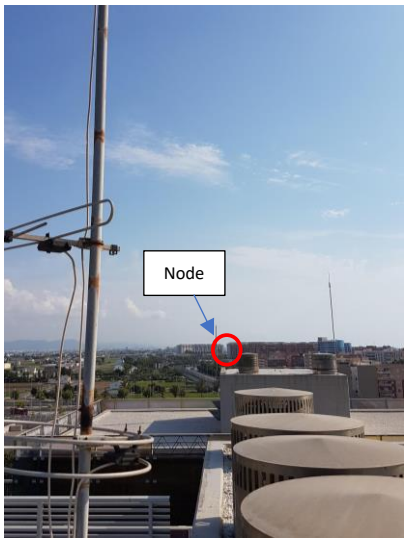

Figure 53: Node from Gateway's View

As also stated in the planning section, the node was installed in the planned locations on top of a 1.5 meters high tripod. The coordinates (latitude and longitude) of the locations where the node was installed (W), the distance to the gateway and the description of the site are shown in Table 46.

Location	Description	Latitude (N)	Longitude (E)	Distance to GW
GW	Building 8E – Access F – Roof	39°28'41.680''	-0°20'02.384''	-
1	"Carrer Camí a la Mar"	39°29'46.948''	-0°19'48.591''	2.05 km
2	Unnamed Road near Port Saplaya	39°30'20.218''	-0°19'48.187''	3.07 km
3	Port Saplaya – Sea Port's Breakwater	39°30'38.471"	-0°19'05.923"	3.86 km
4	Breakwater near Port Saplaya	39°31'21.909"	-0°18'46.462"	5.28 km
5	"Camí de la Mar" near Cuiper	39°31'56.237''	-0°19'32.014''	6.06 km
6	Albuixech	39°32'34.015''	-0°19'16.778''	7.27 km
7	Industrial Park near Masalfasar	39°33'07.812''	-0°18'56.571''	8.38 km
8	Breakwater near Puebla de Farnals	39°33'00.738"	-0°17'38.762"	8.71 km

Table 46: Device's Locations with GPS Coordinates and Distance to GW

The GPS Coordinates found in Table 46 follow the WGS84 (World Geodesic System 1984) datum standard. The distances shown in Table 46 are distances in the horizontal plane, due the imprecision of the GPS when measuring height.

The installation of the node was similar in all the locations. An example of the installation of the node in Location 4 is shown in Figure 54, where the node is installed in a breakwater near Port Saplaya.

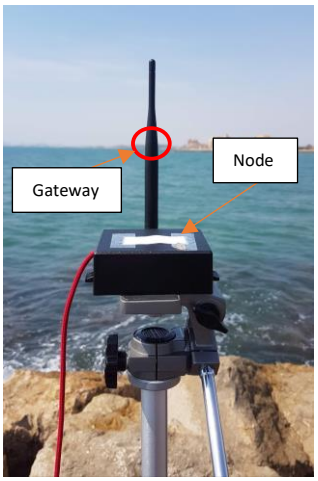

Figure 54: Node Installation and Gateway from Node's View.

The out-of-band management interface (MQTT) was provided to the node, as in previous experiments, by the TL-MR3020 router-AP combo along with a Huawei 3G gateway to provide access to the internet via Wi-Fi to the node.

The out-of-band management interface for the gateway was provided by the same router-AP combo as for the node but without the 3G modem, having in this case a wired connection to UPV's network.

The LoRa link established between the devices is shown in Figure 55, where the remote location is the location where the node is placed in each of the tests. The LoRa message is sent in an uplink channel (node to gateway).

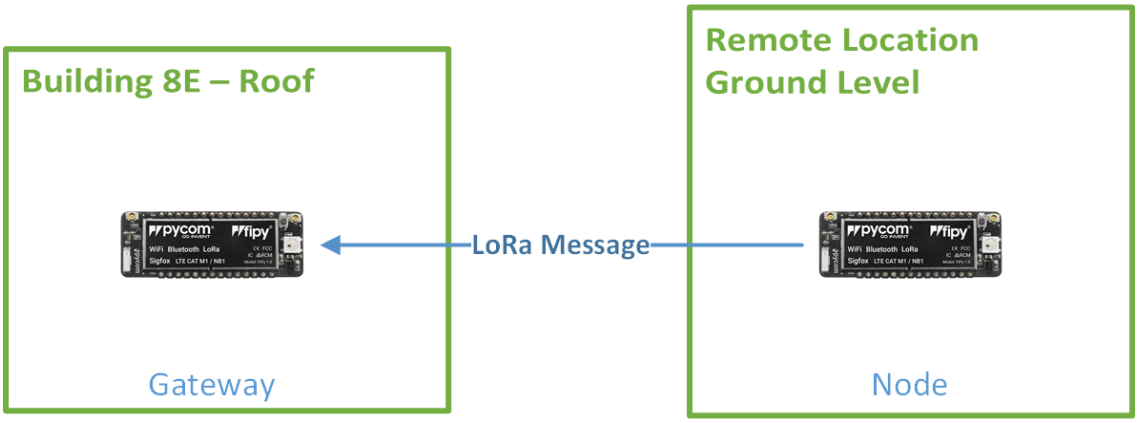

Figure 55: LoRa Link between Node and Gateway

The program routines remain the same as in the previous experiments, both for the gateway and the node.

12.3 Results Analysis

After the UPV in-campus experiment was concluded, an extra test with longer node-gateway distances was conducted. The results help to show the limits of the NLoS model proposed.

In this new model, as previously stated, for the agricultural scenario, the path between both devices participant of this experiment is mostly only obstructed by vegetation, leading to a Near Line of Sight scenario where the Fresnel zone is obstructed and the Line of Sight might be by vegetation and other small objects.

The results of this test shed light on the behaviour of the LoRa PHY communications layer in an environment where the signal path is only obstructed by small objects. This scenario would represent a country-side deployment of LoRa using the hardware used.

However, in the port environment, the Fresnel zones are obstructed by two groups of buildings, instead of vegetation.

Therefore, in this experiment there are two scenarios: the first one where the Fresnel zone is only obstructed by the ground, vegetation and small objects as shown in Figure 56 and the second one where the Fresnel zone is almost totally obstructed by the ground and two groups of buildings as shown in Figure 57.

Figure 56: Gateway view in 1st Scenario

Figure 57: Gateway view in 2nd Scenario

On the one hand, the results obtained with the first scenario where the Fresnel zone is less obstructed, the degradation of the SNR, RSSI and PoS occurs over a long distance and at a low rate, achieving distances over 8 kilometres.

On the other hand, the results obtained with the second scenario where the Fresnel zone is almost totally obstructed show a severe degradation of the SNR and RSSI (and therefore of the PoS) with the distance, achieving little more than 5 kilometres.

12.3.1 First Scenario

In the first scenario (Agricultural), the results show that at distances lower than 3 kilometres the reception of the packets is almost perfect for all the radio configurations used. From there, the PoS starts to degrade.

At a distance of 2 kilometres, the SNR (the factor on which the correct reception of a packet depends) is of -3 dB, and the RSSI is of -105 dB, which according to the manufacturer of the communications IC indicates that with all the radio configurations used, the error rates in the reception should be lower or equal than 1% (PoS 99%). As shown in Figure 58, the data obtained (percentage of correct (PoS) and incorrect packets) lays between the specified parameters.

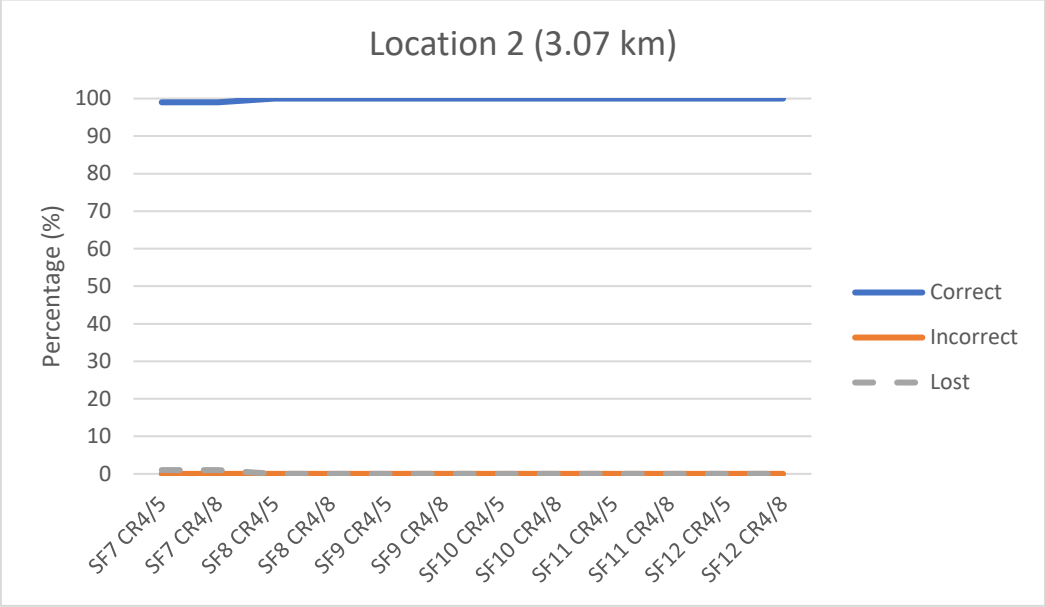

Figure 58: Percentage of Correct and Incorrect Packets Received at Location 2

When further increasing the distance, losses start to appear in the configurations where a lower Spreading Factor and Coding Rate was used. An example of this is found at the results from Location 5 shown in Figure 59.

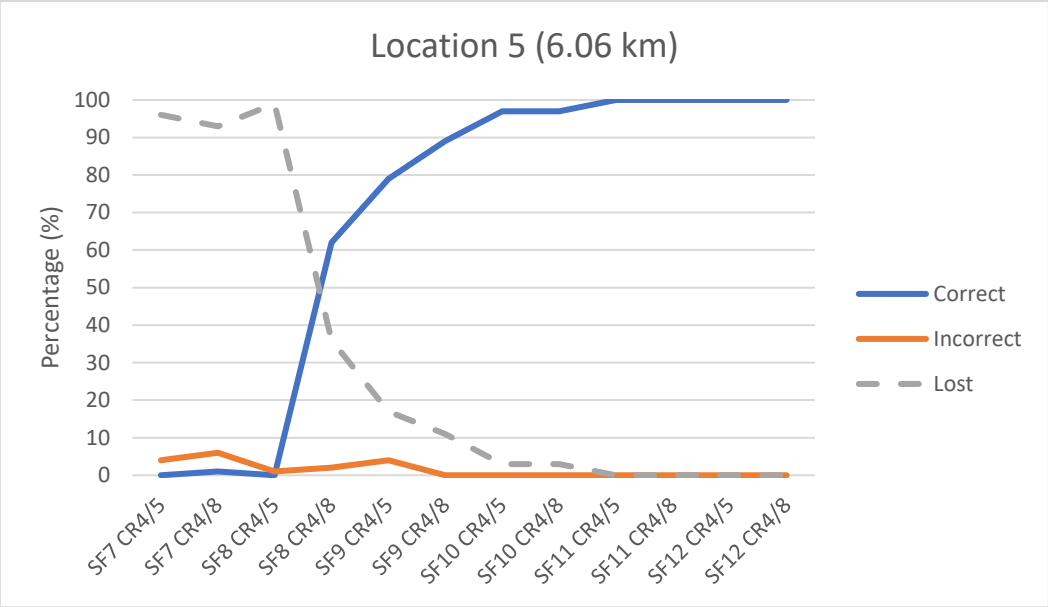

Figure 59: Percentage of Correct and Incorrect Packets Received at Location 5

In this location, most of the packets received with SF 7, which is the configuration most vulnerable to the distance (from the ones used), are erroneous and the PoS is very low. From the SF 8 with a CR of 4/8, the PoS starts increasing until SF 11, where the PoS achieves values of 100%.

Finally, in the last location where the proposed LoS conditions could be accomplished (with a scenario similar enough that the data is relevant), the only SF which achieves a PoS higher or equal to 99% is the SF 12. The PoS of all the radio configurations tested in this location is shown in Figure 60.

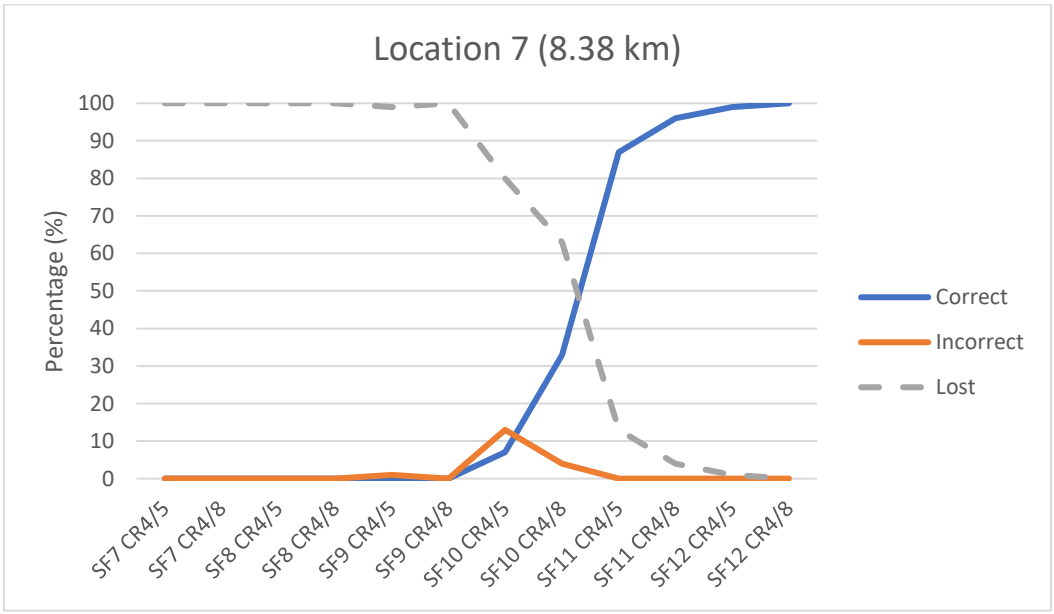

Figure 60: Percentage of Correct and Incorrect Packets Received at Location 7

The evolution of the PoS in the first scenario for all the radio configurations with a CR of 4/8 (the most reliable radio configuration) is shown in Figure 61.

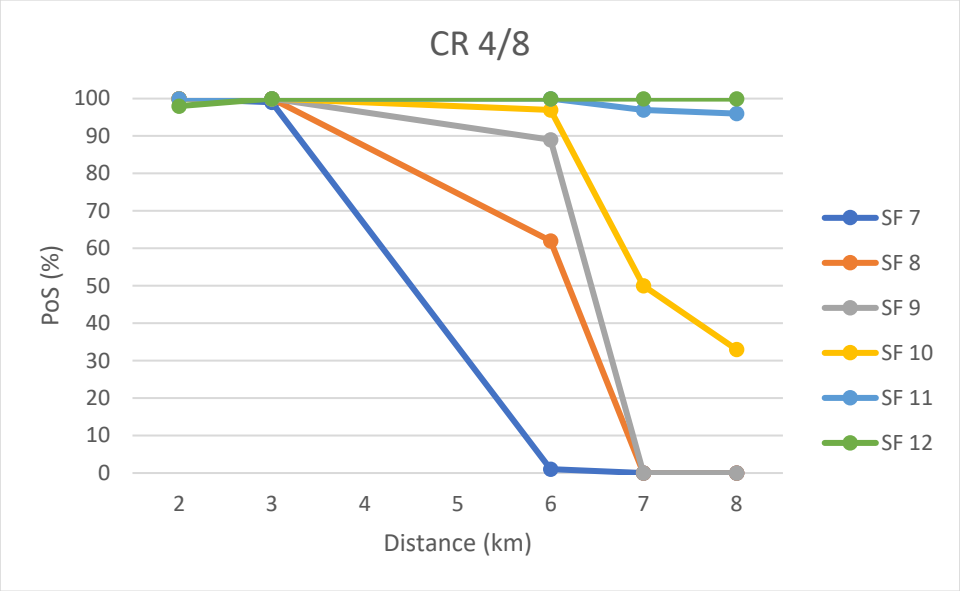

Figure 61: Evolution of the Probability of Success for the different SFs

The PoS of the lower SF quickly diminishes in the first 6 km, while the PoS of the SF greater than 10 remains usable until the 8 km, where only SF 11 and 12 maintain a PoS good enough for the 95 percentile, which is an industry standard for a good transmission scenario.

The evolution of the SNR in the first scenario when using SF 12 and CR 4/8 is shown in Figure 62, where the evolution of the SNR with the distance between the gateway and the node is represented. The SNR is one of the values on which the correct reception of a given radio configuration depends.

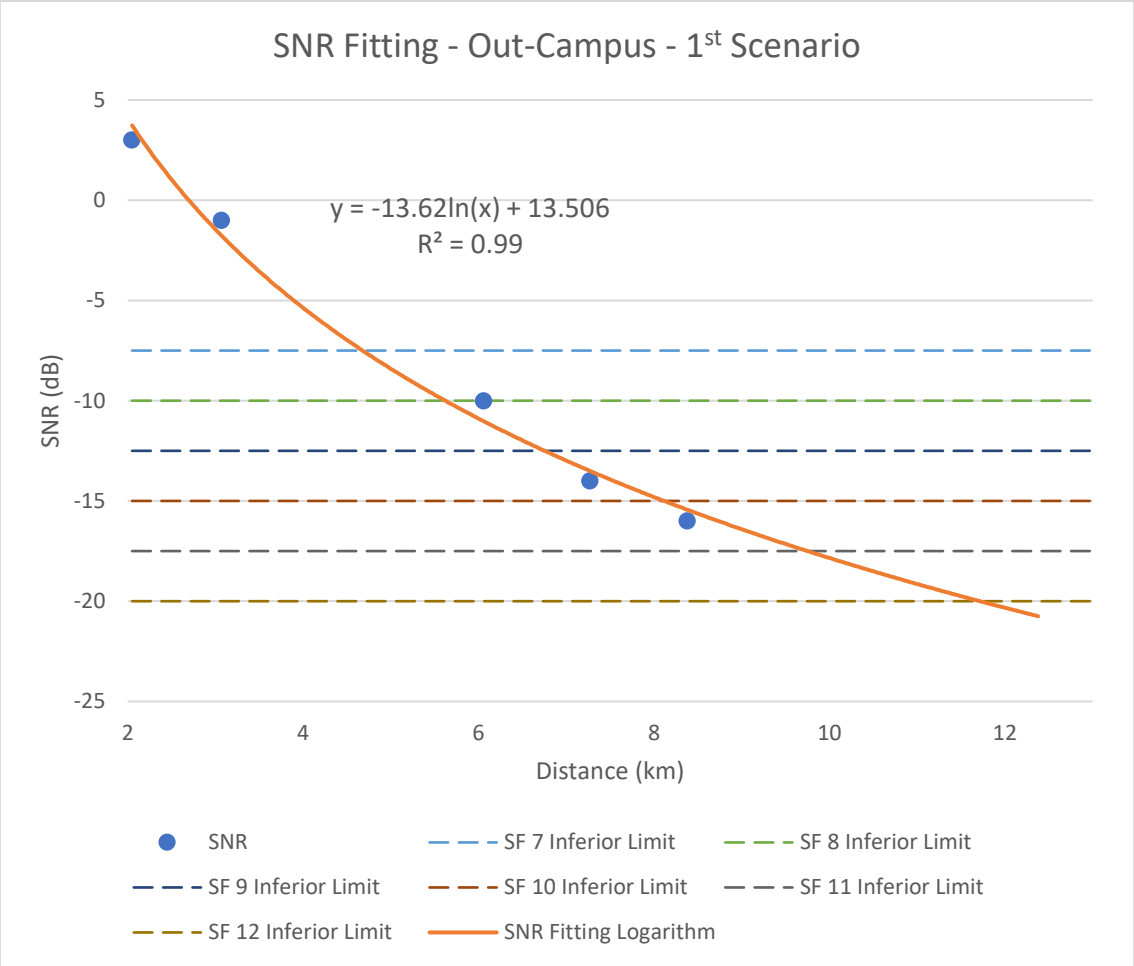

Figure 62: SNR Fitting for the 1st Scenario of the Out-Campus Experiment

With the progression observed in Figure 62 and knowing that the SNR in the last location was of -16 dB, a location a few kilometres further away from the gateway would show significant signs of degradation in the most reliable SF and radio configuration used: SF12 CR 4/5 and 4/8.

The data shows that with the least squares fitting with a logarithmic function obtained for the SNR data of the experiment, the maximum distance when using a SF of 12 in the conditions of the experiment should be of around 11.5 km.

12.3.2 Second Scenario

The second scenario (Port) presents a much stronger degradation on the signal received per kilometre of distance between node and gateway. This results on a lower PoS than the first scenario for the same radio configurations at similar distances.

At a distance of 3.9 kilometres, as shown in Figure 63, the signal shows a degradation equivalent to that of Location 5 of the first scenario at 6 km. The PoS at this distance (percentage of correct packets) shows that the radio configurations that have a SF of 7 or 8 present a severe degradation, receiving almost only erroneous packets. As shown in Figure 63, this improves with higher SFs.

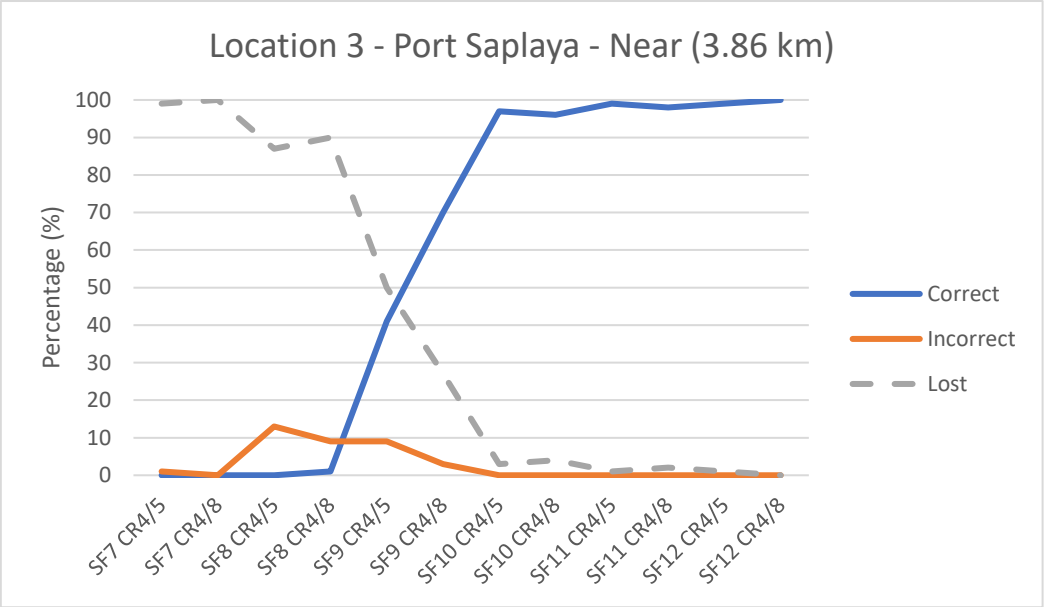

Figure 63: Percentage of Correct and Incorrect Packets Received at Location 3

Further increasing the distance to 5.3 km induces a descent in the PoS of all the radio configurations, leaving as usable and mostly reliable only the radio configurations which use the SF 12. The SNR at this location is already very low at -17.5 dB, which according to the manufacturer makes almost unusable any SF lower than 12, which coincides with the data shown in Figure 64.

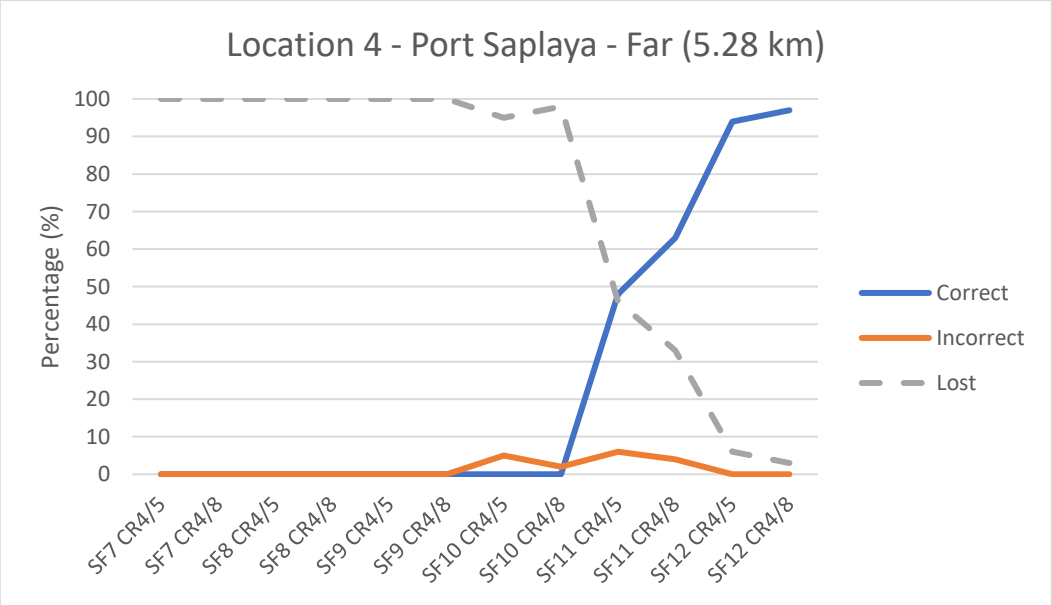

Figure 64: Percentage of Correct and Incorrect Packets Received at Location 4

Finally, in the last location of this scenario, at a distance of 8.7 km, all the radio configurations tested fail to communicate as no correct neither incorrect packet is received. The results are shown in Figure 65.

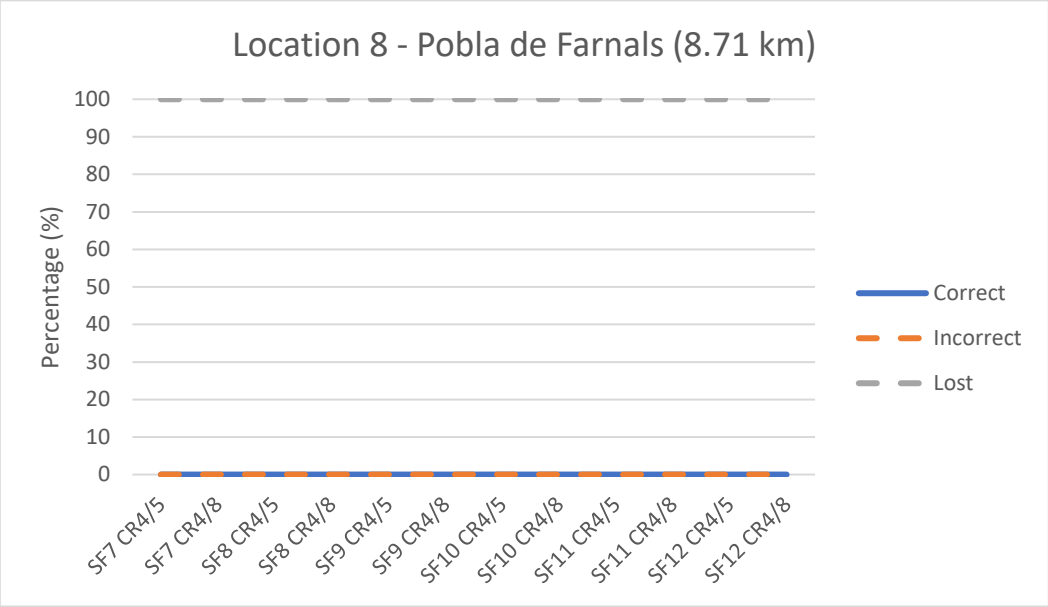

Figure 65: Percentage of Correct and Incorrect Packets Received at Location 8

The evolution of the SNR in the second scenario when using SF 12 and CR 4/8 is shown in Figure 66, where the SNR is represented varying according to the distance between the gateway and the node.

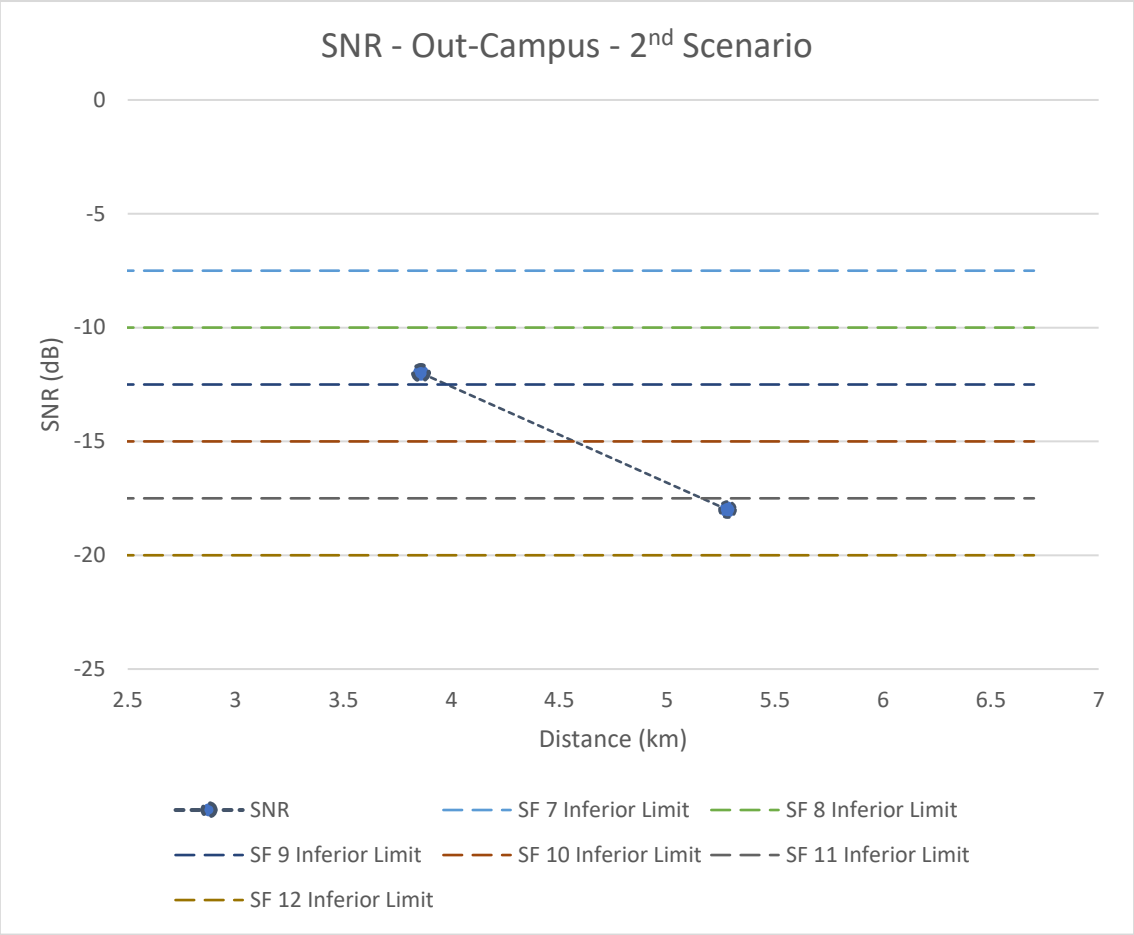

Figure 66: SNR for the 2nd Scenario of the Out-Campus Experiment

In Figure 66, there is no logarithmic fitting because of the limited number of points with valid data. Only a discontinuous line joining the two points has been represented. With the data obtained and observing the evolution, the most resilient radio configuration could work until 6 km approximately.

12.3.3 Bitrates vs Radio Configurations

Choosing a higher SF configuration or extra bits of data redundancy via CR provides of higher link budgets and therefore allows for extra distance, but this comes at the cost of the transmission speed or bitrate. A comparison between different CRs and the evolution of the bitrate with the SF is shown in Figure 67.

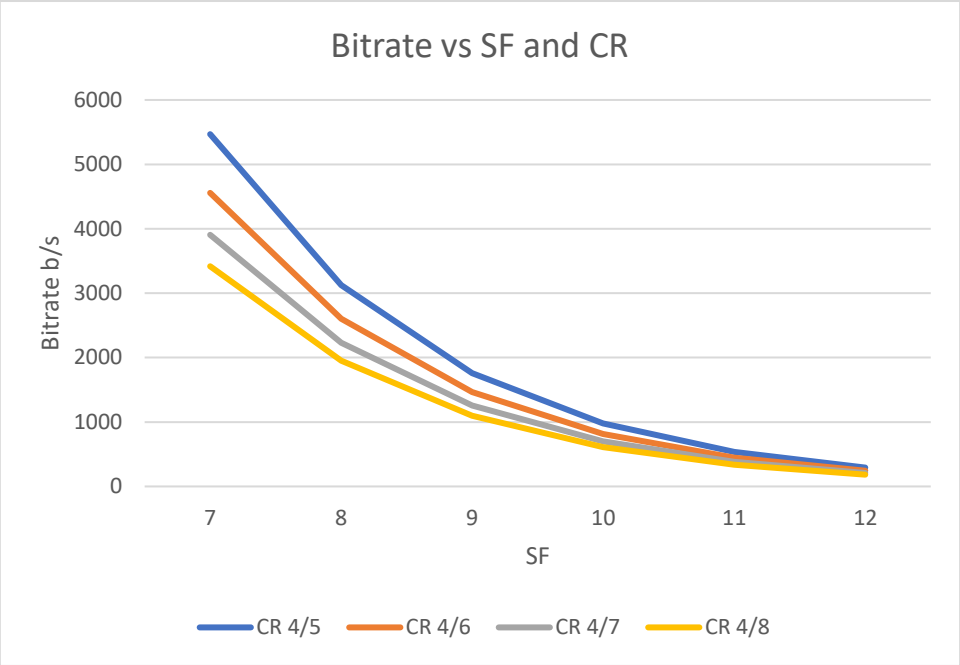

Figure 67: Bitrate vs SF and CR of a LoRa transmission

Chapter 13: CONCLUSIONS

The following conclusions can be extracted from the work carried out in this document:

- Depending on the type, size, number and location of obstacles encountered in the signal path, the transmission distance varies significantly.
- Different obstructions to the Fresnel zones have a great impact on the signal degradation and, therefore, on the maximum distance and quality of a communication.
- In a countryside or agricultural environment, where vegetation and small constructions are in the signal path, the distance that can be achieved with the LoRa hardware and configuration used in the Out-Campus experiment is of about 11.5 km.
- In the UPV Campus Reference Implementation for modelling a Smart City environment, the coverage achieved for an 80% PoS (Probability of Success) was almost complete (1.4 km long).
- In a Smart City and Smart Campus environment where buildings are present, for a ground-level node placement, both the number of obstacles, their composition and placement in relation to the node's location have a great impact on signal degradation.
- For simultaneous non-orthogonal transmissions (in the same channel and spreading factor), the LoRa radio can distinguish between them with only 6 dB of difference between the received power of the signals. This elevates the PoS in congested scenarios.
- While LoRa's channel capacity is small, it can be further expanded with the use of multiple simultaneous channels, enabling the high-density deployments necessary for a Smart City scenario.
- For low-density implementations, cheaper hardware as that of a node can be used in the gateway to reduce costs without great performance impact.

Chapter 14: FUTURE RESEARCH

The results of the experiments have shown the great potential of the LoRa communications technology. There are a few extra experiments whose realization would be useful for future studies. An extension of the experiments already conducted in this work may also prove useful for future research. In the next sections, some ideas are proposed about the continuation of the experimental work.

14.1 NEW EXPERIMENTS

There are some experiments that would present interest for the scientific community. These experiments would provide more use-cases for LoRa and could provide interesting insights in the technology's limitations and advantages.

An example of future possibilities for the experimentation are the industrial IoT and Wireless Sensors areas of study. These future studies could analyse the effects that the obstacles and the increased multipath propagation intrinsic to an indoor scenario would have in the correct reception of the information sent across the network.

14.2 FURTHER DEVELOPMENT

Some of the experiments conducted contain enough data to measure some of the most interesting parameters but not enough for other parameters which need a higher statistical sample (for example, PoS). Also, extra locations could be added to improve the models. Therefore, these experiments would benefit from further development to obtain all the data and accuracy required.

The data collected in this work will be used in a research paper that is expected to be published soon after the presentation of this work. Also, the insights of the technology obtained during the realization of this project may serve to guide future research and to decide which lines of research are worth continuing.

14.3 LINE OF RESEARCH

With all the data collected and analysis conducted, the work presented in this document could lead to the addition of the LoRa communications technology to some European research projects being conducted in different research institutes and research lines of the UPV. In this context, LoRa would fit as a long-range communications technology to provide sensor networks to the Cities and Industries of the future.

One of the objectives could be an implementation of the IPv6 stack over LoRa prepared to offer the necessary robustness for an industrial environment where some of the transmitted data need to be guaranteed with a certain QoS (Quality of Service).

REFERENCES

[1] K. Ashton, “That 'Internet of Things' Thing,” *RFID Journal,* p. 1, 22 6 2009.

[2] Semtech Corporation, “LoRa™ Modulation Basics,” Semtech Corporation, 2015.

[3] Federation of American Scientists, “Continuous Wave Radar,” [Online]. Available: https://fas.org/man/dod-101/navy/docs/es310/cwradar/cwradar.htm.

[4] LoRa Alliance Technical Committee, *LoRaWAN Regional Parameters Specification,* 1.1A ed., N. Sornin, Ed., 2017.

[5] RS Components Limited, “Building a Raspberry Pi Powered LoRaWAN Gateway,” [Online]. Available: https://www.rs-online.com/designspark/building-a-raspberry-pi-powered-lorawan-gateway. [Accessed 08 01 2018].

[6] Cisco Systems, Inc., “Cisco Wireless Gateway for LoRaWAN,” [Online]. Available: https://www.cisco.com/c/en/us/products/routers/wireless-gateway-lorawan/index.html. [Accessed 08 01 2018].

[7] LoRa Alliance Technical Committee, *LoRaWAN Specification,* 1.1 ed., N. Sornin, Ed., 2017.

[8] LoRa Alliance Technical Committee, *LoRaWAN Backend Interfaces Specification,* 1.0 ed., A. Yegin, Ed., 2017.

[9] IEEE Standards Association, *IEEE Std 802.11ah™-2016,* IEEE, 2016.

[10] T. Adame, A. Bel, B. Bellalta, J. Barcelo and M. Oliver, “IEEE 802.11ah: The WiFi Approach for M2M Communications,” *IEEE Wireless Communications,* 2014.

[11] M. Qutab-ud-din, A. Hazmi, L. F. Del Carpio and A. Goekceoglu, “Duty Cycle Challenges of IEEE 802.11ah Networks in M2M and IoT Applications,” in *European Wireless 2016*, Oulu, 2016.

[12] A. Ba, K. Salimi and P. Mateman, “A 4mW-RX 7mW-TX IEEE 802.11ah Fully-Integrated RF Transceiver,” in *Radio Frequency Integrated Circuits Symposium (RFIC)*, Honolulu, 2017.

[13] GSMA, “Extended Coverage – GSM – Internet of Things (EC-GSM-IoT),” [Online]. Available: https://www.gsma.com/iot/extended-coverage-gsm-internet-of-things-ec-gsm-iot/. [Accessed 08 01 2018].

[14] GSMA, “3GPP Low-Power Wide-Area Technologies GSMA White Paper”.

[15] 3GPP, “IoT Summary,” [Online]. Available: http://www.3gpp.org/images/articleimages/iot_summary_large.jpg. [Accessed 08 01 2018].

[16] Sigfox S.A., “Modules | Sigfox Partner Network,” [Online]. Available: https://partners.sigfox.com/products/module. [Accessed 08 01 2018].

[17] Ingenu, Inc., "The Making of RPMA," Ingenu, 2016.

[18] Ingenu, Inc., “RPMA Development kit,” [Online]. Available: http://www.ingenu.com/get-started/hardware/rpma-devkit/. [Accessed 08 01 2018].

[19] Sierra Wireless, “The Opportunity for LTE-M/Cat-M1”.

[20] European Union - ETSI, “ETSI EN 300 220-1 Final Draft V3.1.1,” Europe, 2016.

[21] D. Magrin, M. Centenaro and L. Vangelista, “Performance evaluation of LoRa networks in a smart city scenario,” in *IEEE International Conference on Communications*, Paris, 2017.

[22] G. Pasolini, C. Buratti, L. Feltrin, F. Zabini, R. Verdone, O. Andrisano and C. De Castro, “Smart City Pilot Project Using LoRa,” in *European Wireless*, Catania, 2018.

[23] P. Jörke, S. Böcker, F. Liedmann and C. Wietfeld, “Urban channel models for smart city IoT-networks based on empirical measurements of LoRa-links at 433 and 868 MHz,” in *IEEE 28th Annual International Symposium on Personal, Indoor, and Mobile Radio Communications (PIMRC)*, Montreal, 2017.

[24] M. Tome, P. Nardelli and H. Alves, “Long-range Low-power Wireless Networks and Sampling Strategies in Electricity Metering,” *IEEE Transactions on Industrial Electronics,* p. Early Access, 2018.

[25] S. Thielemans, M. Bezunartea and K. Steenhaut, “Establishing transparent IPv6 communication on LoRa based low power wide area networks (LPWANS),” in *Wireless Telecommunications Symposium*, Chicago, 2017.

[26] R. Sanchez-Iborra, J. Sánchez-Gómez, J. Santa, P. J. Fernández and A. F. Skarmeta, “IPv6 communications over LoRa for future IoV services,” in *IEEE 4th World Forum on Internet of Things*, Singapore, 2018.

[27] H. H. R. Sherazi, G. Piro, L. A. Grieco and G. Boggia, “When Renewable Energy Meets LoRa: A Feasibility Analysis on Cable-less Deployments,” *IEEE Internet of Things Journal,* 2018.

[28] K. Tzortzakis, K. Papafotis and P. P. Sotiriadis, “Wireless self powered environmental monitoring system for smart cities based on LoRa,” in *Panhellenic Conference on Electronics and Telecommunications*, Xanthi, 2017.

[29] M. Loriot, A. Aljer and I. Shahrour, “Analysis of the use of LoRaWan technology in a Large-Scale Smart City Demonstrator,” in *Sensors Networks Smart and Emerging Technologies (SENSET)*, Beirut, 2017.